Master's thesis

NTNU
Norwegian University of Science and Technology
Faculty of Engineering
Department of Marine Technology

Torbjørn Reitan Fyrvik

Methods for Ocean Mapping with Combined ASV and AUV Platforms

Master's thesis in Marine Technology
Supervisor: Asgeir J. Sørensen
Co-supervisor: Jens E. Bremnes
June 2022

NTNU
Kunnskap for en bedre verden

Torbjørn Reitan Fyrvik

Methods for Ocean Mapping with Combined ASV and AUV Platforms

Master's thesis in Marine Technology
Supervisor: Asgeir J. Sørensen
Co-supervisor: Jens E. Bremnes
June 2022

Norwegian University of Science and Technology
Faculty of Engineering
Department of Marine Technology

NTNU
Norwegian University of
Science and Technology

NTNU Trondheim
Norwegian University of Science and Technology
Department of Marine Technology

MASTER OF TECHNOLOGY THESIS DEFINITION (30 SP)

Name of the candidate:	Torbjørn Reitan Fyrvik
Field of study:	Marine Cybernetics
Thesis title (Norwegian):	Metoder for havkartlegging med kombinert ASV- og AUV-plattformer
Thesis title (English):	Methods for Ocean Mapping with Combined ASV and AUV Platforms

Background

Increasing levels of autonomy in the marine domain opens for novel operations where multiple agents consisting of homogeneous and heterogeneous networks of underwater vehicles, surface vehicles, air vehicles and satellites can collaborate to perform tasks and missions. Deploying two or more agents in a combined operation expands the application scenarios that these units can be used for. Specifically, if the agents operate collaboratively rather than independently, more complex tasks can be solved, while increasing operational efficiency, reducing risks, costs and environmental impact, and enabling scalability in data collection. Operations that combine multiple agents do, however, impose stringent requirements on the communication between the agents. Moreover, collaborative control becomes of utmost importance to not only reduce operational risk, but also in updating mission objectives to achieve desired performance. To ensure safe and successful operations, new control methods are needed for multi-vehicle operations. A case study of an ocean mapping and monitoring operation using an autonomous underwater vehicle (AUV) supported by an autonomous surface vehicle (ASV) will be conducted.

Scope of Work

1. Review relevant literature on autonomy, robotic organizations, marine agents, mathematical modelling of marine vessels, AUV navigation, and hybrid dynamical systems.
2. Install and get familiar with necessary software tools and operating systems for marine robots, including the LSTS toolchain (Dune, Neptus, IMC), OBS/VCS, ROS, and Linux.
3. Implement a software framework based on the LSTS toolchain to be used for experimental work; define multiple vehicles for use in homogeneous and heterogeneous networks.
4. Develop new collaborative control methods for combined ASV and AUV operations.
5. Implement algorithms in the software framework; demonstrate and validate the methods using simulations.
6. Describe the experimental set-up for combined ASV and AUV operations. Develop and implement control method onboard an ASV to track an AUV in the AUR-Lab; demonstrate and verify the methods with field experiments. This constitutes the basis of Paper 1.
7. Expand on and modify the control methods in single-AUV to multi-AUV operation; demonstrate and validate the new methods in simulation and field experiments. This constitutes the basis of Paper 2.
8. Write the two papers, as well as relevant literature and details of robotic organizations, in a final report.

Specifications

The student shall at startup provide a maximum 2-page week plan of work for the entire project period, with main activities and milestones. This should be updated on a monthly basis in agreement with supervisor.

Every weekend throughout the project period, the candidate shall send a status email to the supervisor and co-advisors, providing two brief bulleted lists: 1) work done recent week, and 2) work planned to be done next week.

The scope of work may prove to be larger than initially anticipated. By the approval from the supervisor, described topics may be deleted or reduced in extent without consequences about grading.

The candidate shall present personal contribution to the resolution of problems within the scope of work. Theories and conclusions should be based on mathematical derivations and logic reasoning identifying the steps in the deduction.

The report shall be organized in a logical structure to give a clear exposition of background, problem/research statement, design/method, analysis, and results. The text should be brief and to the point, with a clear language. Rigorous mathematical deductions and illustrating figures are preferred over lengthy textual descriptions. The report shall have font size 11 pts., and it is not expected to be longer than 70 A4-pages, 100 B5-pages, from introduction to conclusion, unless otherwise agreed. It shall be written in English (preferably US) and contain the elements: Title page, abstract, preface (incl. description of help, resources, and internal and external factors that have affected the project process), acknowledgement, project definition, list of acronyms, table of contents, introduction (project background/motivation, objectives, scope and delimitations, and contributions), technical background and literature review, problem formulation, method, results and analysis, conclusions with recommendations for further work, references, and optional appendices. Figures, tables, and equations shall be numerated. The original contribution of the candidate and material taken from other sources shall be clearly identified. Work from other sources shall be properly acknowledged using quotations and a Harvard citation or Vancouver reference style (e.g. natbib Latex package). The work is expected to be conducted in an honest and ethical manner, without any sort of plagiarism and misconduct, which is taken very seriously by the university and will result in consequences. NTNU can use the results freely in research and teaching by proper referencing, unless otherwise agreed.

The thesis shall be submitted with an electronic copy to the main supervisor and department according to NTNU administrative procedures. The final revised version of this thesis definition shall be included after the title page. Computer code, pictures, videos, data series, etc., shall be included electronically with the report.

Start date: 15 January 2022
Due date: 11 June 2022

Supervisor: Asgeir J. Sørensen
Co-supervisor: Jens E. Bremnes

Trondheim, 11.06.2022

Professor Asgeir J. Sørensen
Supervisor

Preface

This master's thesis marks the final piece of fulfillment of my master's degree in Marine Technology with a specialization in Marine Cybernetics at the Norwegian University of Science and Technology (NTNU). The work presented in this thesis was conducted between January and June 2022 under the supervision of Professor Asgeir J. Sørensen and Ph.D. candidate Jens E. Bremnes.

Spending much of my youth on the water, and having never lived far from the coast, I have always had a strong connection with the ocean. The field of Marine Cybernetics has allowed me to combine this connection with an interest in technology and innovation. In particular, I have been fascinated by the development of networked marine robots, and when I was presented with the opportunity to work with autonomous surface and underwater vehicles, I knew this would be an appropriate topic for my master's thesis.

The main goal of the work presented in this thesis is to contribute to the transition towards autonomous systems in the marine space. Specifically, I hope that my work can help create useful systems for environmental mapping of the ocean, closing the gap of knowledge about this space that is essential for our survival as a species. Largely due to lack of knowledge, the ocean has long been disregarded as insignificant and unworthy of environmental protection, and I wish for my work to help reverse this mindset.

The work presented in this thesis is done independently by me, with supervision and support from Sørensen and Bremnes. I have actively defined the research content of the thesis, including the formulation of the task. All written content and mathematical expressions are produced by me, unless otherwise stated. Chapter 2, which introduces relevant theory, is primarily based on my Project thesis from the fall of 2021 and work done in two module courses in the same period, namely *TMR06 - Autonomous Marine Systems* and *TMR16 - Hybrid Systems Theory for Marine Applications*. The software integration, experimental setup and field trials were completed in collaboration with Bremnes at Trondheim Biologiske Stasjon in April and May 2022 with support from the staff there.

I have found the thesis work insightful and enjoyable, and I hope I get a chance to continue working with these topics in the future.

Acknowledgements

This thesis would not have been possible without the people working behind the scenes.

I would like to thank my supervisor Professor Asgeir J. Sørensen. For many years, he has helped me find my path to the completion of a master's degree at NTNU. This willingness for me to perform well has been apparent throughout the master's thesis work, during which he has encouraged me to aim high, while assisting me with valuable knowledge and insights throughout. I am grateful for the enthusiasm, the opportunities, and the trust that he has given me.

I am also grateful for the support and commitment from my co-supervisor Ph.D. candidate Jens E. Bremnes. His thoughts, ideas, and experience were instrumental in designing, implementing, and testing the proposed control methods, as well as improving the quality of the written presentation of the work in the thesis and each paper. In addition to the help towards my thesis, I am thankful for the non-thesis-related conversations about the state of the world and the belaying on the climbing wall in Korsvika.

The AUR-Lab staff at Trondheim Biologiske Stasjon also deserve appreciation. This project would not have been possible without their technical knowledge and logistical support.

Lastly, I would like to thank everyone who has made this year in Trondheim not only survivable, but rather enjoyable. My parents Jorunn and Torkel, Leo, and many, many more. You know who you are.

Torbjørn Reitan Fyrvik

Trondheim, Norway

June 11, 2022

Abstract

Recent developments in technology have reduced robots' dependency on human operators. This trend has allowed for greater levels of autonomy (LoA) in systems, leading to increased human safety and cost-efficiency, and reduced environmental impact. This is also the case for the marine industry, where agents with various LoA are gaining traction. Moreover, several autonomous agents deployed together in robotic organizations have additional benefits, such as solving increasingly complex tasks.

One example of a robotic organization is an autonomous surface vehicle (ASV) providing mission support for one or multiple autonomous underwater vehicles (AUV). During underwater operation, AUVs depend on surface support for navigation and communication with operators, as well as potential intervention during missions. While the AUVs survey the seabed, the ASV stays in their vicinity on the surface to communicate acoustically with the AUVs, providing navigational aid and relaying information from AUVs to operators. Information also goes the other way, that is, from human operators to the AUVs, such as mission updates, mission aborts or other requests. When these vehicles are combined, new properties and behaviors emerge. While the emergent properties yield a more powerful system for environmental mapping of the ocean, some of the emergent behaviors might constitute new risks. Appropriate control methods that manage these emergent risks need to be designed.

This master's thesis contains two academic papers, which propose control methods for the robotic organization where an ASV aids a single or multiple AUVs, respectively, with navigation and communication. The proposed controllers are based on emergent risks related to the hazardous events of loss of communication and the ASV getting too close to an AUV. Represented as hybrid dynamical systems, the controllers ensure safe operation. The controllers are demonstrated and validated in numerical simulations and field trials.

To contextualize the appended papers, the thesis presents background literature on related topics, and describes details about the experimental setup for the ASV-AUV test missions. This includes a detailed explanation of networking within the robotic organization, as well as hardware modifications necessary to conduct field trials. A summary and a discussion of the most important results from the appended papers are also included.

The proposed controllers performed well in both numerical simulations and physical field trials. The controller for single-AUV operation kept the ASV sufficiently close to the AUV to maintain communication, while preventing collision by maintaining distance between the vehicles. The controller for multi-AUV operation ensured to eventually re-establish acoustic communication with each AUV by consecutively transiting between each AUV's vicinity, while also preventing collision with each AUV by prioritizing collision avoidance.

Thus, the work presented in this thesis and appended papers represents a step towards more efficient, safe, and successful marine environmental mapping.

Sammendrag

Nyvinning innen teknologi har redusert hvor avhengige roboter er av menneskelige operatører. Denne trenden har muliggjort høyere automasjonsnivå (LoA) i en rekke systemer, som igjen har fordeler som høyere sikkerhet for mennesker og effektivitet, samt redusert miljøpåvirkning. Dette er også tilfelle i marin sektor, hvor agenter med varierende LoA øker i popularitet. Flere agenter sjøsatt sammen i robotorganisasjoner kan gi systemer økte kapabiliteter, som å løse mer komplekse oppgaver.

Et eksempel på en robotorganisasjon er en autonom overflatefarkost (ASV) som gir operasjonsstøtte til én eller flere autonome undervannsfarkoster (AUV). AUVer avhenger av støtte fra overflaten for navigasjon og kommunikasjon med operatører når de er under vann. Når AUVene kartlegger havbunnen kan ASVen holde seg på overflaten i nærheten av undervannsrobotene for å gi denne operasjonsstøtten. Slik kan ASVen gi navigasjonsstøtten AUVene trenger, samt etablere kommunikasjon mellom farkostene og operatører. Dette kan være oppdateringer fra AUVene, eller endringer i oppdrag, avbrytelser, eller andre forespørsler fra operatørene. Nye egenskaper og oppførsler oppstår når disse agentene blir satt sammen i en robotorganisasjon. Selv om dette er egenskapene som gjør systemet såpass godt egnet til miljøkartlegging, kan de også lede til fremvoksende risiko. Det er derfor et behov for kontrollmetoder som tar hånd om fremvoksende risiko.

Denne masteroppgaven inneholder to akademiske artikler som presenterer kontrollmetoder for robotorganisasjonen hvor en ASV gir operasjonsstøtte til henholdsvis én eller flere AUVer. De foreslåtte regulatorene er basert på fremvoksende risiko relatert til to hasardiøse hendelser: tap av kommunikasjon og at ASVen havner for nært en av AUVene. Regulatorene er presentert som hybride dynamiske systemer, og sørger for sikre og pålitelige opperasjonsvilkår. Kontrollmetodene er demonstrert og validert med numeriske simuleringer og feltforsøk.

Som en kontekstualisering av artiklene presenterer masteroppgaven litteratur knyttet til relevante emner, og beskriver detaljer rundt det eksperimentelle oppsettet for operasjoner med ASV og AUVer. Denne beskrivelsen inkluderer detaljer rundt nettverkstilkoblingene, og nødvendige modifiseringer som ble gjort på farkostene. I tillegg presenteres et sammendrag av de viktigste resultatene fra de to vedlagte artiklene, samt diskusjon av disse.

Regulatorene utførte oppgavene sine godt i både numeriske simuleringer og fysiske feltforsøk. Regulatoren for operasjon med én AUV holdt ASVen tilstrekkelig nære AUVen for å ivareta akustisk kommunikasjon, samtidig som den unngikk å havne for nært AUVen. Regulatoren for operasjon med flere AUVer sørget for at akustisk kommunikasjon med hver AUV ble gjenopprettet til slutt, samtidig som den også unngikk kollisjon ved å prioritere kollisjonsunngåelse

Arbeidet som er lagt fram i denne masteroppgaven og de vedlagte artiklene representerer et steg mot mer effektiv, trygg og vellykket havkartlegging.

Table of Contents

List of Figures

List of Tables

List of Acronyms

AI: Artificial intelligence

ASV: Autonomous surface vehicle

AUV: Autonomous underwater vehicle

DOF: Degrees-of-freedom

DP: Dynamic positioning

DR: Dead-reckoning

DVL: Doppler velocity log

GNSS: Global navigation satellite system

GPS: Global positioning system

HI: Human independence

HRI: Human-robot interface

IMC: Inter-Module Communication

IMU: Inertial measurement unit

INS: Inertial navigation system

LAUV: Light AUV

LBL: Long baseline

LoA: Levels of autonomy

NIST: National Institute of Science and Technology

OBS: Onboard System

ROS: Robot operating system

TCP: Transmission Control Protocol

UAV: Unmanned aerial vehicle

UMS: Unmanned system

UMV: Unmanned maritime vehicle

USBL: Ultra-short base line

VCS: Vehicle Control Station

Chapter 1

Introduction

1.1 Background and Motivation

In recent years there have been large developments in field robotics, enabled by new and improved sensor, computer, communication, and navigation technologies [1]. Reduced dependency on human operators leads to increased human safety and has proven to be cost-efficient and more environmentally friendly [2, 3]. Therefore, a transition towards higher levels of autonomy (LoA) is often beneficial.

Traditionally, complex marine operations have been conducted with manned, manually operated surface ships and submarines with advanced sensor systems [4]. Recently, however, due to the benefits of increased human independence (HI) and higher LoA, agents with some degree of autonomy have also gained significant traction in the marine domain. Agents are systems that both sense and act upon their environment, and the term often comes with a notion of intelligence [5]. There exists a wide range of integrated platforms and sensors with various LoA designed for use in marine applications. Two examples of such agents are autonomous surface vehicles (ASVs) and autonomous underwater vehicles (AUVs) [6]. ASVs are surface-going sensor-carrying platforms, while AUVs are sensor-carrying platforms with possibilities of under- and on-surface operation, as well as under ice.

Previously, many of the tasks requiring robotic intervention have been solved by single agents or multiple agents operating independently from each other. However, some tasks are too complex for agents to solve alone, and there is increased focus on combining multiple marine agents in robotic organizations [7]. This can expand the range of tasks that these agents can do with a potential increase in operational efficiency and reduction of risk, creating powerful systems for mapping and monitoring the marine environment [4, 6]. These systems have the potential to close the knowledge gap on the ocean, bringing humanity closer to understanding the mysteries of its vastness.

One combination that has received much attention is that of an ASV providing mission support for one or several AUVs in operation, replacing the manned support vessel that AUVs rely on [6]. This mission support may include aiding AUVs with navigation or enabling intervention. Importantly, ASVs can serve as communication hubs, relaying information between the AUV and remote operators through WiFi, radio, or satellite communication [8].

The development of collaborative control for this robotic organization is in the early stages

and more research is needed. Research groups have designed and tested various control strategies for an ASV aiding one or several AUVs. However, the proposed strategies often lack autonomy or require excessive control. Higher LoA are beneficial for this type of operation, as autonomy will lead to increased operational efficiency, reduced costs and risks, and lower impact on the environment. Moreover, this is enabling technology which makes possible a scaling-up of automatic data collection. Excessive control also increases emissions and costs while potentially lowering performance. Thus, more robust control strategies for autonomous operation of an ASV providing mission support for AUVs should be designed. This will help drive the development where multi-vehicle systems operate more independently, further expanding the benefits of marine robotic organizations.

1.2 Research Questions

The overarching goal of this thesis is to develop enabling technology that will contribute to close the knowledge gap that exists in the marine environment. To reach this goal, the case of ASV-aided AUV operation for environmental mapping is considered. This yields a more specific scientific goal, namely, to develop control methods for an ASV providing mission support for one or several AUVs. In trying to meet the main scientific goal, the thesis aims to answer the following research questions:

1. What are the advantages and disadvantages of combining autonomous agents in robotic organizations?
2. How can an ASV be combined with one or multiple AUVs in a robotic organization for environmental mapping?
3. Which properties and behaviors emerge from combining an ASV with one or multiple AUVs in a robotic organization?
4. How can an ASV be used to provide mission support for one or multiple AUVs while managing emergent risks?

1.3 Research Methods

To answer the above research questions, the thesis employs various research methods, both quantitative and qualitative. These research methods include a review of relevant literature, the definition of a case study with model expansion, a theoretical analysis, numerical simulations, and field trials.

A qualitative review of relevant literature is conducted. Theory is presented on autonomy, robotic organizations, marine agents, mathematical modelling of marine vessels, AUV navigation, hybrid dynamical systems, and risk.

To define a context in which the research questions can be answered, a case study is presented. The qualitative case study is that of an ASV providing mission support for one or several AUVs. In the case study, mission support includes providing position fixes for the AUVs and relaying mission information both ways between vehicles and operators real-time. The AUVs' task is to map the seabed, an application that requires high navigational precision to accurately georeference the collected data. For the data to be of sufficiently

high quality, the ASV's navigation-aiding role thus has critical importance for the mission. Although they are given pre-defined plans to follow, the AUVs might deviate from their plans as needed to perform closer inspections of certain areas, or if aborting the mission is necessary. This autonomous behavior necessitates autonomy on the side of the ASV as well. To provide reliable mission support, the ASV must stay close enough to AUVs to maintain secure acoustic connection to the AUVs, while preventing inter-vehicle collisions.

Moreover, a theoretical analysis of the case study is undertaken to evaluate the details of this operation. The result is a qualitative description of control objectives and strategies for combined ASV and AUV control. These objectives and strategies are further specified quantitatively in mathematical expressions that describe the proposed control methods.

Next, the proposed control methods are demonstrated and validated quantitatively using numerical simulations. Various AUV behaviors in diverse situations are tested to ensure robustness of the methods.

Lastly, field trials are conducted to further demonstrate and validate the proposed control methods quantitatively. The resulting behavior is closely analyzed to ensure that the control methods meet specifications.

1.4 Main Contributions

This thesis presents several contributions that are listed below.

- Novel control methods for an ASV providing mission support for 1) a single AUV, and 2) a swarm of AUVs.
- Formulation of control methods for ASV and AUV robotic organizations modeled as hybrid dynamical systems.
- A software framework for testing and implementing control methods in heterogeneous robotic organizations.
- A physical implementation of heterogeneous marine vehicles in a network.
- Results from numerical simulations and field trials.

The first two contributions, as well as the last, are mainly achieved in the papers. The individual contributions of the papers are included below for reference.

Paper 1: *The main scientific contribution [of this paper] is the development of a tracking controller for an ASV providing mission support for a single AUV. This is useful for aiding an AUV with USBL position fixes, as well as functioning as a communication gateway between the AUV and human operators. The tracking controller has collision avoidance properties and ensures communication between the vehicles is maintained, allowing the ASV to perform its gateway role while managing emergent risks. Moreover, formulating the control algorithm as a hybrid dynamical system represents another scientific contribution.*

Paper 2: *The primary scientific contribution [of this paper] is a supervisory switching controller algorithm for an ASV aiding multiple AUVs in operation. The mission support includes providing USBL fixes to augment the AUVs' inertial navigation error, as well as*

relaying relevant data between AUVs and operators. The proposed supervisory switching controller ensures that each AUV eventually gets a USBL fix (liveness property), while also avoiding collision with all AUVs (safety property). A secondary contribution is the formulation of the controller as a hybrid dynamical system.

1.5 Thesis Outline

The thesis is outlined as follows:

Chapter 2 presents the theory and background requisite for the appended papers, including relevant literature on autonomy, robotic organizations, marine agents, mathematical modelling of marine vessels, AUV navigation, hybrid dynamical systems, and risk.

Chapter 3 provides an in-depth description of the robotic organization used in the field trials, including software and hardware modifications made to prepare the vehicles for testing, as well as justification for the chosen tuning parameter values.

Chapter 4 presents the results from numerical simulations and field trials with both simulated and physical AUVs.

Chapter 5 provides conclusions and suggests areas of further work.

Lastly, two academic papers are included in the **Appendices**, namely:

Paper 1: *Hybrid Tracking Controller for an ASV Providing Mission Support for an AUV*

Paper 2: *Hybrid Control Approach for an ASV Aiding Multiple-AUV Operation*

Chapter 2

Marine Autonomous Systems and Control

This chapter presents literature relevant to the thesis, as well as the appended papers. This includes details about autonomy, robotic organizations, marine agents, mathematical modelling of marine vessels, AUV navigation, hybrid dynamical systems, and risk.

2.1 Agents and Robotic Organizations

In recent years there have been large developments in field robotics, enabled by new and improved sensor, computer, communication, and navigation technologies [1]. One area that is tightly connected to these developments is the field of Artificial Intelligence (AI), which has the concept of agents at its core. Russel and Norvig [5] define an *agent* as anything that can be viewed as perceiving its environment through sensors and acting upon that environment through effectors. Moreover, they make the distinction that *intelligent agents* take the best possible action in a situation.

Agents can have varying degrees of autonomy. Autonomous systems, operations and processes are often associated with unmanned systems (UMS). However, many manned systems have elements of autonomy, such as ships with complex automation capable of dynamic positioning (DP). It is therefore important to distinguish between these related but not equivalent types of systems [9].

Perhaps the most widely accepted definition of UMS is that provided by the National Institute of Standards and Technology (NIST), which states that a UMS is:

> *a powered physical system, with no human operator aboard the principal components, which acts in the physical world to accomplish assigned tasks. It may be mobile or stationary. It can include any and all associated supporting components* [10].

NIST goes on to list examples of UMS, such as unmanned ground vehicles, unmanned aerial vehicles (UAV), unmanned maritime vehicles (UMV) – unmanned underwater vehicles or unmanned water surface borne vehicles – unattended munitions, and unattended ground sensors.

Moreover, NIST provides a standard definition of autonomy with respect to UMS. Although NIST's definition applies exclusively to UMS, it can be rewritten to apply to all systems, both manned and unmanned. Thus, the rewritten definition of autonomy is:

> *a [system's] own ability of integrated sensing, perceiving, analyzing, communicating, planning, decision-making, and acting/executing, to achieve its goals as assigned by its human operator(s) through designed Human-Robot Interface (HRI) or by another system that the [system] communicates with. [A system's] autonomy is characterized into levels from the perspective of HI, the inverse of HRI* [10].

This definition makes apparent that UMS are a sub-category of autonomous systems.

Different taxonomies have been proposed for LoA, normally defined in terms of HI. It is worth noting that no one taxonomy is more correct than the others; rather, the chosen LoA should be appropriate to the system and problem at hand [11]. Utne, Sørensen and Schjølberg [9] suggest four LoA, presented in Table 2.1. Examples of marine systems and operations for each LoA are also given in the last column, inspired by Utne [12]. In the present work, the term *autonomous system* will refer to a system that can be placed in one or a combination of the LoA presented in Table 2.1.

Reduced dependency on human operators leads to increased human safety and has proven to be cost-efficient and more environmentally friendly [2, 3]. Therefore, a transition towards higher LoA is often beneficial. However, for most complex systems it is nearly impossible, and not desired, to take the direct step from fully manned and manual operation to fully unmanned and highly autonomous operation. Rather, a gradual transition towards higher LoA is more appropriate [9]. In addition to technical feasibility, this approach has other advantages. For one, it allows for extensive testing at each stage of development to ensure proper and safe functionality. This can have positive impacts on health, safety, and environment. Moreover, incremental LoA gradually has an assurance benefit. By experiencing and/or observing the safe operation of systems with higher LoA, operators, owners and other stakeholders can build trust in the systems. Thus, the move towards higher LoA might become more feasible.

As described above, single agents can solve increasingly complex tasks while increasing human safety and reducing costs and environmental impact. However, combining multiple agents to solve tasks can unlock new potential. These teams of agents, called *robotic organizations*, can be used to solve even more complex tasks, enhancing the benefits of single-agent operation. Some potential benefits of collaborating robots are scalability, efficiency, and agility in capacity, as well as increased resilience and robustness. Robotic organizations are gaining significant traction for use in a wide variety of applications [13].

Robotic organizations can be homogeneous or heterogeneous. *Homogeneous organizations* consist of teams of the same vehicle, while *heterogeneous organizations* combine different types of vehicles.

While autonomous systems and robotic organizations come with many advantages, there are also certain drawbacks to these technology. For instance, agents can only act intelligently if they are able to accurately sense their environment. The situational awareness capabilities of agents have increased significantly, but some environments are still challenging for agents to accurately sense. One example is sea ice, which, in good light and visibility, can be easy for a human to see, but notoriously difficult for robots to detect [8].

Table 2.1: Levels of autonomy for marine systems and operations [9, 12].

LoA	System description	Overall risk aspects	Examples
1: Automatic operation (Remote control)	Human operator directs and controls all functions; some functions are preprogrammed. System states, environmental conditions and sensor data are presented to operator through HRI (human-in-the-loop/human operated).	Operator experience, procedures and training are essential.	ROV/subsea inspection and intervention.
2: Management by consent	System automatically makes recommendations for mission or process actions related to specific functions, where system prompts human operator at important points for information or decisions. At this level, system may have limited communication bandwidth, including time delay due to, e.g., physical remoteness. System can perform many functions independently of human control, when delegated to do so (human-delegated).	The HRI is increasingly important. Software and the control software, including anti-collision sensors, constitute an increasing risk with higher autonomy levels.	DP system, AUV inspection task with support by surface vessel.
3: Semi-autonomous operation or management by exception	System automatically executes mission-related functions when and where response times are too short for human intervention. Human operator may override or change parameters and cancel/redirect actions within defined timelines. Operator's attention is only brought to exceptions for certain decisions (human-supervisory control).	Risk depends largely on the situation awareness capabilities of the system and the operator. Risk related to erroneous operator actions are lower, but boredom of the operator and unforeseen incidents are challenges.	DP system, energy management systems. AUVs in ocean monitoring and surveillance.
4: Highly autonomous operation	System automatically executes mission- or process-related functions in unstructured environment with capability to plan and re-plan mission or process. Human operator may be informed about progress, but the system is independent and "intelligent" ("human-out-of-the loop"). In manned systems, "human-in-the-loop" with a more supervisory role may intervene.	Risk reduction is completely dependent on a robust and resilient system design, but also on online risk management. Efficient and high integrity machine learning and adaptive functionality are essential.	AUV in ocean monitoring and surveillance without support of surface vessel. AUVs inspecting subsea installations.

However, technological advancements are being made in this field, and it is likely that the situational awareness challenge is overcome as the technology matures further.

Another challenge is agents' lack of ability to improvise. While they can be trained for many scenarios, there is always a possibility that an agent encounters a situation where it does not know how to evaluate the best decision. Training agents to have the same improvisational ability as humans remains an unsolved challenge. Nonetheless, new simulation technologies enable almost unlimited testing in virtual environments, allowing this challenge to be solved by maturing technology, too.

Furthermore, when multiple agents are combined in a robotic organization, new challenges arise due to the increased complexity of multi-agent systems. Still, robotic organizations have such a high potential in terms of solving complex tasks that researchers are investing significant resources into overcoming these challenges. Moreover, there are low additional costs and complexity involved in adding new agents in already established robotic organizations. These benefits therefore outweigh the drawbacks.

2.2 Marine Autonomous Agents

Traditionally, complex marine operations have been conducted with manned, manually operated surface ships and submarines with advanced sensor systems [4]. Recently, however, due to the benefits of increased HI and LoA, autonomous agents have also gained significant traction in the marine space. There is a clear trend where autonomous UMVs are starting to outperform traditional vehicles in solving complex tasks. These improvements are due to UMVs' characteristics such as deployability, scalability, and reconfigurability that reduce operational time and cost, as well as risk reduction with any in-the-loop operators being physically removed from the hazardous environments common to marine operations [4]. Areas of current research surrounding autonomous marine vehicles include path planning and following, collision avoidance, and maneuvering in dynamic environments for applications such as transportation, seafloor mapping, and in the oil and gas industry [7].

There exists a wide range of integrated platforms and sensors with various LoA designed for use in the above applications. These agents include, but are not limited to, small satellites, UAVs, ASVs, and AUVs [6]. Since the variation in these vehicles' temporal and spatial coverage span orders of magnitude, they have been combined in what is called the observational pyramid, presented graphically in Figure 2.1 [14].

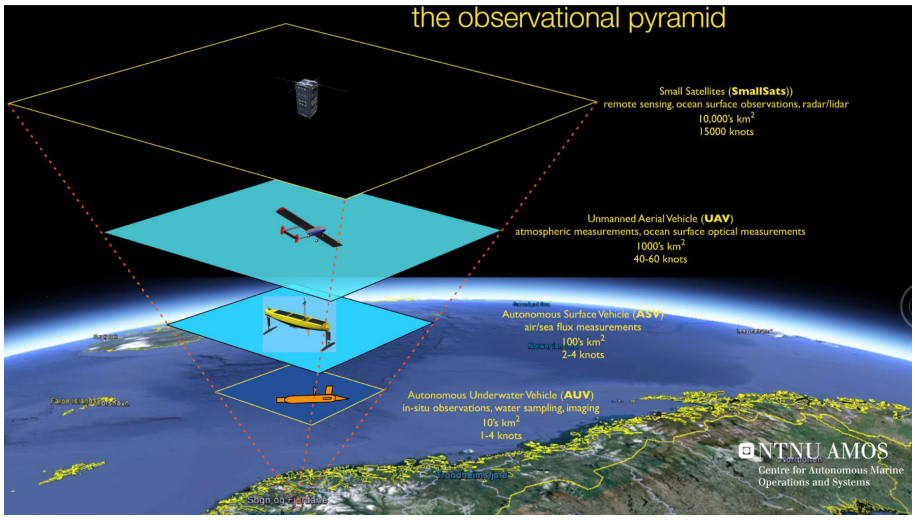

Figure 2.1: Observational pyramid for marine operations with various temporal and spatial coverage [14].

Complementing Figure 2.1, Figure 2.2 shows the temporal and spatial coverage of marine agents. The figure highlights how different agents are appropriate for different applications. Notice that the figure is a comprehensive overview of agents in the marine space, while this thesis focuses on a subset of agents: an ASV and one or multiple AUVs. Following is a description the agents presented in the observational pyramid (Figure 2.1), their applications, and potential combinations of agents in marine robotic organizations. As they are the focus of this thesis, ASVs and AUVs are presented in more detail than the rest. The introduction of the different agents is largely based on Sørensen et al. [8].

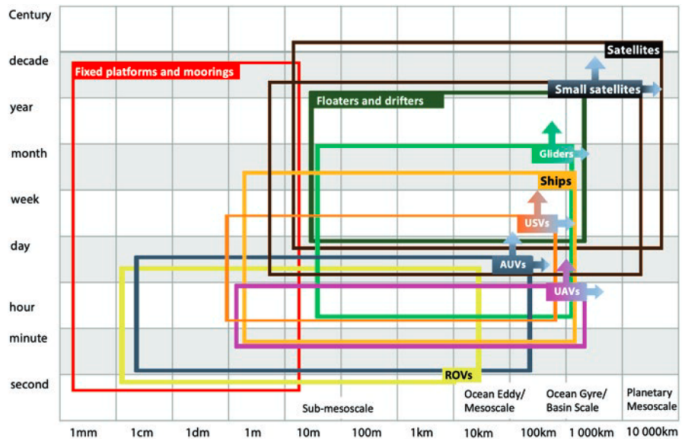

Figure 2.2: Temporal and spatial coverage of various platforms used in marine operations. Abbreviations: ROVs remotely operated vehicles, AUVs autonomous underwater vehicles, USVs unmanned surface vessels (same coverage as ASVs), UAVs unmanned aerial vehicles [8].

2.2.1 Small Satellites

Small satellites consist of a hull, antennas, payload sensors, and a control system. After launch, they operate for three to five years in a 450-500 km orbit. With a unique 2D mapping coverage, small satellites have advantages over other platforms when it comes

to mapping, and they have great communication capabilities. However, their mapping depends on good visibility and usually comes with low resolution, deployment is costly, and there is a risk of loss of data or platform.

Although satellites can be used for mapping, typically with optical sensors, the most important usage is connecting other agents in a robotic network. Their unique coverage and communication capabilities mean that satellites are useful as communication links between remote vehicles and operators.

2.2.2 Unmanned Aerial Vehicles

UAVs consist of a fixed wing shape, global navigation satellite system (GNSS), a launch and recovery system, and a control system. The vehicles come in different sizes with varying range, wind and endurance capabilities, functionality, and sensors. UAVs operate supervised within or beyond line of sight. Like satellites, UAVs have good 2D mapping abilities, and can operate in areas inaccessible with other platforms. The limitations of UAVs include limited payload capacity and endurance, sensitivity to cold temperatures and winds, as well as the potential of loss of vehicle.

While they are efficient as sensor carriers, UAVs also perform well as communication hubs. These vehicles can be outfitted with advanced communication suites and can therefore relay information between far-away water-borne vehicle and on-shore operators.

2.2.3 Autonomous Surface Vehicles

ASVs are surface-going sensor-carrying platforms that consist of the vehicle itself, a propulsion system, navigational sensors, payload module(s) and a control system. These vehicles have a variety of applications, as they come in a range of sizes with various principles of propulsion, such as combustion engines, batteries, sun, and wind. ASVs do not rely on other vehicles for power and their spatial and temporal coverage is thus dictated by the on-board power supply and/or production. Typical navigational sensors include GNSS, compass and inertial navigation system (INS), described in further detail in Section 2.5. ASVs can be deployed in supervised operation or work autonomously if communication bandwidth is limited.

ASVs' characteristics give these vehicles certain advantages compared to other marine agents. Importantly, ASVs have a unique capability in performing 2D mapping due to their large coverage, low dependency on a supporting ship during operation and high payload capacity. The lower dependency on supporting ships as compared to other agents means that operations can also be more flexible, cost-efficient, environmentally friendly, and time efficient. The high payload capacity also enables more high-quality data collection. Since ASVs can typically communicate with operation centers via 4G, radio or satellite, some data can be transmitted during operation, reducing the risk of losing data, i.e., that collected data gets lost during a mission. Furthermore, ASVs can operate in shallow waters, enabling them to reach environments unreachable with other platforms. In addition, ASVs can provide navigational aid and serve as a communication hub for underwater agents in robotic organizations, making them excellent for aiding AUV operations [8], described in further detail in Section 2.3.

At the same time, there are some inherent limitations to ASV operation. Since the agents operate independently and often far from possible human intervention, their operation

comes with significant risk. There is a risk of loss of data, loss of mission, and, in the worst-case scenario, loss of vehicle. Moreover, since ASVs are sensitive to ice, waves and current, their applicability is limited in harsh environmental conditions. This dependency on favorable weather windows reduces the availability and quality of data. Since ASVs often cannot operate highly autonomously due to lack of technological development there is also still a need for trained operators. Additionally, operational regions might be limited due to other ship traffic.

ASVs can be used in a wide variety of applications. Two examples of recent ASV-based operations are presented by Ludvigsen et al. [15] and Dias et al. [16]. Ludvigsen et al. [15] used an ASV fitted with a hyperspectral irradiance sensor and an acoustic profiler to measure the behavior of zooplankton in the high Arctic polar night. Dias et al. [16] showed how coordinated efforts between ASVs and UAVs can be used in clean up and mitigation efforts after oil spills. These are just two examples that showcase the potential of ASVs, but the future holds great potential for the deployment of ASVs in more complex and challenging applications [17].

2.2.4 Autonomous Underwater Vehicles

AUVs are sensor-carrying platforms with possibilities of under- and on-surface operation. These agents consist of the vehicle itself, acoustic and potentially other forms of navigation, and a control system. Larger AUVs also have launch and recovery systems. The vehicles come in various sizes and functionalities with different depth and thrust ratings, as well as payload sensors. A diverse range of sensors can be used for navigation, but some common ones are GNSS, underwater acoustic positioning, compass, INS, Doppler velocity log (DVL) and cameras. These are described in further detail in Section 2.5. Since they are untethered, AUVs carry their own power supply, which dictates their spatial and temporal coverage. Moreover, not being tethered means that AUVs have only limited communication capabilities. AUV operation can be supervised if the communication capabilities are sufficient, or autonomous when communication is limited.

There are several advantages of AUVs as compared to other marine agents. They have a relatively high payload capacity, which enables them to collect diverse types of data. This couples well with AUVs' unique 3D mapping capabilities, allowing the vehicles to map data not only in the horizontal plane but also at various depths. Due to their independence from umbilicals and human operators, AUVs can also reach areas where other platforms have low to no accessibility, such as under ice.

On the other hand, there are certain disadvantages of AUVs. As with ASVs, AUV operations without the possibility of human intervention have an inherent risk associated with loss of data and loss of vehicle. Next, since the power supply is carried on board, the operational time and spatial coverage are limited. AUVs also need trained operators for launch and recovery, operational planning and troubleshooting until better systems are in place. Furthermore, ship traffic and environmental conditions such as ice can limit operations. Also important is the dependency on a surface communication hub to transmit data, as well as a network of pre-installed transponders or surface vessels that track the AUVs for accurate navigation. AUVs are vulnerable to strong currents that make positioning difficult, and differences in water layers can be problematic for the acoustic communication, making navigation less accurate and consequently lowering the quality of collected data.

AUVs are getting increasingly popular for environmental (and commercial) mapping and

monitoring. Some applications include detection and monitoring of Arctic [18] and Subtropical [19] ocean fronts, tracking and sampling of deep chlorophyll [20], habitat mapping [21], monitoring of harmful algae blooms, and inspections of subsea pipelines [22, 23]. However, there is still much development happening in this field, and the next decade will likely see many novel applications.

2.3 Marine Robotic Organizations

Previously, many of the tasks requiring robotic intervention have been solved by single agents. However, some tasks are too complex for single agents to solve alone, and there is increased focus on combining multiple agents in robotic organizations in the marine space too [7]. This can further expand the range of tasks that these agents can do [4], with the possibility to create powerful systems for mapping and monitoring the marine environment [6]. Nilssen et al. [24] show how integrated operations with robotic organizations can increase efficiency, also in the marine space. Many other researchers have later joined the call for marine robotic organizations as a way forward that can reduce costs and increase the complexity of tasks that can be solved [6, 7, 25].

Until recently, most research in the marine robotic space has been focused on single-agent operations, or formation control problems for multi-vehicle control [1]. With the limited research into other aspects of robotic organizations, the development of the enabling technologies for these organizations is faster than the necessary operational community capability to use the technologies. This is particularly relevant for marine robotic organizations since solutions for land-based robotic organizations are incapable of dealing with the challenges of marine space. For instance, the underwater domain comes with additional challenges regarding communication with multipath arrival structure, channel spread and low data exchange rates [4].

The following subsections present some possible homogeneous and heterogeneous marine robotic organizations.

2.3.1 Multiple AUV Operation

One homogeneous organization that has received much attention is that of multiple AUVs deployed in a swarm. By combining these units, the underwater application potential is drastically increased [26]. Sotzig and Lane [27] proposed a framework for coordinated control of multiple AUV operations. The researchers justify the need for such a framework by pointing to benefits of multi-vehicle operation. They mention force-multiplier effects such as simultaneous data gathering and system redundancy, the ability to collect data with spatial and temporal variation, as well as possible combinations in heterogeneous networks.

There are many examples of multi-AUV operations, and only a few are presented here. Fiorelli et al. [26] proposed a concept for adaptive sampling with a swarm of AUVs. The concept was implemented and tested to do temperature gradient climbing in Monterey Bay. Wang et al. [28] used a homogeneous AUV swarm to investigate a water parameter field of interest. This group points out that the most common solution for information exchange between an AUV and the control center is the use of a satellite link when the AUV surfaces. In their work, they suggest using a remote fusion center for the communication link to overcome problems of the AUVs having to surface.

2.3.2 Multiple ASV Operation

Another homogeneous organization possibility is that of multiple ASVs. Like multi-AUV operations, multi-ASV operations allow for greater spatial and temporal coverage, increased asset redundancy and greater efficiency in sampling. Peng et al. [25] provide an overview of recent developments in coordinated control of multiple ASVs. Some examples of multiple ASV applications include a swarm of ASVs following a leading ASV [29] and sonar imaging of underwater environments [30].

2.3.3 ASV-Aided AUV Operation

A promising heterogeneous marine robotic organization, which forms the case study of this thesis and the appended papers, is that of an ASV aiding one or several AUVs in operation, taking over the role of the potentially expensive manned research vessel. Surface vehicles can employ WiFi, radio or GNSS and spread-spectrum communications for navigation and communication with operators, but since these signals do not propagate far in water, they are unsuitable in underwater applications. Therefore, ASVs can serve as communication hubs, relaying information between underwater vehicles and the control center [8]. As will be investigated in Section 2.5, ultra-short baseline (USBL) acoustic navigation systems can be used for accurate positioning of an AUV relative to an ASV, augmenting the unbounded error in inertial navigation [31–33]. With higher position accuracy from USBL navigation, AUVs can save power on less accurate INS [13]. An additional benefit of ASV-aided AUV operation is a reduced risk of collision between the AUVs and other ships. Since the ASV can be equipped with Automatic Identification System (AIS), other ships can observe the ASV. If the ASV is patrolling the safety zone around the AUVs, it can prevent ships from colliding with the units during surfacing [34]. In the case that the ASV uses spread-spectrum communication, a satellite would likely be used as an extended link between the ASV and operators. With WiFi and radio this link between operators and the ASV can be direct. Therefore, the case study in this paper does not consider the inclusion of a satellite in the robotic organization.

Among the research done on ASVs and AUVs combined in robotic organizations, most is focused on specific aspects of operations, such as launch and recovery systems, path planning, or control systems. At the same time, there is a lack of field experience with these operations being part of commercial survey campaigns [22]. However, some of the research developments and potential applications of ASV-aided AUV operation are presented below.

One tracking strategy for an ASV providing mission support for a single AUV is to maintain a constant formation. This is the strategy employed by Norgren et al. [34], who use an ASV and an AUV to map an area to search for a World War II airplane wreck. With a constant range and bearing to the AUV, the ASV functions as a communication hub, relaying information to an onshore control center and providing position fixes to the AUV. Another example is the Ocean Infinity project, a successful commercial implementation of these robotic organizations that has shown how deep-sea mapping operations are made possible with a team of up to eight AUVs, each aided by an ASV [35]. Like the ASV in Norgren et al. [34], each ASV maintains a constant range and bearing to the AUV that it aids. Similarly, Fallon et al. [36] show that satisfactory inertial navigation error augmentation can be achieved with the ASV moving in zigzag or circular patterns around the AUV. Although this strategy is reliable, the ASV in each application is always moving, leading to potentially excessive control action and propeller noise that affects the acoustic signals. Norgren et al. [34] point to how only 63% of acoustic signals were successfully

captured. Moreover, it is desirable that one ASV can provide mission support for multiple AUVs.

Another tracking strategy is to provide the ASV with a pre-defined track to follow. One group that employs this strategy is Vasilijević et al. [37], who present results from field trials of a coordinated navigation system for an ASV and an AUV for ocean sampling and environmental monitoring. In this navigation system the ASV performs station-keeping in the middle of the AUV's operational area. Thus, successful missions depend on the AUV not surfacing or aborting in the center of the area, and the area being small enough that reliable acoustic communication is maintained throughout. Another example of this tracking strategy is Zhang et al. [38], who use an ASV to provide situational awareness and potential intervention for two AUVs, enabling novel data collection and tracking of the deep chlorophyll maximum layer in the North Pacific Ocean. Similarly, Antonelli et al. [39] employ the same tracking strategy with an ASV aiding AUVs performing geotechnical surveys. The main challenge with this strategy is the dependence on a pre-defined plan. The strategy relies on a priori knowledge of the AUVs' movement and does not consider autonomous AUV behavior or aborted plans. With the dependence on pre-defined plans, the strategy thus gives the robotic organization lower LoA and limits possible AUV strategies, such as adaptive sampling, where the AUVs' paths are unknown.

To reach higher LoA and minimize propeller usage, there have been further efforts towards designing more autonomous control algorithms for an ASV that can move adaptively while aiding one or multiple AUVs. Willners, Toohey and Petillot [40] propose an ASV controller that chooses the optimal waypoint in a domain about the ASV defined by its maximum speed. The controller uses two cost functions that depend on the distance to each potential waypoint, as well as the bearing relative to the ASV's heading. By choosing the waypoint with the lowest cost, the controller minimizes fuel consumption. Expanding on these results, Sture, Norgren and Ludvigsen [41] propose an optimal controller that also takes AUV depth into consideration and enables a trade-off between fuel consumption and navigational accuracy for the AUVs. These proposed controllers solve the problem in a cost-optimal manner, but also come with additional layers of complexity. Controllers that are not optimization-based might therefore be easier to modify and tune for operators.

The above examples highlight the potential of ASV-aided AUV operations, but there are many other possible applications.

2.3.4 Other Configurations

It should be noted that numerous other configurations of marine agents in robotic organizations exist as well. One example is the use of air-borne vehicles, such as UAVs, in joint operation with ASVs and/or AUVs to increase spatial coverage. Other surface vehicles or underwater vehicles like gliders and ROVs, respectively, can also be used in different applications with various benefits [6]. However, since this thesis is focused on ASV-aided AUV operation, these other configurations will not be described in further detail here.

2.4 Modeling of Marine Vessels

This section draws mainly on Fossen [42]. Please refer to that work and the references therein for more details.

2.4.1 Kinematics of Marine Vessels

In marine applications, several reference frames are used. This thesis makes use of an Earth-fixed reference frame and a body-fixed reference frame, presented in Figure 2.3. When using the Earth-fixed reference frame, measurements of position and orientation are done relative to a fixed origin, while in the body-fixed reference frame, the origin follows the moving body. Here, the body-fixed origin will be defined as the mean oscillatory position in the average water plane.

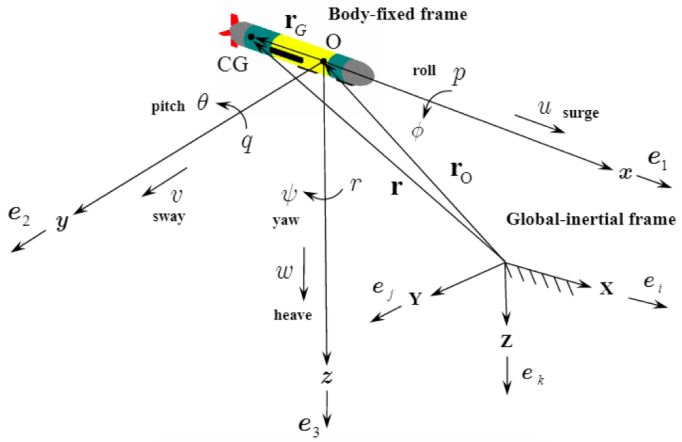

Figure 2.3: Reference frames for a marine vessel [43]. Note that in the figure the Earth-fixed reference frame and its NED components are presented as the Global-inertial reference frame with components XYZ.

The 6 degree-of-freedom (DOF) Earth-fixed generalized position vector of a marine vessel is expressed as $\eta = [p^T \quad \Theta^T]^T = [N \quad E \quad D \quad \phi \quad \theta \quad \psi]^T \in \mathbb{R}^6$, representing North, East and Down positions, and roll, pitch, and yaw orientations, respectively. Similarly, the 6 DOF body-fixed velocity vector is expressed as $\nu = [v^T \quad \omega^T]^T = [u \quad v \quad w \quad p \quad q \quad r]^T \in \mathbb{R}^6$, representing surge, sway and heave translational velocities, and roll, pitch, and yaw rotational velocities, respectively.

The kinematic relationship between the Earth-fixed ($\dot{p} \in \mathbb{R}^3$) and the body-fixed ($v \in \mathbb{R}^3$) translational velocities is expressed as

$$\dot{p} = J_1(\Theta)v, \tag{2.1}$$

where $J_1(\Theta) \in \mathbb{R}^{3\times3}$ is the Euler angle transformation matrix for translational motion with orientation $\Theta \in \mathbb{R}^3$, given by

$$J_1(\Theta) = \begin{bmatrix} c\psi c\theta & -s\psi c\phi + c\psi s\theta s\phi & s\psi s\phi + c\psi c\theta s\phi \\ s\psi c\theta & c\psi c\phi + s\psi s\theta s\phi & -c\psi s\phi + s\psi s\theta c\phi \\ -s\theta & c\theta s\phi & c\theta c\phi \end{bmatrix}, \tag{2.2}$$

using $s \cdot = sin(\cdot)$ and $c \cdot = cos(\cdot)$. Similarly, the kinematic relationship between the Earth-fixed ($\dot{\Theta} \in \mathbb{R}^3$) and body-fixed ($\omega \in \mathbb{R}^3$) rotational velocities is expressed as

$$\dot{\Theta} = J_2(\Theta)\omega, \tag{2.3}$$

where $J_2(\Theta) \in \mathbb{R}^{3\times3}$ is the Euler angle transformation matrix for rotational motion, given by

$$J_2(\Theta) = \begin{bmatrix} 1 & s\psi t\theta & c\psi t\theta \\ 0 & c\psi & -s\psi \\ 0 & s\phi/c\theta & c\phi/c\theta \end{bmatrix}, \quad c\theta \neq 0, \tag{2.4}$$

using $s\cdot = sin(\cdot)$, $c\cdot = cos(\cdot)$ and $t\cdot = tan(\cdot)$. Note that $J_2(\Theta)$ is undefined if $\theta = \pm\frac{\pi}{2}$ (rad), a case in which a quaternion can be used. Combining (2.1) and (2.3), the 6 DOF kinematic vessel model becomes

$$\dot{\eta} = \begin{bmatrix} J_1(\Theta) & 0_{3\times3} \\ 0_{3\times3} & J_2(\Theta) \end{bmatrix} \nu = J(\Theta)\nu, \tag{2.5}$$

where $0_{3\times3} \in \mathbb{R}^{3\times3}$ is a matrix of zeros and the block matrix $J(\Theta) \in \mathbb{R}^{6\times6}$ is the Euler angle transformation matrix for combined translational and rotational motions.

2.4.2 Vessel Dynamics

It is common to separate the vessel dynamics model into a low-frequency (LF) model and a wave-frequency (WF) model. The LF motions are assumed to be caused by second-order wave loads, other environmental loads (e.g., current, wind and ice), mooring and thrust forces. WF motions, on the other hand, are caused by first-order wave loads, which are well represented by a linear model under the assumption of small amplitudes. In a marine control system, it is undesirable to control for WF motions since this requires large control action and consequently causes unnecessary wear and tear on the ship's machinery. Thus, the LF motions are the focus in the following discussion.

The nonlinear LF vessel model for the 6 DOF body-fixed motions is represented as

$$M\dot{\nu} + C_{RB}(\nu)\nu + C_A(\nu_r)\nu_r + D(\kappa, \nu_r) + G(\eta) = \tau_{env} + \tau_{thr}. \tag{2.6}$$

The right-hand side of (2.6) represents generalized external forces on the vessel, where generalized forces refer to forces in surge, sway and heave, and moments in roll, pitch, and yaw. $\tau_{env} \in \mathbb{R}^6$ represents the environmental forces (e.g., second-order waves, wind, and ice) except current loads, which are accounted for on the left-hand side with the inclusion of relative velocity $\nu_r = \nu - \nu_c$ using current velocity ν_c. $\tau_{thr} \in \mathbb{R}^6$ represents the generalized forces from the propulsion system.

On the left-hand side of (2.6), $M\dot{\nu}$ is the generalized inertial forces, where $M = M_{RB} + M_A \in \mathbb{R}^{6\times6}$ is the sum of the rigid body and added mass matrices. $C_{RB}(\nu) \in \mathbb{R}^{6\times6}$ is the Coriolis and centripetal matrix of the rigid body, and $C_A(\nu_r) \in \mathbb{R}^{6\times6}$ is the corresponding matrix for the added mass. The generalized damping and current forces are accounted for by the damping vector $D(\kappa, \nu_r) \in \mathbb{R}^6$. This vector is the sum of two components as per $D(\kappa, \nu_r) = D_L(\kappa, \nu_r)\nu_r + d_{NL}(\nu_r, \gamma_r)$, where the first and second terms are its linear and nonlinear components, respectively. Since higher speeds result in turbulent flow, the linear damping matrix $D_L(\kappa, \nu_r) \in \mathbb{R}^{6\times6}$ is assumed to decay exponentially to zero with increasing speed. $\kappa \in \mathbb{R}_{>0}$ is a constant that ensures this exponential decay. The nonlinear damping and current vector $d_{NL}(\nu_r, \gamma_r) \in \mathbb{R}^6$ depends on the relative drag angle γ_r. Lastly, $G(\eta) \in \mathbb{R}^6$ represents the generalized restoring forces.

The combination of (2.5) and (2.6) represents the high-fidelity process plant model (PPM) of a ship.

2.5 Autonomous Underwater Vehicle Navigation

A variety of navigational sensors are installed on board an AUV to accurately determine its navigational states. This section describes some AUV navigation technologies in more detail.

2.5.1 GNSS and Other Ubiquitous Sensors

Global Navigation Satellite System

GNSS are satellite-based positioning systems used in almost all mobility-based applications, where global positioning system (GPS) is the most common of several possible systems. GNSS units provide position measurements using electromagnetic waves [44]. If coupled with real-time kinematics (RTK), GNSS technology can achieve very high positional accuracy. However, since electromagnetic energy does not propagate far in water, underwater navigation cannot rely on GNSS; other techniques must be used [45].

Despite the unavailability of GPS signals under water, almost all AUVs are equipped with a GPS receiver. This is because GPS can be used to fix initial position before the AUV leaves the surface, and to augment errors with the other navigation technologies if the AUV surfaces during the mission [45].

Pressure Sensors

Most underwater vehicles are outfitted with pressure sensors, which, together with a priori knowledge of sea water conditions, can accurately measure absolute depth [45]. Since the pressure sensor is very accurate, this depth measurement is prioritized for positioning along the vertical axis. Thus, the AUV navigation problem is reduced to positioning in the horizontal plane [6]. Pressure sensors used on AUVs have sampling rates in the range 0.8-8 Hz [46].

Magnetic Compasses

Due to their low price and power consumption, compasses are also used in most underwater vehicle applications. Magnetic compasses measure the 3D magnetic field at the location of the compass. To calculate AUV heading from the local magnetic field, the compass must be calibrated to the geographical location of operation. Moreover, the electronics in the AUV induce a magnetic field, which will affect the compass measurements, and magnetic compasses become less accurate at high latitudes [45].

Gyroscopes

Gyroscopes measure the AUV's changes in orientation by use of physical laws related to rotation. Examples of available technologies include mechanical gyrocompasses and gyroscopes based on laser, fiber optic or micro electromechanical systems (MEMS) technology. Optical gyroscopes are popular, but high-performance requirements drive the price up. Additionally, they have high power and space requirements, meaning they are normally limited to use in large and expensive AUVs [45]. Rotation-based heading sensors are more common and accurate than magnetic compasses for underwater applications, meaning gyroscopes are preferred over magnetic compasses [6, 47]. However, since magnetic compasses are cheaper, they are often used in low-budget applications [47]. Sampling rates for gyroscopes are near-continuous [46].

Doppler Velocity Log

DVL uses Doppler shifts in frequencies to measure linear velocities and altitude. Four transceivers facing downward emit acoustic pulses that, if the AUV is sufficiently close to the seabed, are detected after seabed reflection. Measuring the Doppler shift in the reflected signals, the DVL unit can calculate the vehicle speed relative to the stationary seabed. The maximum distance to the seabed for DVL to be available ranges from 30 m for high-frequency units to 500 m for low-frequency units. Vegetation or a soft seabed can, however, absorb most of the energy in the signals, reducing this range significantly [45]. DVL units have sampling rates in the range 0.5-5 Hz [46].

2.5.2 Proprioceptive Navigation

Proprioceptive navigation refers to navigation where a vessel's self-motion is used to deduce its position. The two main categories of proprioceptive navigation systems are attitude-heading reference systems (AHRS) and INS combined with DVL. While AHRS is cheaper, the more expensive INS/DVL combination gives more accurate position estimates [45].

Attitude-Heading Reference Systems

AHRS are commonly used to estimate AUV orientation. These systems normally consist of a 3-axis gyroscope, a 3-axis linear acceleration sensor and a heading sensor that is either magnetic- or rotation-based. The gyroscope's measured rotation rates are integrated to get orientation estimates. The heading sensor augments accumulated integration error in heading, while the accelerometers measure the gravitational vector to augment roll and pitch errors [45]. AHRS typically have sampling rates in the range 100-200 Hz [6, 46].

Inertial Navigation Systems

INS consist of the same sensors as AHRS but have the additional capability of estimating position. This is done by rotation of measured linear accelerations to the common navigation frame, followed by double integration with respect to time. Inertial measurement units (IMU) are one common INS implementation and, like AHRS, have sampling rates in the range 100-200 Hz [46]. INS rely on signals from GNSS or acoustic networks for the

initial position measurements. The operation when vehicles navigate without direct measurements of position and velocity but rely solely on INS estimates is called *dead-reckoning* (DR) [6, 45].

Due to the lack of sensors that can measure position and velocity directly during DR, sensor noise in the accelerometers translates to an error in position and velocity that increases over time called *drift*. In fact, the position drift increases without bound as the AUV stays in DR and the distance travelled increases. Therefore, AUVs rely on other sensors to augment the error. One option for augmentation is for the AUV to surface to get GPS signals. However, frequent surfacing can be inconvenient or even impossible in some operations, such as deep-water or under-ice applications. Due to these factors, surfacing therefore increases risk. Another option is coupling INS with DVL. This allows for augmentation of the velocity drift, which also reduces position drift, but position drift will remain unbounded. Moreover, DVL augmentation requires the AUV to be sufficiently close to the seabed, which might not be possible in some operation formats. Acoustic positioning is a more viable technology to augment the position drift, as explained in more detail in Section 2.5.3 [45].

How fast the error grows depends on DVL availability, ocean currents, vehicle speed, calibration errors, errors in lever arms or rotation of the sensors, as well as noise levels in the IMU. Assuming that DVL is not available and that the other factors remain constant, the drift's dependency on IMU noise can be estimated. For IMU acceleration noise ε_a (in RMS), the expected position drift Δp is given by (2.7), where t is the time spent in DR.

$$\Delta p = \frac{1}{2}\varepsilon_a \times t^2 \tag{2.7}$$

Experimentally, position drift is normally 0.5–2% of distance traveled if DVL is available. Errors down to 0.1% are obtainable for large and expensive INS systems, while AUVs that rely solely on a compass and a speed estimate can have errors up to 10%. IMUs that have power and space requirements compatible with typical AUV operations have position drift rates of about 1 km/h [45].

External aiding with position fixes is necessary to augment the position drift in inertial navigation. The required position fix frequency depends on the required navigational accuracy and IMU noise. To understand how position drift is affected by IMU noise, consider two IMUs from Kongsberg Seatex: MRU 5 and MRU 5+ MK-II. While the rated acceleration noise of the MRU 5 unit is $\varepsilon_{a,5} = 0.002$ m/s^2 RMS, the more high-end MRU 5+ MK-II has a rated acceleration noise of $\varepsilon_{a,5+} = 0.0003$ m/s^2 RMS.

Specifying a maximum acceptable position drift Δp_{max}, (2.7) can be rewritten to estimate the maximum acceptable period between position fixes as per

$$T_{max} = \sqrt{\frac{2\Delta p_{max}}{\varepsilon_a}}. \tag{2.8}$$

Using $\Delta p_{max} = 2$ m, as well as the rated acceleration noise of the MRU 5 and MRU 5+ MK-II, the acceptable periods between position fixes become $T_{max,5} = 44.7$ s and $T_{max,5+} = 115$ s, respectively. Interestingly, with the inversely quadratic relationship between acceleration noise and acceptable position fix period, an almost ten-fold increase in precision corresponds to less than a three-fold increase in acceptable time between position fixes.

2.5.3 Acoustic Positioning

Acoustic baseline sensors have historically been the preferred method of underwater navigation [6]. The two most common and relevant sensors are long baseline (LBL) and USBL. Both make use of acoustic transceivers on the vehicle to find relative position compared to transponders in the operational area. Knowing the exact location of these transponders, absolute position can be calculated.

Long Baseline

In LBL systems three or more acoustic transponders are placed around the AUV's operational area and used as beacons. When the AUV acoustic modem sends out a ping, each beacon responds in a unique way, allowing the AUV to recognize the signals and calculate the range to each beacon. Knowing the exact position of each beacon, the AUV can trilaterate its position [45].

With LBL systems using low frequency bands for signal transmission (e.g., 12 kHz), the AUV can operate as far as 10 km from the beacons with an absolute position error of 1-10 m. Using short-range systems with transmission frequencies up to 300 kHz, however, the maximum range is reduced to 100 m, while the error can be in the order of millimeters [45].

Since LBL navigation requires beacons being deployed before the operation, it is not an ideal method for AUVs moving across longer distances. Moreover, the LBL installation can be expensive and time consuming, driving the price up for areas that do not see much traffic [45].

Ultra-short Baseline

Instead of a single receiver on each modem, such as that used in LBL systems, USBL modems have multiple receiving elements. USBL uses only one top-side modem, which is of the same type as the beacons used in LBL navigation. What distinguishes USBL from LBL is that with multiple receiving elements, a single modem can detect phase differences. This allows for the system to calculate the bearing to the AUV. Knowing both range and bearing, the relative position of the AUV can be calculated with only one beacon. Like for LBL, knowledge of the beacon location allows for subsequent calculation of absolute position [45]. The sampling rates of the USBL signals lie in the range 0.2-2 Hz [46].

USBL navigation is limited to the communication range of the acoustic modems. With long-range systems, the AUV is confined to an operational area in the order of 10 km^2.

USBL (and LBL) communication range also depends on water conditions, where natural phenomena like salinity, temperature and turbidity can limit the signal transmission and consequently reduce communication range [8]. For instance, rivers can deposit large amounts of sediments and change the water quality significantly in river deltas. Moreover, ambient noise caused by propellers or other sources of acoustic interference can significantly deteriorate acoustic signals or prevent transmission altogether.

Another limitation on the communication range is navigational uncertainty. Specifically, uncertainty in the bearing estimate of the USBL modem ($\Delta\beta$) translates to a transverse position uncertainty (Δd) that increases with range (r) as per

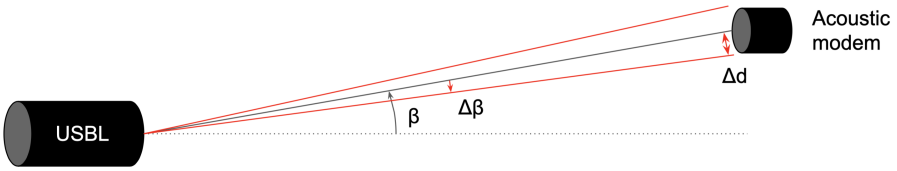

Figure 2.4: Uncertainty in USBL navigation. β is measured bearing with uncertainty $\Delta\beta$, where Δd is the corresponding transverse position uncertainty.

$$\Delta d = \Delta\beta \cdot r, \tag{2.9}$$

for small angles $\Delta\beta$. This is graphically illustrated in Figure 2.4. As a result of the transverse uncertainty's proportional relationship with range, the navigational uncertainty decreases as the AUV moves further from the USBL modem. This can lead to increased operational risk, as well as reduced data quality, since data collected by the AUV cannot be mapped geographically with the same precision.

One example of a USBL modem is EvoLogics's S2C R 18/34 USBL. The stated range of the modem is 3500 m, but experience shows that under typical conditions the signal is good only up to about $d_1 = 500$ m and sporadic to $d_2 = 800$ m, after which no signals are received.[1]

2.5.4 Map-Based Navigation

To overcome the challenges related to deploying beacons for acoustic positioning, another navigation technique is map-based or terrain-aided navigation. This technique consists of matching what the vehicle senses in its surroundings to an a priori map of the environment. Geophysical parameters that can be mapped a priori and sensed during operation include bathymetry, magnetic field, or gravitational anomalies. If there is sufficient local variation in the parameters, the vehicle's measurements can be matched with the corresponding location on the map, allowing for localization of the AUV. However, this technique requires detailed maps of the operational area, and there is large computational complexity related to matching sensed data to the map [45].

2.5.5 Cooperative Navigation of Multiple Vehicles

AUV Swarm navigation

Since new technology enables two or more AUVs to communicate with each other, homogeneous AUV swarms can also increase position accuracy where mobile transponder networks can be created by the AUVs. In applications where two or more AUVs will at least sporadically be within acoustic communication reach of one another, the unbounded DR drift can thus be augmented. If one vehicle in a team of AUVs is equipped with a more accurate IMU, this vehicle can aid the other vehicles' navigational efforts [45, 48, 49].

[1] Range estimates from e-mail conversation in October 2021 with Jens E. Bremnes. Bremnes is a Ph.D. candidate at NTNU AMOS, works with autonomy for underwater vehicles in the AUR-Lab (https://www.ntnu.edu/aur-lab), and has operational experience with AUVs both in open water and under ice.

ASV-Aided AUV navigation

Another option for cooperative navigation is mounting the USBL modem on an ASV instead of a manned research vessel. The ASV is outfitted with a GPS receiver, so that it can follow the AUV and provide position fixes. Hovering on the surface above the AUV, the ASV functions as a communication hub, aiding the AUV with navigation while relaying information between the AUV and operators in a remote control center. This operation can be used to reduce estimation bias in the observer during DR with USBL fixes from the ASV [33], or to reduce power consumption in the AUV by using a less accurate INS [13]. It is worth noting that this operation also has challenges related to implementation. Norgren et al. [34] observed that only 63% of the pings sent out by the transceiver were detected by the ASV-mounted transponder in a sea trial where an ASV aided the navigation of an AUV. The low detection rate was believed to be due to sub optimal placement of the acoustic modem head on the ASV hull surface but could also be caused by ASV propeller noise since the ASV was always moving during the field trials. Caution must therefore be exercised to ensure that the implementation is successful.

Moreover, the limitations of USBL systems lead to various modes of operation for the ASV and AUV heterogeneous organization. Figure 2.5 shows the three operational modes with respect to communication between the ASV and the AUV, and consequently also the availability of USBL-aided navigation. The availability of DVL is not considered in this simplified representation. Firstly, operational mode 1 (AUV in dark blue region) is when the two agents have reliable communication. A few USBL position updates might be lost in this mode, but the general trend is that the signals are received at a mostly consistent, high sampling rate. Secondly, operational mode 2 (AUV in light blue region) is when the AUV is near the limit of the range of the acoustic signals, meaning USBL signals will be more sporadic and therefore also less reliable. Lastly, operational mode 3 (AUV in white region) is when the AUV is fully outside the ASV's range of communication. In this operational mode, the AUV will be in DR until returning to operational mode 2. If DVL were considered and had similar differences in signal availability, its inclusion would add several sub-cases to each operational mode described here.

The size and shape of the regions that define the AUV's operational modes are determined by the reach of the acoustic modems. The USBL signals become more sporadic when the AUV moves further from the ASV and when the water conditions worsen, and they may also depend on bathymetry. Additionally, as the AUV moves further from the ASV or the acoustic quality of the water is reduced, the USBL signal sample time and noise also increase.

2.6 Hybrid Dynamical Systems

It is common that, when described mathematically, systems are characterized as either continuous-time systems or discrete-time systems. Some systems, however, have both continuous- and discrete-time dynamics. These systems are referred to as hybrid dynamical systems. Goebel, Sanfelice and Teel [50] present a detailed mathematical framework for analyzing such systems, and while a short introduction is provided here, the reader is referred to that work and the references therein for more details.

The mathematical framework presented by Goebel, Sanfelice and Teel [50] refers to continuous time dynamics as *flow* dynamics, and discrete time dynamics as *jump* dynamics.

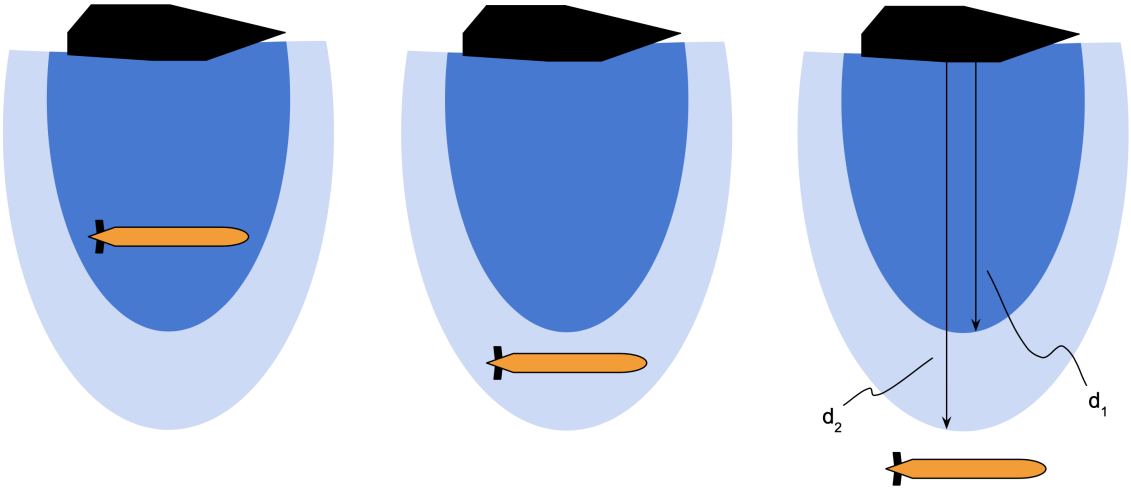

(a) Operational mode 1: Good communication.

(b) Operational mode 2: Sporadic communication.

(c) Operational mode 3: No communication.

Figure 2.5: ASV (black) and AUV (orange) communication. The dark blue area of range d_1 represents the USBL communication range of the ASV, the white area is outside the ASV's communication range, and the light blue area of range d_2 is a transition between the other two regions. Note that the shapes might not be representative of real-life conditions. (Based on [13]).

Using these concepts, the general model of a hybrid dynamical system is expressed as

$$\mathcal{Q} = \begin{cases} \dot{x} \in \mathcal{F}(x) & \text{for } x \in \mathcal{C}, \\ x^+ \in \mathcal{G}(x) & \text{for } x \in \mathcal{D}, \end{cases} \tag{2.10}$$

where $\mathcal{C} \in \mathbb{R}^n$ is the flow set, $\mathcal{F} : \mathbb{R}^n \rightrightarrows \mathbb{R}^n$ is the flow map, $\mathcal{D} \in \mathbb{R}^n$ is the jump set, and $\mathcal{G} : \mathbb{R}^n \times \mathbb{R}^m \rightrightarrows \mathbb{R}^n$ is the jump map. The differential inclusion $\mathcal{F}(x)$ describes how the hybrid state x is allowed to change continuously when it belongs to the flow set $\mathcal{C}$. Similarly, the difference inclusion $\mathcal{G}(x)$ describes how the state is allowed to change discretely when it belongs to the jump set $\mathcal{D}$.

The hybrid dynamical systems framework might appear to be overly complex for some systems that exhibit continuous- and discrete-time dynamics, but it has certain advantages. Importantly, the framework allows for stability analysis of a wide range of systems, such as systems that have logic variables, mechanical systems that experience impacts and systems with computer-based sampling [50, 51].

2.7 Risk Aspects

There exists a plethora of textbooks on risk, and as many definitions of the concepts that surround it. This paper uses the definitions of Rausand and Haugen [52], who define *risk* as "The combined answer to the three questions: (1) What can go wrong? (2) What is the likelihood of that happening? and (3) What are the consequences?" Moreover, the authors define *hazard* as, "A source or condition that alone or in combination with other factors can cause harm," and *hazardous event* as, "An event that has the potential to cause harm."

In marine autonomous systems, there is risk associated with loss of mission, loss of data and damage to or loss of vehicle, to mention some [8]. Loss of mission refers to vehicles having to abort missions earlier than planned due to unforeseen events. The unforeseen events can constitute several hazards, such as, for instance, violation of operational constraints, worsening environmental conditions, time constraints, or failing machinery or other components. Loss of data refers to collected data being lost of deteriorated. This can happen if data-collection sensors fail or are calibrated wrongly, or if the navigational accuracy is too low, meaning accurate georeferencing is not possible. Damage to or loss of vehicle refers to a vehicle being damaged or unretrievable, respectively. The risk of damage to or loss of vehicle is heightened by the presence of hazards such as sea ice, poor environmental conditions, ship traffic, man-made objects, complex bathymetry, lacking communication and navigation capacities, and failing components.

When autonomous agents are combined in robotic organizations, new properties and behaviors emerge. In fact, one can argue that this is the main motivation for robotic organizations: to achieve new properties that can be used to solve more or different tasks than the agents are capable of individually [53]. The emergent behaviors can, however, also constitute new risks that do not exist for the individual agents. Robotic organizations must therefore be evaluated for emergent hazards and hazardous events, as well as corresponding risks.

In the case of ASV-aided AUV operations, there are two hazardous events that stand out. The first of these hazardous events is that of loss of communication between the ASV and AUVs. For the robotic organization to operate as desired, the communication link between the vehicles must be maintained. Loss of communication can have serious consequences, such as loss of mission, loss of data, and damage to or loss of vehicle. Another hazardous event is the ASV getting too close to an AUV, which can lead to collision between the vehicles. The event of an agent breaching another agent's safety zone emerges as a new hazardous event in multi-vehicle systems. Like loss of communication, collision between vehicles can have severe consequences, such as loss of mission, loss of data, and damage to or loss of vehicle.

While there exist many other hazardous events for ASV-aided AUV operation, the two presented here might be the most apparent that also have the most serious consequences. Therefore, risk reduction for these hazardous events constitutes the main motivation of the control methods proposed in the appended papers.

Chapter 3

Experimental Setup for ASV-AUV Operation

This chapter presents details behind the development of the two appended papers. It describes the robotic organization deployed in the Trondheimfjord during field trials, as well as modifications necessary for this work and future developments. The field trials were conducted using equipment and experiential support from AUR-Lab. Figure 3.1 presents a graphic illustration of the network, described in more detail in the following text.

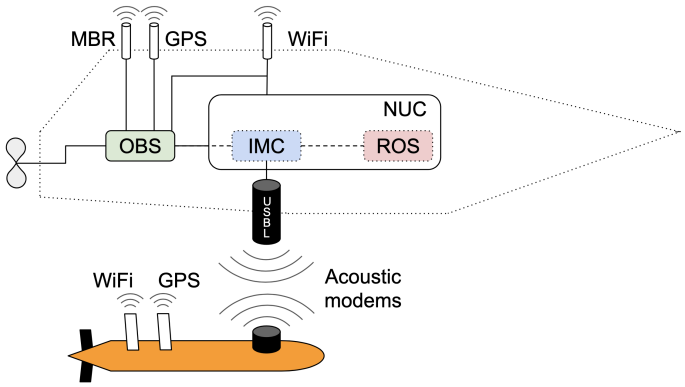

Figure 3.1: Network chart for robotic organization. The ASV is the dashed outline on top and the AUV is the orange vehicle underneath. The vehicles communicate via WiFi (AUV on surface) or acoustics (AUV underwater).

3.1 Vehicles and Network

The robotic organization of focus in this thesis and appended papers consists of an ASV and one or multiple AUVs, shown in Figure 3.2, as well as any operators supervising the operation. These entities constitute nodes in the network that communicate with each other. This section presents details about the nodes and describes the communication pathways that were implemented.

(a) ASV Gretha. (b) LAUV Fridtjof.

Figure 3.2: The vehicles used in the field trials, pictured in the Trondheimfjord.

3.1.1 Autonomous Surface Vehicle

AUR-Lab's ASV is a Pioner 17 from Maritime Robotics named Gretha. Gretha is 5.2 m long, 2.15 m wide, has a draft of 0.3 m and weighs 810 kg without payloads. While the vehicle's rated top speed is 6 kn, its rated endurance is 24 hours at 3 kn. The ASV comes with a square 1 m x 1 m moonpool for mounting sensors, as well as three circular, smaller ones.

The on-board communication suite consists of a WiFi hotspot with more than 50 m range, LTE coverage through a 4G module, and Kongsberg MBR broadband with 15 km range. Operators can steer the ASV on-site via WiFi during launch and recovery, or from a control center via the MBR broadband. Additionally, an EvoLogics S2C R 18/34 USBL modem was installed in the square moonpool to facilitate acoustic communication with the AUV.

3.1.2 Autonomous Underwater Vehicles

AUR-Lab operates four light AUVs (LAUV) from OceanScan: Fridtjof, Harald, Roald, and Thor [54]. In terms of software, these four vehicles are mostly interchangeable, but they have different uses. The smallest of the four, Fridtjof, is a bottom-tracking AUV equipped with a side-scan sonar (SSS) and a forward-looking sonar (FLS). This type of operation is the focus of the present work. Thus, and since it is the easiest to handle due to its small size and weight, Fridtjof was the AUV used for implementation and field trials of the single AUV tracking controller. However, soon before field trials were to be conducted, Fridtjof experienced a leak in its main payload compartment. Thus, the LAUV was not available for testing. Due to logistical challenges, none of the other LAUVs were available either, meaning field trials had to be conducted with simulated AUVs. If possible, Fridtjof would also have been deployed with one or two of the other LAUVs for multi-AUV field trials. Although the field trials were conducted with simulated AUVs, Fridtjof's specifications are presented here to display which type of vehicle would be used in the field trials if available. Moreover, the simulator is modeled on an LAUV which

hydrodynamics are similar to Fridtjof's.

Fridtjof is 1.80 m long, has a diameter of 20 cm and weighs 25.8 kg. The vehicle's maximum speed is 2 m/s, and the rated endurance is 8 hours at maximum speed. Fridtjof's on-board communication suite consists of a WiFi antenna with 1 km range, GSM coverage through a 3G module, and an Iridium SBD module with global coverage, as well as an underwater acoustic modem. When the AUV is on the surface and within range, it communicates with the ASV via WiFi. During underwater operation, however, the vehicles' communication is limited to acoustic communication with the USBL modem. The period of USBL fixes is set to 5 s, while full acoustic report period is set to 30 s, which is the minimum update period. However, these waiting times can be significantly higher if acoustic distortion prevents successful transmission of one or several updates.

3.2 Software

Figure 3.3 illustrates how the hardware and software components onboard the ASV are connected. The following text describes the network in more detail.

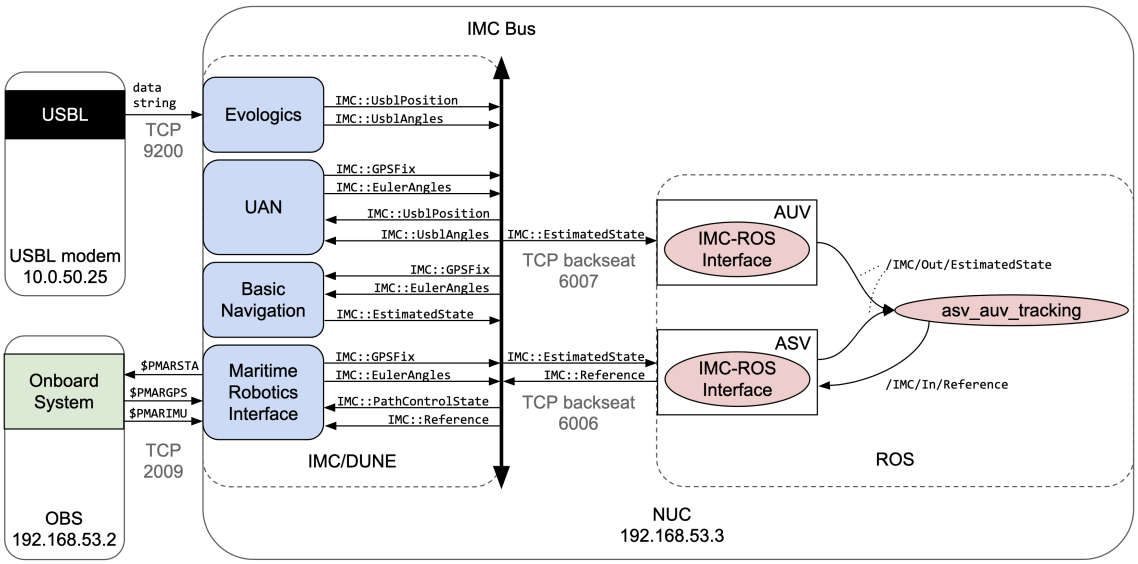

Figure 3.3: Network nodes and connections onboard the ASV (see Sections 3.2.1-3.2.6 for details about the components). Each physical unit (OBS, NUC and USBL) is indicated with black lines, and their IP addresses are included under the names. The software components on the NUC unit (IMC/DUNE and ROS) are indicated with dashed lines, and the colors match those used in Figure 3.1. IMC messages are shown as straight arrows going in and out of the IMC bus, while ROS topics are illustrated by curved arrows. The blue rectangles are DUNE tasks, and the red circles are ROS nodes. TCP ports are numbered with dark grey text. This example shows the case of single-AUV; multi-AUV operation would have similar IMC-ROS interface nodes for additional AUVs. Only the most relevant IMC messages and ROS topics are shown.

3.2.1 Onboard System and Vehicle Control Station

During simulation and field missions, Gretha is operated with Maritime Robotics's in-house Onboard System (OBS) for control, navigation, and communication. OBS, marked

by a green rectangle in Figure 3.3, runs on a designated OBS computer, which monitors and controls essential parts of the ASV operation, from navigation with GPS and communication via WiFi or radio, to low-level actuator control. The user interface of OBS is called Vehicle Control Station (VCS). VCS allows operators to choose between different modii operandi, such as a station-keeping, heading control, manual control, external control and many more. Moreover, the software allows for monitoring the ASV's navigational states, sensors, power consumers, etc. VCS also comes with a built-in simulator of Gretha, which enables rapid testing and prototyping before running field trials on the water.

3.2.2 LSTS Toolchain

The LAUVs operated by AUR-Lab come with the LSTS toolchain, which consists of DUNE[1] on-board software, the Inter-Module Communications (IMC)[2] protocol, and Neptus[3] command and control software [55].

DUNE: Unified Navigational Environment is a runtime environment for vehicle on-board software. It enables control of unmanned vehicles' motion, navigation, communication, sensors, and actuators, to mention some. The base entity of a program in DUNE is the task, indicated by blue rectangles in Figure 3.3. A *task* is a subprogram that executes some functionality by subscribing and publishing to IMC *messages* [56]. There is great diversity in tasks' functionalities. Some tasks interface hardware with IMC, such as `MaritimeRoboticsInterface` and `Evologics` in Figure 3.3. Other tasks can translate higher-level goals into low-level commands or use low-level sensor measurements to estimate states. An example of the latter is `BasicNavigation` in Figure 3.3. All tasks, as well as the DUNE core library, are compiled into a single binary executable.

When a DUNE instance is started, an initialization file for the specified vehicle determines which tasks are run for that vehicle, and sets relevant parameters. Since the default LAUV simulator in DUNE (lauv-simulator-1) has similar hydrodynamics to Fridtjof, Fridtjof's DUNE instance was initialized with the initialization file for lauv-simulator-1 [54]. The initialization file for Gretha, however, had to be made specifically for this project. Like Fridtjof, Gretha's initialization file is based on the initialization file for lauv-simulator-1, but also starts the custom *MaritimeRoboticsInterface* task (see Section 3.2.4), as well as the *Evologics* task. This second task is essentially an EvoLogics USBL driver written for DUNE, which creates and publishes `IMC::UsblPosition` and `IMC::UsblAngles`, which are converted to `IMC::GPSFix` and `IMC::EulerAngles` by the *UAN* task. UAN is short for underwater acoustic navigation. This allows for the USBL signals to be converted into `IMC::EstimatedState` messages, the default navigation message in DUNE, in the *BasicNavigation* task. By running the *Evologics* task and connecting it to the installed USBL modem via a Transmission Control Protocol (TCP) port (see Section 3.2.6), the ASV can provide the AUV with USBL fixes and monitor its states.

As mentioned above, DUNE tasks communicate using IMC messages, represented by straight arrows in Figure 3.3. The IMC protocol is a message framework created to facilitate communication between heterogeneous vehicles, sensors, and human operators, as well as in-vehicle communication [55]. The protocol outlines which types of data and messages that can be passed between tasks. The entire IMC protocol is defined in a single XML document, which can be compiled in C++, C# or Java. The IMC protocol has a

[1] https://github.com/LSTS/dune
[2] https://lsts.pt/docs/imc/master/index.html
[3] https://github.com/LSTS/neptus

bus structure, where all DUNE tasks have access to all messages, illustrated graphically in Figure 3.3. This makes the system modular, as tasks can be replaced without changing the whole program structure, if they subscribe and publish to the same IMC messages. Each DUNE instance has its unique IMC ID. This ID is included in the header of IMC messages published by that node so that other tasks can identify the publishing source of the message.

Neptus is the user interface of DUNE, which allows human operators to interact with the unmanned systems. In Neptus the operator can command and control vehicles in the planning, simulation and execution phases of missions, and the interface allows for multi-vehicle mission control.

3.2.3 Robot Operating System

The source code for the hybrid tracking controllers was written in Python using Robot Operating System (ROS)[4]. ROS is an open-source set of libraries and tools created to make building robots easier. The software is based on packages created by its users, making it very modular and useful in a range of applications. ROS's numerous possibilities, as well as the unparalleled online community, makes the software a popular choice for robotic operations. Thus, ROS was chosen due to its simplicity, modularity, and online support.

The base entity of a ROS program is the *node*, marked by red circles in Figure 3.3. Nodes perform computation to execute some functionality, and a ROS program typically consists of many such nodes connected in a network. The main difference to a DUNE task is that each ROS node is compiled as a separate executable, while all DUNE tasks are compiled in a single executable. This means that to communicate with other nodes, each node must be connected to a program called master, which connects nodes together.

Like DUNE, ROS also uses message passing for nodes to communicate with each other. In ROS, this is done by nodes subscribing and publishing to *topics*. Topics, represented by curved arrows in Figure 3.3, are buses of information through which nodes can share information. By subscribing and publishing to topics, nodes can communicate without direct connection to or knowledge of each other. Several nodes can subscribe and publish to the same topics.

In the network presented in Figure 3.3, each vehicle's navigational states are published to the `/IMC/Out/EstimatedState` topic. The *asv_auv_tracking* node subscribes to this topic to compute waypoints for the ASV, published on the `/IMC/In/Reference` topic. There is one *IMC-ROS Interface* node for each vehicle, each corresponding to a DUNE instance with a unique IMC ID. When the *asv_auv_tracking* node receives messages over the `/IMC/Out/EstimatedState`, it therefore must use the IMC ID in the header of the message to determine which vehicle has published the navigational states in DUNE.

3.2.4 MaritimeRoboticsInterface Task

For OBS to integrate with the LSTS toolchain, the *MaritimeRoboticsInterface* task was created. The task functions as a two-way software bridge between OBS and IMC. To present the navigational states of Gretha in IMC, the task listens to the `$PMARGPS` and `$PMARIMU`, published by the OBS computer on TCP port 2009. These messages get con-

[4] https://www.ros.org

verted to the IMC messages `IMC::GPSFix` and `IMC::EulerAngles`, respectively, which get published to the IMC bus. Like for the acoustic navigation, *BasicNavigation* subscribes to these messages and converts them to `IMC::EstimatedState`, the navigation message which is accepted by the *IMC-ROS Interface* nodes in ROS.

For OBS to accept waypoints from DUNE, the *MaritimeRoboticsInterface* task subscribes to `IMC::PathControlState` and `IMC::Reference`. `IMC::PathControlState` is the message that is published when commands such as station-keeping and more complex plans are provided by the operator through Neptus. `IMC::Reference` is another IMC message used to give commands to a DUNE instance. In this network, it is the message used to send tracking set-points from the controller in ROS to the ASV. Thus, the *MaritimeRoboticsInterface* task allows for monitoring the ASV's navigational states in DUNE, and consequently in ROS, as well as sending commands from both Neptus and the ROS tracking script node.

3.2.5 IMC-ROS Interface

Since the source code for the ASV controller was written in ROS, another interface was necessary between ROS and IMC. This interface was based on the *imc_ros_bridge* package.[5] The package has a launch file, `bridge.launch`, which initiates a node that subscribes to specified IMC messages to publish them as ROS topics and vice versa. However, the package does not apply directly to multi-vehicle operations and is lacking a conversion of the `IMC::Reference` IMC message, so the package had to be modified to suit the network at hand.

To achieve this, a conversion was specified between `IMC::Reference` and the topic `/IMC/In/Reference` in ROS. Then, a new launch file, `multibridge.launch` was created. This launch file starts *IMC-ROS Interface* nodes for each of the DUNE instances in the robotic organization. The ASV node subscribes to `IMC::EstimatedState` and `/IMC/In/Reference`, before converting and publishing them to `IMC/Out/EstimatedState` and `IMC::Reference`, respectively. The AUV nodes do not incorporate the Reference part since no waypoints are sent from ROS to the AUVs.

3.2.6 Transmission Control Protocol Ports

Communication between the different units in the network is achieved by TCP, which is a communication protocol that facilitates exchange of messages between devices that are connected to the same network. As shown in Figure 3.3, the USBL modem and OBS computer are connected to the NUC computer via TCP ports 9200 and 2009, respectively. Moreover, the ROS nodes for the ASV and AUV are connected to the TCP backseat driver ports 6007 and 6006, respectively, and multi-vehicle tests were conducted with additional AUVs connected to TCP backseat driver ports 6008 and 6009.

[5] https://github.com/smarc-project/imc_ros_bridge

(a) Cage before mounting to hull.

(b) Profile view.

(c) Corner view.

(d) Front view.

Figure 3.4: Protective cage for the USBL modem made from welded steel profiles and pipes. The pipes have circular cross-section holes drilled in them to minimize acoustic signal reflection.

3.3 Hardware

3.3.1 USBL Modem Cage

The EvoLogics S2C R 18/34 USBL modem used for acoustic communication needs to be in a downward-facing underwater position for good communication with underwater vehicles. To achieve this, the modem was mounted in the square moonpool on the ASV. However, the external part of the modem was very exposed, protruding 13cm under the ASV hull. During launch and recovery of the ASV on a custom cradle, there would be a high risk of large loads on and potential damage to the modem in this configuration.

Therefore, a protective cage was built around the USBL modem. This was designed to withstand the resulting load from the entire boat's weight on top of the cage. Moreover, it was desirable to minimize the acoustic reflection from the cage, as this could infringe with the modem's ability to provide accurate and reliable USBL fixes, so holes were drilled in the cage's corner pipes. The resulting cage on the boat can be seen in Figure 3.4.

3.3.2 Ballast

During preliminary field trials it was found that Gretha performed poorly when tracking waypoints. Rather than staying at the desired heading, the vehicle would consistently start moving in circles. It was hypothesized that this undesirable behavior was a result of poor tuning and/or the vehicle being ballasted incorrectly. Upon inspection, the bow seemed to dive unnaturally deeply into the water, validating the hypothesis that the boat was poorly balanced. This is likely due to the vehicle's heavy batteries, which are all located at the bow of the vehicle, creating a forward moment.

To counteract this forward moment, ballast was added to the ASV's stern end. 180 kg of sandbags, as well as 40 kg of bricks, were safely stored in appropriate compartments. This ballasting was believed to be more than necessary to counteract the forward moment. However, it was expected that a slight backward moment would increase the maneuverability of the under-actuated vehicle with only one propeller at stern.

This modification significantly improved the tracking behavior of the ASV, but the performance was still not satisfactory. Thus, it was deemed necessary to also tune the vehicle's controller, as described in Section 3.4. Moreover, the added mass in the vehicle significantly increased its displacement and consequently slowed it down. After the modification, the ASV's maximum observed speed was 4.5 kn. Therefore, most of the sandbags were removed in later field trials, decreasing the total added ballast to 100 kg. This yielded stable controller performance with a more satisfactory maximum speed at 4.9 kn = 2.5 m/s.

3.3.3 ASV WiFi Access Point

Although the stated range of the installed WiFi antenna is more than 50 m, connection issues caused significant difficulties in the early field trials. The issues were experienced when connecting the operator's computer to the on-board computer to initiate tracking. It was possible to overcome this issue by staying close to the ASV, but this approach is neither safe nor feasible for an AUV at the beginning or end of its mission, as well as potential mid-mission surfacing or aborts. Indeed, having the AUV stay close to the AUV increases the risk of collision between the vehicles. Since the vehicles need to communicate using WiFi when the AUV is on the surface, the ASV WiFi range thus had to be improved. It is also desirable that the vehicles can communicate via WiFi during pop ups and at the end of the operation even when they are not close to one another, further emphasizing the need for a better WiFi range.

To achieve a better WiFi range, the old ASV antenna was replaced with an Ubiquiti Rocket M2HP access point integrated with two Laird TRA9023P antennas. This combination can yield a range of several kilometers under favorable conditions. After the new installation, no more connection issues were experienced.

3.4 Tuning

3.4.1 Execution Level

Yaw Controller

As described above, the additional ballast in the ASV was not sufficient to achieve desired tracking behavior. Thus, the execution level yaw controller of the ASV also had to be tuned. Several tuning combinations with P, PI, PD and PID controllers were tried, but in the end a PID controller with a sufficiently large integral component allowed the ASV to accurately track waypoints.

Surge Speed Reference Model

Field trials revealed that large heading errors at high speeds led to slow and unstable response, with the ASV starting to do pirouettes instead of following its set-point. Specifically, when the ASV was set to turn while accelerating, it was not able to achieve its desired heading. Since the ASV controller was designed and tuned for low-speed applications, it did not perform well in the high-speed transits necessary in an AUV-tracking application. Therefore, a surge speed reference model based on heading error had to be implemented.

The reference model for the surge speed set-point is a combination of a feed forward controller and a proportional controller that makes the ASV slow down during turns to facilitate more stable turning. The feed forward component (u_{ff}) is a minimum forward speed required regardless of heading error for the ASV to maneuver properly. Even at maximum heading error, the ASV must have a forward speed to maneuver because the vehicle cannot turn if it is stationary. The proportional controller determines the variable part of the commanded speed, increasing linearly from zero at $\frac{\pi}{2}$ rad or higher absolute heading error to a maximum at zero heading error. The size of the maximum commanded speed is determined by a proportional gain, while the actual maximum speed of the vehicle is dictated by its dynamics. Field trials showed that this maximum speed is $u_{max} = 2.5$ m/s. The resulting surge speed reference model is expressed as

$$u_{cmd} = \begin{cases} u_{ff} + k_u \cdot (\frac{\pi}{2} - |\psi_e|) & \text{for } |\psi_e| < \frac{\pi}{2}, \\ u_{ff} & \text{otherwise.} \end{cases} \tag{3.1}$$

In (3.1), u_{ff} is the feed forward speed, k_u is the proportional gain, and $\psi_e = \psi_{asv} - \psi_{wp}$ is the heading error of the ASV. The resulting behavior is represented graphically in Figure 3.5.

The surge speed reference model makes the ASV slow down if large heading changes are required when new waypoints are received. u_{ff} and k_u are tuning parameters that can be tuned to achieve satisfactory performance. Low values of u_{ff} give more stable behavior, while higher values yield higher speed and indirectly better maneuverability when the ASV's absolute heading error is large. Low values of k_u give more stable behavior when the absolute heading error is large, while higher values can give faster response.

The feed forward speed was initially set to $u_{ff} = 0.4$ m/s, while the proportional speed

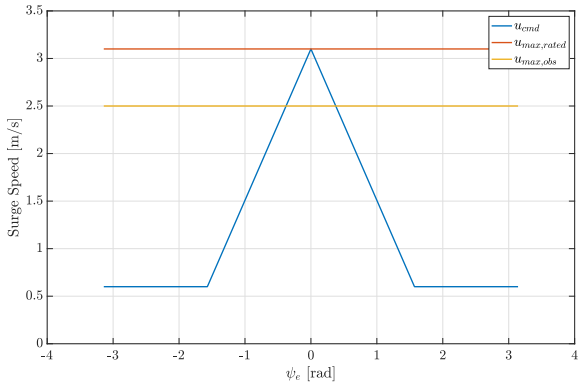

Figure 3.5: ASV surge speed reference model; commanded speed as a function of heading error (ψ_e). The commanded ASV surge speed (u_{cmd}) has a maximum at the ASV's rated maximum speed ($u_{max,rated}$), but the surge speed is in reality saturated at the observed maximum speed ($u_{max,obs}$) for $|\psi_e| < \frac{\pi}{10}$.

gain was set to $k_u = 1.72$ m/s to get a maximum commanded speed $u_{cmd,max} = 3.1$ m/s. This is approximately equal to the ASV's rated maximum speed.

During field trials, the feed forward speed was increased to $u_{ff} = 0.6$ m/s to achieve faster response during sharp turns, and the proportional gain was reduced correspondingly to $k_u = 1.59$ m/s to maintain the maximum commanded speed equal to the vehicle's rated maximum speed. Although the observed maximum ASV speed was lower than the rated maximum speed, meaning the surge speed saturated for $|\psi_e| < \frac{\pi}{10}$, the proposed tuning combination yielded good result, with fast yet stable response. The problem of unstable behavior with pirouettes was eliminated; the reference model worked well. Therefore, the tuning parameters were not modified further to meet the observed maximum speed.

3.4.2 Supervisory Level

As described in the appended papers, there are several tuning parameters related to the proposed tracking controllers. These include the parameters defining the various domains (α_{inner} and α_{outer} in Paper 1, α in Paper 2, and δ_r in both papers), as well as the parameters determining the jump dynamics of the controllers (ε in both papers and T Paper 2). The final selection of the tuning parameters for both papers is presented in Table 3.1, while a justification for the selection is provided in the following text.

Paper 1	**Paper 2**
$\alpha_{inner} = 5$	$\alpha = 5$
$\alpha_{outer} = 17.5$	$T = 10$ s
$\delta_r = 20$ m	
$\varepsilon = 10$ m	

Table 3.1: Final selection of tuning parameters.

Paper 1

The first selection of values for the domain-defining parameters was based on a priori knowledge of the system. Each parameter was set to achieve a behavior that was believed to be safe but also sufficiently fast. For instance, the inner boundary safety factor was initially adjusted to $\alpha_{inner} = 3$, yielding an inner boundary of the safety domain ($r_{inner} =$ 30 m) that was believed to prevent collision in the worst-case scenario where the AUV was moving straight towards the ASV at maximum speed. Similarly, the outer boundary safety factor was initially set to $\alpha_{outer} = 11.7$, yielding an outer boundary of the safety domain ($r_{outer} = 300$ m), thought to be small enough to maintain reliable and accurate USBL fixes throughout the safety domain, while minimizing control action and consequently propeller usage. This was primarily based on previous field experience with USBL communication, showing that USBL fixes become sporadic for $r > 500$ m. Furthermore, an initial value for δ_r was chosen to achieve a target circle radius r_t that was deemed appropriate, first believed to be in the middle between the inner and outer boundaries of the safety domain in the single-AUV application and maintained the same for multi-AUV. As for the tuning parameter defining the jump dynamics of the hybrid controller, the acceptable distance to the target circle before changing to standby mode was set to $\varepsilon = 30$ m.

These tuning parameters worked well for the initial simulation study for single-AUV operation but were adjusted during field trials for improved performance. Since the dynamics of the ASV were found to be much slower than those of the ASV simulator used during simulation-based testing, the inner boundary of the safety domain had to be increased to $\alpha_{inner} = 5$, giving $r_{inner} = 50$ m. Moreover, since the ASV was significantly slower than its rated top speed ($u_{max,test} = 4.9$ kn vs. $u_{max,rated} = 6$ kn), the safety factor for the safety domain's outer boundary had to be increased to $\alpha_{outer} = 17.5$, giving $r_{outer} = 200$ m. This was for the ASV to quickly reach the target circle during tracking, even with the AUV moving away from the ASV. The ASV only provides reliable USBL fixes when it is in the AUV's vicinity, and its propeller is turned off. Although the ASV could have drifted further from the ASV and still maintained USBL communication, it was found that the AUV operated too long without reliable USBL fixes if the safety domain's outer boundary was larger. For similar reasons, it was found that the target circle needed to be smaller than believed at first. This is since the ASV ended up spending more time tracking the AUV than doing collision avoidance. Thus, the final value for the margin from the safety domain's inner boundary was set to $\delta_r = 20$ m, giving a target circle radius r_t ranging from 20 m if the AUV is deeply submerged to 70 m if the AUV is on the surface. Lastly, the acceptable distance to the target circle before jumping to standby mode was reduced to $\varepsilon = 10$ m to make a smaller target domain, appropriate for a target circle closer to the safety domain's inner boundary.

Paper 2

For Paper 2, the selection of most of the tuning parameters followed the same reasoning as those for Paper 1. The safety factor for the anti-collision domain was set such that the $\alpha = \alpha_{inner}$, giving $r_{avoid} = r_{inner} = 50$ m. This selection is appropriate because the dynamics of the single-vehicle operation are identical to the dynamics during the ASV's collision avoidance interaction with a single AUV. Similarly, δ_r and ε were kept the same as in Paper 1. T, the time that the ASV should remain in standby before transiting to the next AUV, is dictated by the nominal periods of USBL fixes $T_{fix} = 5$ s, and full AUV status reports $T_{report} = 30$ s. Although T should arguably be set higher than $T_{report} =$ to

ensure transmission of the full report, it was kept at T =10 s in the field trials. This is because as a proof-of-concept with simulated vehicles, all AUV states are already known, the T =10 s waiting time is sufficient to showcase the controller behavior. Thus, the lower waiting time significantly reduces the duration of each test run.

Chapter 4

Results and Discussion

This section presents the results of the controllers implemented in the appended papers. The controller for an ASV providing mission support for a single AUV was tested in a simulation study, in field trials with a simulated AUV in Trondheim, and with a physical AUV in Ny-Ålesund, Svalbard. The controller for multi-AUV operation was tested in a simulation study and in field trials with simulated AUVs in Trondheim. For more details, please refer to the appended papers.

4.1 Single-AUV Operation

4.1.1 Simulation Study

Using the default LAUV simulator in DUNE and the Gretha simulator in VCS, two test cases of typical AUV operation were simulated. In Case 1, the AUV first does overview scans of two areas before performing closer inspection of detected areas of interest. In Case 2, the AUV does the same two overview scans as in Case 1, but then continues to another area to do a third overview scan instead of performing closer inspection. AUVs normally operate on altitude control during seabed surveys, but without loss of generality, depth control is used in these test cases for simplicity. The hybrid tracking controller's performance was analyzed by running it on the ASV and studying the vehicle's resulting behavior.

Case 1

Figure 4.1 presents the results from the simulation of Case 1. Figure 4.1a shows how, despite the AUV's large operational area, the ASV does not move much. While the AUV travels 4.25 km, the ASV moves less than 620 m during the entire simulation, which is only 15% of the AUV's traveled distance. Moreover, the ASV is in standby mode for 2891 s (89% of simulation), while it is in transit mode for only 357 s (11% of simulation, 28 s collision avoidance, 329 s tracking). This is largely because each overview scan is small enough that the ASV stays mostly within the safety domain. Such behavior is beneficial because it reduces wear and tear on the propulsion system, lowers energy usage, and improves the acoustic environment. Figure 4.1b helps explain how the ASV can stay mostly stationary in standby mode. Until $t = 835$ s, the ASV is drifting in the middle of

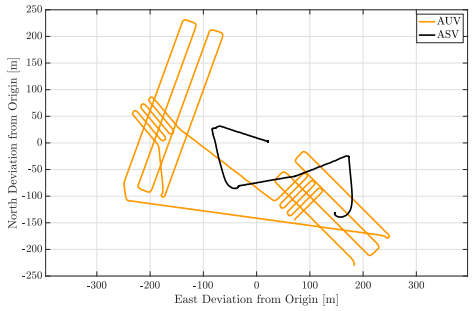

(a) North and East movement of the AUV and the ASV relative to the origin, defined as the center point of the operation, for two overview scans and two detailed inspections.

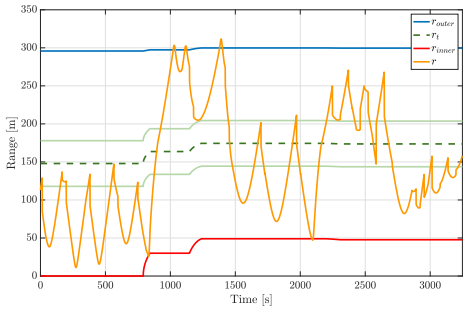

(b) Range (r), outer safety boundary (r_{outer}), target circle (r_t) surrounded by the target domain boundaries in lighter green, and the inner boundary (r_{inner}).

Figure 4.1: Single-AUV simulation, Case 1.

the AUV's lawnmower path, with the AUV sufficiently submerged that collision avoidance is not necessary. However, when the AUV transits to the Western part of its operational area, collision avoidance is initiated when the ASV breaches the inner boundary at $t = 835$ s, before tracking is initiated when the ASV breaches the outer boundary at $t = 1022$ s and again at $t = 1378$ s. One more collision avoidance is required at $t = 2095$ s, but apart from that the ASV is in standby mode.

Case 2

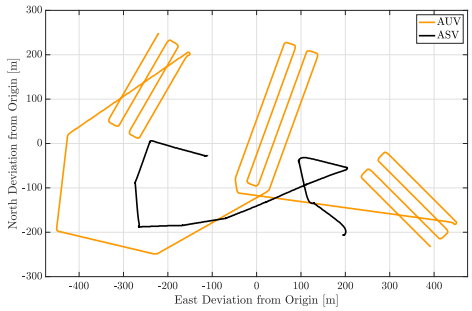

(a) North and East movement of the AUV and the ASV relative to the origin, defined as the center point of the operation, for three overview scans in various locations.

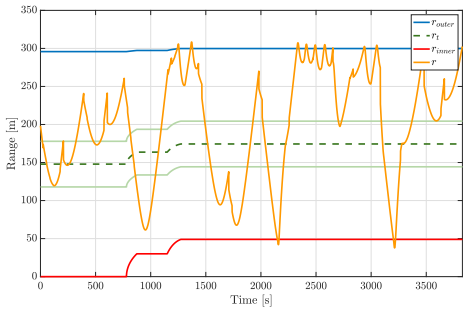

(b) Range (r), outer safety boundary (r_{outer}), target circle (r_t) surrounded by the target domain boundaries in lighter green, and the inner boundary (r_{inner}).

Figure 4.2: Single-AUV simulation, Case 2.

Figure 4.2 presents the results from the simulation of Case 2. Since the AUV transits to a different area for the third overview scan, the ASV has to move further, as seen in Figure 4.2a. The AUV moves 4.99 km, while the ASV travels 1.19 km during the 1-hour simulation. Although the ASV does more tracking than in Case 1, the total distance traveled is still only 24% of that of the AUV, confirming that the ASV moves conservatively. This is validated by Figure 4.2b, which shows the ASV-AUV range compared to the boundaries of the safety domain. For most of the operation, the ASV is drifting within the safety domain; it spends 3115 s (81% of simulation) in standby mode and only 714 s (19% of simulation) in transit mode (680 s tracking and 34 s collision avoidance). Tracking

is initiated at $t = 1240$ s, 2325 s, and 2930 s, and collision avoidance at $t = 2150$ s, and 3200 s, but the ASV quickly moves to the target domain to re-enter standby mode every time.

4.1.2 Field Trials in Trondheim

After the controller was validated in numerical simulations, field trials were conducted in the Trondheimfjord in April and May 2022 with Gretha and a simulated AUV. Like in the simulation study, two operational cases (Case 3 and Case 4) were tested. The testing cases for the field trials are simpler than those used in simulation because of the unpredictable and unforgiving environment of the ocean. The results from the simulation study and the field trials are therefore intended to complement each other.

Case 3

In Case 3, the ASV and AUV both start some distance from the operational area, which consists of a stretched-out lawnmower pattern. The length of the pattern is larger than in the simulation cases to showcase the ASV's tracking abilities. Rather than a constant altitude control law, the simulated AUV operates in the surface with a zero-depth set-point during the test to better illustrate the controller's behavior. This gives a worst-case condition with respect to the size of the anti-collision domain.

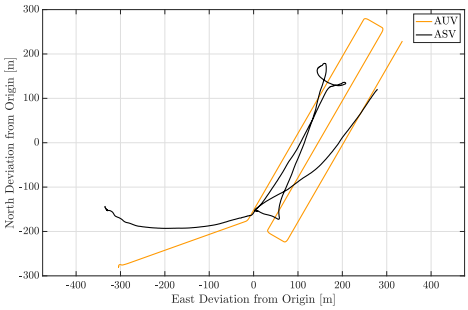

(a) North and East movement of the AUV and the ASV relative to the origin, defined as the center point of the operation, for a stretched-out lawnmower operation.

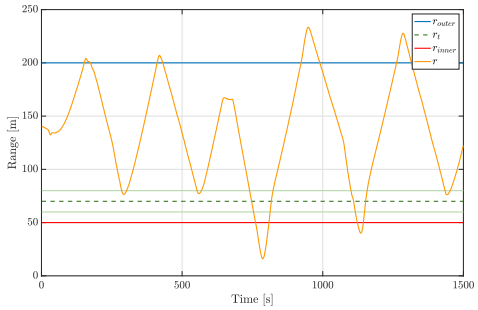

(b) Range (r), outer safety boundary (r_{outer}), target circle (r_t) surrounded by the target domain boundaries in lighter green, and the inner boundary (r_{inner}).

Figure 4.3: Single-AUV field trial, Case 3.

Figure 4.3 presents the results from the field trial of Case 3. Like in the simulated cases, the ASV travels significantly shorter than the AUV by not following the underwater vehicle to the extremities of the operation. The total distance traveled by the AUV in Case 3 is 1.98 km, while the ASV travels 1.68 km, or 85% of that of the AUV. Figure 4.3b explains the ASV's movement in Case 3 in more detail. Corrective action is taken quickly when the AUV breaches the safety domain, thus initiating a collision avoidance maneuver, which limits the range to the interval $r \in [17 \text{ m}, 233 \text{ m}]$. The ASV maintains safe operation without excessive control action, as verified by the total time spent in each operation: 798 s (53%) in standby mode and 702 s (47%) in transit mode (633 s tracking and 69 s collision avoidance). The portion spent in transit is larger than for the simulated cases because of the layout of the AUV's operational area, and since the outer boundary of the

safety domain was reduced to 200 m, with the target circle closer to the inner boundary, to achieve better performance.

Case 4

In Case 4, the AUV actively tries to breach the inner boundary, to generate challenging scenarios, by moving in an unpredictable manner, often straight towards the ASV. In essence, the AUV behaves as an adversary or a pursuer. Although this behavior is unlikely during nominal operation, it is difficult to predict how an autonomous vehicle will behave, for instance if it follows an adaptive sampling control law. Therefore, Case 4 is mainly focused on how the hybrid tracking controller prevents possibly dangerous situations when the AUV operates with high levels of autonomy. Like in Case 3, the AUV remains on the surface in Case 4.

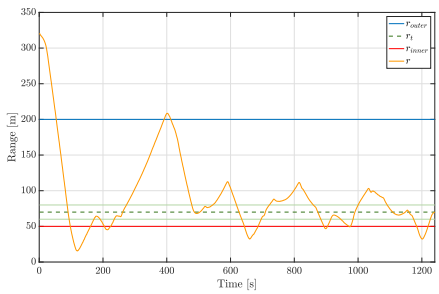

Figure 4.4: Single-AUV field trial, Case 4: range (r), outer safety boundary (r_{outer}), target circle (r_t) surrounded by the target domain boundaries in lighter green, and the inner boundary (r_{inner}).

Figure 4.4 presents the time-series of range for Case 4. The figure shows how the ASV repeatedly breaches the safety domain's inner boundary, each time initiating a collision avoidance maneuver. Even with the AUV moving straight towards the ASV at maximum speed, it was not possible to obtain a range smaller than $r = 15.5$ m at any point during the test. This verifies the ASV's collision avoidance properties. Like in Case 3, the corrective action in Case 4 is also efficient, with only 409 s (33%) spent in transit mode (232 s tracking and 177 s collision avoidance), compared to 833 s (67%) in standby mode. For closer inspection of the behavior seen in Figure 4.4, four snapshots of the vehicles during the collision avoidance period $t \in [$ 98 s, 235 s] are presented in Figure 4.5. The first snapshot (Figure 4.5a) shows the ASV in collision avoidance at $t = 120$ s. As seen in Figure 4.4, the ASV reaches the target domain and enters standby mode at $t = 88$ s. Because of the ASV's inertia, the vehicle is still drifting towards the AUV when collision avoidance is initiated at $t = 98$ s. Thus, it takes another 22 s until the ASV has turned around and started moving away from the AUV at $t = 120$ s, as seen in Figure 4.5b, reaching the minimum range $r = 15.5$ m.

The ASV then quickly moves away from the AUV and reaches the target domain at $t = 180$ s to enter standby mode (Figure 4.5b). Since the AUV is still moving the same direction, the ASV breaches the inner boundary again at $t = 215$ s (Figure 4.5c), but since the ASV is now stationary and its heading is already close to the desired heading, it only takes 20 s before the ASV reaches the target domain again at $t = 235$ s (Figure 4.5d). After this, the AUV changes heading, meaning further ASV transit is not necessary.

4.1.3 Field Trials in Ny-Ålesund, Svalbard

Complete field trials with physical AUVs were not possible to conduct as planned due to a leak in one of the LAUVs and other logistical issues. This was partly because all the other LAUVs at Trondheim Biologiske Stasjon had been sent to Ny-Ålesund, Svalbard,

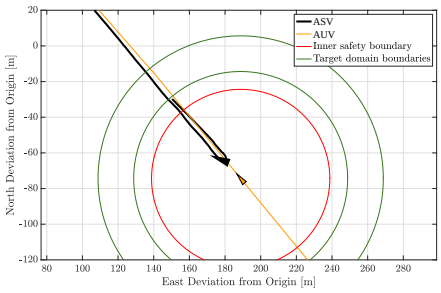

(a) $t = 120$ s. Collision avoidance.

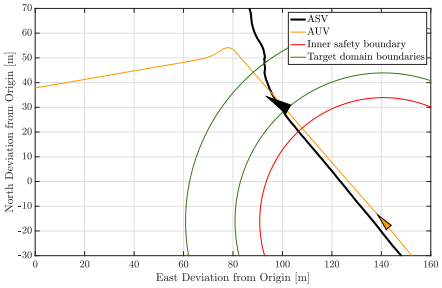

(b) $t = 180$ s. Standby.

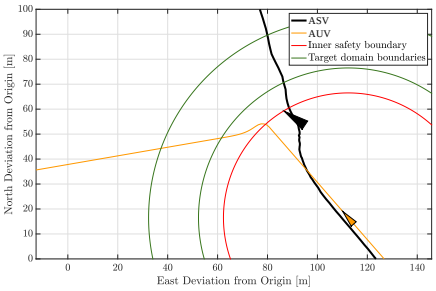

(c) $t = 215$ s. Collision avoidance.

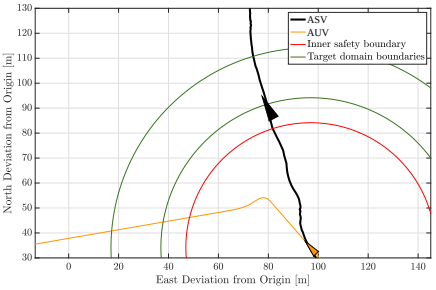

(d) $t = 235$ s. Standby.

Figure 4.5: Single-AUV field trial, Case 4: snapshots of position and heading for the ASV (labeled as USV) and the AUV during collision avoidance. The red circles indicate the anti-collision domain around each AUV, while the green circles symbolize the boundaries of the target domain.

to be used in a research campaign there. However, a chance presented itself when co-supervisor Jens E. Bremnes went to Ny-Ålesund to participate in the mission campaign. Using a Mariner ASV from Maritime Robotics, he tested the control methods developed in this thesis to track LAUV Roald, which is slightly larger than Fridtjof but has the same software setup. Time was limited to test the single-AUV controller, but it was possible to conduct one simple trial, called Case 5 in the following description.

Case 5

In Case 5, Roald first moves Northeast in a yoyo maneuver between depths of 10 m and 50 m, before the vehicle surfaces at $t = 277$ s and remains on the surface for about 300 s to give time for Iridium communication. During this time on the surface, Roald moves West, before going underwater again at $t = 587$ s and moving Southwest at varying depths. At $t = 900$ s, the AUV surfaces again and remains on the surface for the remainder of the operation. The resulting North and East movement of both vehicles is shown in Figure 4.6. The AUV was programmed to transmit an acoustic report every 30 seconds, containing its estimated state, as well as fuel level and health status. Rather than estimating the AUV's states between acoustic reports, the ASV estimated stationary AUV states between updates, as reflected in the data. One of the network connections was not properly established during Case 5, so the ASV did not receive the AUV's GPS fixes via WiFi during surface operation. Therefore, the AUV's estimated position does not change when the AUV is in the surface. Dashed lines are used to indicate the believed AUV state between position fixes.

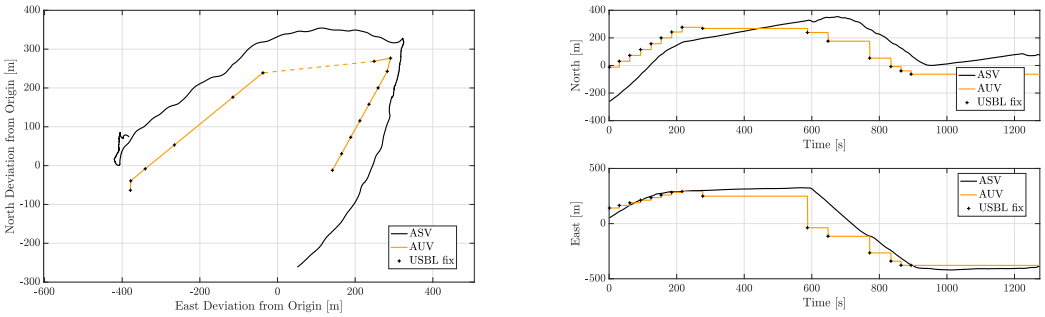

(a) North vs. East.

(b) North and East vs. time.

Figure 4.6: Single-AUV field trial, Case 5: North and East movement of the two vehicles relative to the origin, defined as the center point of the operation. The dashed line indicates estimated AUV path in the 310 s time interval $t \in$[277 s, 587 s], for which there are no position fixes.

As seen in Figure 4.6, the ASV follows the general path of the AUV. The lack of position fixes during surface operation leads to a big jump in the AUV's estimated state when it goes underwater again at $t = 587$ s. This jump is indicated by a dashed line in Figure 4.6a. Moreover, the ASV appears to consistently steer starboard of its desired heading. This is likely explained by the mounting of the USBL modem on the ASV. Since the ASV in Ny-Ålesund is not outfitted with a moonpool, the USBL modem was instead attached to a metal rod on the starboard side of the vessel in an ad-hoc manner, as shown in Figure 4.7. Consequently, the drag profile of the hull was asymmetric, leading the ASV to deviate from its heading set-point. Due to the limited time and resources in the Ny-Ålesund field campaign, this issue was not resolved. Although the tracking is not as good as one would want, the range between the vehicles is displayed in Figure 4.8 for further investigation.

Figure 4.7: Mounting of USBL modem on the ASV in Ny-Ålesund, leading to asymmetric drag on the hull.

Figure 4.8 shows that the controller behaves as expected. Since the AUV states are estimated as constant between position fixes, the raw data range curve in Figure 4.8a

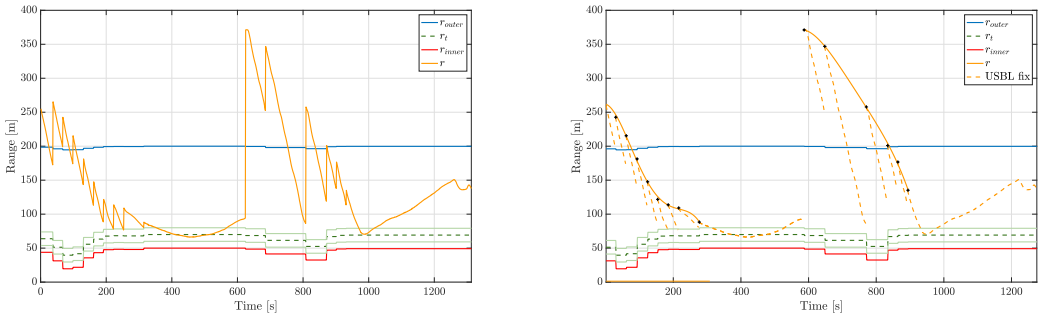

(a) Raw data.

(b) Estimating range between USBL fixes.

Figure 4.8: Single-AUV field trial, Case 5: range (r), outer safety boundary (r_{outer}), target circle (r_t) surrounded by the target domain boundaries in lighter green, and the inner boundary (r_{inner}).

has discontinuous jumps at position updates. When the ASV assumes that the AUV remains in one location, the believed range decreases rapidly as the ASV moves towards that location. However, the believed range is updated to the actual range when a position fix is provided since the AUV has moved further in the period between acoustic reports. To estimate the actual range during the field trial, the actual range at USBL fixes is curve fitted in Figure 4.8b. During surface operation, there are no position fixes for longer periods, so the actual range cannot be estimated in those intervals. Therefore, the range to the believed stationary AUV is indicated by dashed lines in the intervals $t \in$[277 s, 587 s] and $t \in$[900 s, 1275 s].

Although the AUV's position data is unreliable for large parts of the operation, the controller behaves as expected based on believed navigational states. After starting some distance away from the AUV, it enters the safety domain at $t = 80$ s and the target domain at $t = 300$ s. It then switches to standby mode and drifts, believing to be close to the AUV. When the AUV goes underwater again at $t = 587$ s, a range update $r = 387$ m is provided, and the ASV immediately switches to transit mode until it reaches the target domain again within 350 s, after which it re-enters standby mode at $t = 925$ s. After this point, it remains within the safety domain of a believed stationary AUV for the remainder of the trial.

Despite the mentioned challenges, the field trial was deemed successful as a proof of concept. The controller behaved well in field trials, acting efficiently for the ASV to stay within the safety domain. The challenges are topic for further work.

The ratios between distance traveled by the ASV and the AUV, as well as the portion of total simulation or field trial time spent in transit mode, are presented in Table 4.1.

Case	$\frac{d_{asv}}{d_{asv}}$	$\frac{t_2}{t_{tot}}$
1	15%	11%
2	24%	19%
3	85%	53%
4	na	33%
5	157%	44%

Table 4.1: Summary of numerical results from five cases of single-AUV operation. d_{asv} is the distance traveled by the ASV, d_{auv} is the distance traveled by the AUV, t_2 is the time spent in transit mode, and t_{tot} is the total simulation time.

4.2 Multi-AUV Operation

4.2.1 Simulation Study

Case 6

Using three instances of the default LAUV simulator in DUNE and the Gretha simulator in VCS, one typical multi-AUV operation was simulated. In Case 6, each AUV does a lawnmower pattern, with the operational areas separated by a few hundred meters. This closely resembles a possible multi AUV operation, where the AUVs can do simultaneous overview scans of the seabed. Like in the field trials for single-AUV operation, the simulated vehicles operate in the surface with a zero-depth set-point during the simulation. This means that the target circle and collision avoidance circle radii are the same for all three vehicles, i.e., $r_{avoid,i} = r_{avoid}$ and $r_{t,i} = r_t$ for each AUV i.

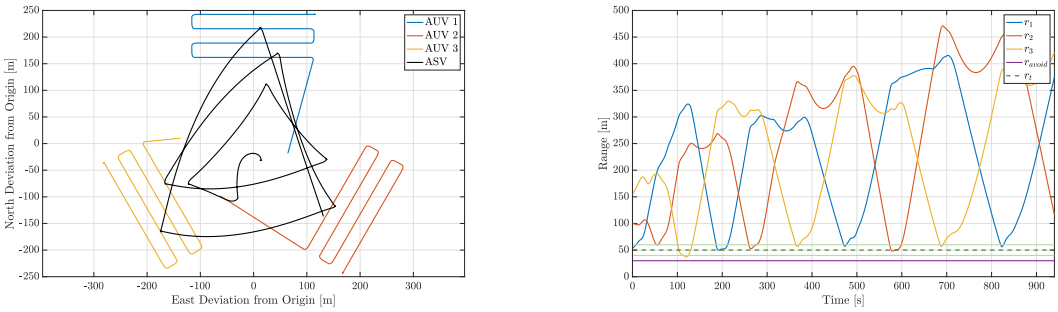

(a) North and East movement of the four vehicles relative to the origin, defined as the center point of the operation.

(b) Range between the ASV and each AUV i (r_i), and radii of the collision avoidance circle (r_{avoid}) and target circle (r_t).

Figure 4.9: Multi-AUV simulation, Case 6.

Figure 4.9 presents the results from the simulation of Case 6. Figure 4.1a shows how the ASV transits between the operational areas of the three AUVs. The triangular path of the ASV highlights how the vehicle does not have to transit to the exact position of the AUV before providing the USBL fix, but rather reduces the traveled distance by stopping when it reaches the target domain. This behavior is desired since it reduces wear and tear on the propeller, lowers energy usage, contributes to a better acoustic environment, and reduces the time between each AUV visit. As seen in Figure 4.9b, the ASV moves towards the AUVs in cyclical order, transiting towards one until the range is within the target domain, waiting $T = 10$ s, and then transiting towards the next AUV. Due to the

orientation of the AUVs' operational areas relative to each other, the ASV never enters the anti-collision zone of any AUV. Since it reaches significantly higher speeds than the AUVs, the ASV quickly transits between the operational areas, so the time between two consecutive visits does not exceed 314 s for any AUV.

4.2.2 Field Trials in Trondheim

Deploying Gretha in the Trondheimfjord and simulating three AUVs with the default AUV simulator in DUNE, two cases of a typical multi-AUV operation were tested on the water. The supervisory switching controller's performance was validated by studying the ASV's resulting behavior.

Case 7

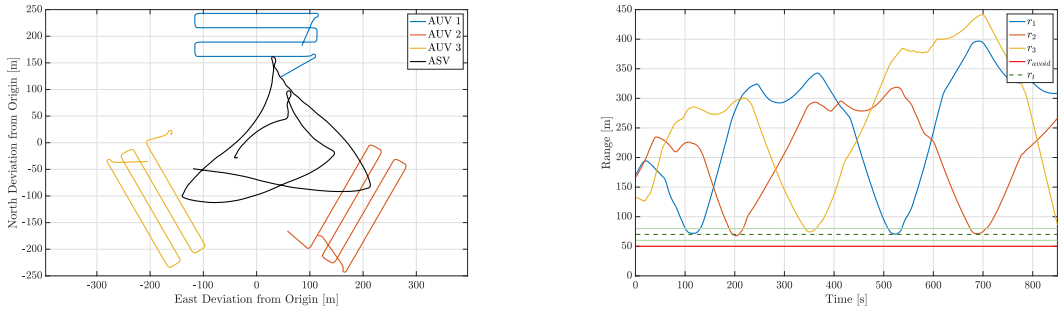

(a) North and East movement of the four vehicles relative to the origin, defined as the center point of the operation.

(b) Range between the ASV and each AUV i (r_i), and radii of the collision avoidance circle (r_{avoid}) and target circle (r_t).

Figure 4.10: Multi-AUV field trial, Case 7.

Field trial Case 7 is identical to simulated Case 6, with the exception that the physical Gretha was used instead of the simulator. Comparing Figure 4.10 to Figure 4.9, it is apparent that the behavior in the field is similar to the simulation. The tracking is slightly poorer due to the environmental loads acting on the ASV, but as seen in Figure 4.10b, the time between two consecutive visits never exceeds 500 s for any AUV. This behavior is largely enabled by the surge speed reference model, giving Gretha fast but stable turning.

Case 8

In field trials Case 8, the AUVs' waypoints are updated manually to create situations that demonstrate the ASV's anti-collision properties, like in Case 4. Therefore, Case 8 is mainly focused on how the supervisory switching controller prevents possibly dangerous situations when the AUVs operate with high levels of autonomy. The AUVs operate in the surface in Case 8 as well.

Figure 4.11 shows how the AUVs repeatedly get so close that the ASV enters their anti-collision domains, requiring corrective action by the supervisory switching controller. This corrective action effectively prevents collision, with no AUV getting closer to the ASV than AUV 3 at $t = 40$ s with $r_3 = 15$ m. Although it is longer since AUV 1 has received a visit than the two other vehicles towards the end of case, the ASV focuses its control action

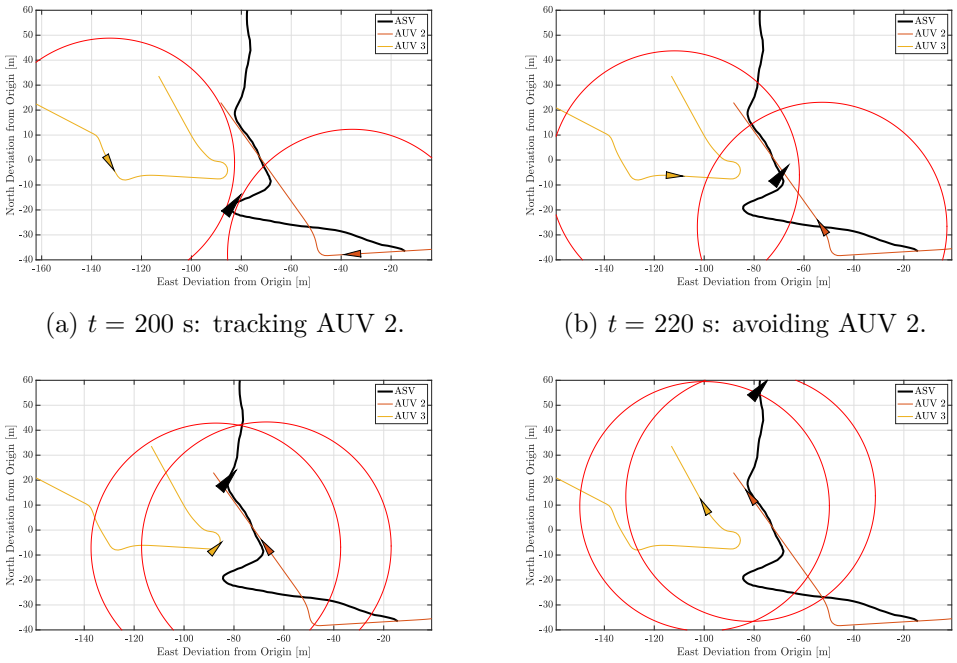

(a) $t = 200$ s: tracking AUV 2.

(b) $t = 220$ s: avoiding AUV 2.

(c) $t = 240$ s: avoiding AUV 3.

(d) $t = 260$ s: avoiding AUV 2.

Figure 4.12: Multi-AUV field trial, Case 8: snapshots of position and heading for the ASV, AUV 2 and AUV 3 during collision avoidance. The red circles indicate the anti-collision domains.

on AUV 2 and 3. This shows how anti-collision gets priority over USBL fixes. Since both AUV 2 and 3 are within the anti-collision domain in the time frame $t \in [200 \text{ s}, 260 \text{ s}]$, snapshots of the position and heading of these vehicles, as well as the ASV, are shown in Figure 4.12 for further analysis.

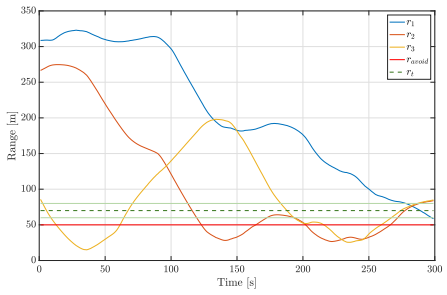

Figure 4.11: Multi-AUV field trial, Case 8: range between the ASV and each AUV i (r_i), and radii of the collision avoidance circle (r_{avoid}) and target circle (r_t).

Following the results from Figure 4.11, at $t = 200$ s (Figure 4.12a), the ASV is transiting towards AUV 2. However, it then enters the anti-collision domain of AUV 2 and turns around to prevent collision. This is shown in Figure 4.12b at $t = 220$ s, where the ASV is moving away from AUV 2. At $t = 240$ s (Figure 4.12c), the range to AUV 3 has gotten smaller than that of AUV 2, as verified by Figure 4.11. This means that the ASV switches to collision avoidance for AUV 3, and consequently turns towards North. By $t = 260$ s (Figure 4.12d), the ASV has moved out of the anti-collision domain of both vehicles. Since the ASV is significantly faster than the AUVs, it quickly moves out of the anti-collision domains despite both AUVs actively moving towards it.

Overall, the designed cases of numerical simulations and field trials gave satisfactory results for both controllers.

Chapter 5

Conclusions and Further Work

This chapter presents conclusions for the presented work, as well as recommended focus areas for further work.

5.1 Conclusions

The work presented in this master's thesis has aimed to develop control methods for an ASV providing mission support for one or several AUVs through investigating the following research questions:

1. What are the advantages and disadvantages of combining autonomous agents in robotic organizations?
2. How can an ASV be combined with one or multiple AUVs in a robotic organization for environmental mapping?
3. Which properties and behaviors emerge from combining an ASV with one or multiple AUVs in a robotic organization?
4. How can an ASV be used to provide mission support for one or multiple AUVs while managing emergent risks?

The research questions have been investigated through theoretic developments, numerical simulations, and field trials in relation to a case study.

Trying to answer the first research question, relevant literature on agents and robotic organizations, including in the marine domain, was reviewed. While there are still-present challenges related to the implementation of robotic organizations, the enabling technologies are maturing, eliminating the existing disadvantages. There are numerous advantages to combining agents in robotic organizations, including increased efficiency and safety, and reduced costs and environmental impact.

In response to the second research question, combined ASV and AUV operation was investigated in more detail. Being more flexible and efficient than traditional research operations, the ASV-AUV combination represents a powerful system for environmental mapping in the marine domain. An ASV can be deployed as a communication hub,

relaying information both ways between AUVs and operators, and providing position fixes for the underwater vehicles. Moreover, this robotic organization is scalable, as many agents can be controller or monitored by few operators. The communication between the ASV and AUVs can happen through acoustic signals underwater and WiFi on the surface, while more details about the network connections were provided in the thesis.

Referring to the third research question, emergent properties and behaviors of the ASV-AUV robotic organization were discussed. While the emergent properties are what give this robotic organization its advantages in environmental mapping, some of the emergent behaviors constitute system-level hazards. Two such hazards are loss of communication and inter-vehicle collision, both with potentially severe consequences. These system-level hazards formed the basis of the controllers presented in the appended papers.

The fourth research question was answered primarily in the appended papers. Paper 1 showed how a hybrid tracking controller that switches between a standby mode and a transit mode can keep an ASV mostly within a safety domain about an AUV performing seabed surveys. By taking control action if the ASV leaves this safety domain and turning off the ASV propeller if it is within the safety domain, the controller ensures reliable acoustic communication between the vehicles while preventing inter-vehicle collision. Similarly, Paper 2 proposed a supervisory switching controller for an ASV tracking multiple AUVs. By continuously evaluating which AUV has received mission support least recently, the controller switches its tracking objective between the different AUVs, ensuring that each AUV eventually receives mission support. Additionally, by prioritizing collision avoidance if the ASV is too close to any AUV, the controller also ensures inter-vehicle collision is prevented. Both of the proposed controllers performed well in numerical simulations and field trials.

In conclusion, the research questions and their answers have led to the development of a robotic organization with great capabilities for environmental mapping. The simulations and field trials show promising results for the proposed control methods.

5.2 Further Work

While the results from numerical simulations and field trials are promising, several topics for further studies have been identified. Some suggestions for further work are presented here.

Most importantly, more comprehensive field trials with physical AUVs are necessary to ensure the reliable and robust behavior of the proposed control methods. This includes validating whether the assumptions around AUV navigation hold. During the preliminary testing with a physical AUV, some challenges related to the experimental setup were discovered, so these should be investigated in further work. More comprehensive field trials should also include a wider variety of longer-duration test cases.

Another area of further work is a more detailed analysis of the system dynamics. This could involve performing a stability analysis of the design hybrid dynamical systems for single- and multi-AUV tracking, using for instance Lyapunov stability analysis for hybrid systems. The decision to design the controllers as hybrid dynamical systems rather than simpler, fully discrete systems, e.g., a finite state machine, was largely driven by this potential for further analysis of the system dynamics.

Moreover, the requirements related to collision avoidance can likely be relaxed to achieve

better performance. In the appended papers, the anti-collision domain is defined as a sphere that the ASV should stay out of. The sphere's radius is based on the furthest distance that the AUV is expected to travel between consecutive USBL fixes. However, this distance is in reality largely dependent on heading and speed; the AUV can travel significantly further in the forward direction than backwards, upwards, or downwards. Tools such as reachability analysis and level-set analysis can be used to define smaller, more realistic anti-collision domains that relax the conservative requirement of the sphere.

Another area of further work is more advanced selection of tuning parameters for the controllers. Further and more extensive field trials will allow for more trial-and-error testing of various values, but other methods should also be considered. For instance, a dynamic selection scheme for the key tuning parameters could be implemented. The simplification $\varepsilon_- = \varepsilon_+ =: \varepsilon$ could also be relaxed to allow for more flexibility in determining the controller behavior.

Furthermore, a state estimator can be implemented to estimate AUV states between position fixes. One example of such an estimator is a Kalman filter. This could possibly contribute to improving ASV tracking performance.

Additionally, expanding the robotic organization presented here is an area of further work. For instance, the role and potential of small satellites and UAVs can be investigated more closely. This is likely to significantly improve the mapping capabilities of the system, but will also come with other emergent risks that must be managed.

Lastly, further work can be focused on re-evaluating to strengthen or debunk some of the basic assumptions that this thesis is based on. Many researchers are turning their eyes on the field of robotic organizations and multi-agent control, and it is a field of rapid development. In coming years, the field is expected to see many creative and innovative solutions. This thesis has attempted to drive this development in the right direction.

Bibliography

[1] M. Aguiar, J.E. da Silva and J.B. de Sousa. 'Minimal time delivery of multiple robots'. In: *59th IEEE Conference on Decision and Control - CDC'2020* (2020), pp. 1572–1577 (cit. on pp. 1, 5, 12).

[2] N. P. Ventikos, A. Chmurski and K. Louzis. 'A systems-based application for autonomous vessels safety: Hazard identification as a function of increasing autonomy levels'. In: *Safety Science* 131 (2020) (cit. on pp. 1, 6).

[3] I.B. Utne, B. Rokseth, A.J. Sørensen and J.E. Vinnem. 'Towards supervisory risk control of autonomous ships'. In: *Reliability Engineering and System Safety* 196 (2020) (cit. on pp. 1, 6).

[4] R. Costanzi et al. 'Interoperability Among Unmanned Maritime Vehicles: Review and First In-field Experimentation'. In: *Frontiers in Robotics and AI* 7 (2020) (cit. on pp. 1, 8, 12).

[5] S. Russel and P. Norvig. *Artificial intelligence, A modern approach*. 3rd. Pearson, 2010 (cit. on pp. 1, 5).

[6] M. Ludvigsen and A.J. Sørensen. 'Towards integrated autonomous underwater operations for ocean mapping and monitoring'. In: *Annual Reviews in Control* 42 (2016), pp. 145–157 (cit. on pp. 1, 8, 12, 14, 17–20).

[7] Å. Eek, K.Y. Pettersen, E.M. Ruud and T.R. Krogstad. 'Formation path following control of underactuated USVs'. In: *European Journal of Control* 62 (2021), pp. 171–184 (cit. on pp. 1, 8, 12).

[8] A.J. Sørensen, M. Ludvigsen, P. Norgren, Ø. Ødegård and F. Cottier. 'Sensor-Carrying Platforms'. In: *POLAR NIGHT Marine Ecology*. Springer, 2020. Chap. 9, pp. 241–275 (cit. on pp. 1, 6, 9, 10, 13, 20, 24).

[9] I.B. Utne, A.J. Sørensen and I. Schjølberg. 'Risk Management of Autonomous Marine Systems and Operations'. In: *Proceedings of the International Conference on Ocean, Offshore and Arctic Engineering, OMAE2017-61645* (2017) (cit. on pp. 5–7).

[10] National Institute of Science and Technology. *Autonomy Levels for Unmanned Systems (ALFUS) Framework*. Volume I: Terminology, version 2, NIST Special Publication 1011-I-2.0. Bantam, 2008. URL: https://nvlpubs.nist.gov/nistpubs/Legacy/SP/nistspecialpublication1011-I-2.0.pdf (cit. on pp. 5, 6).

[11] M. Vagia, A.A. Transeth and S.A. Fjerdingen. 'A literature review on the levels of automation during the years. What are the different taxonomies that have been proposed?' In: *Applied Ergonomics* 53 (2016), pp. 190–202 (cit. on p. 6).

[12] I.B. Utne. *NTNU Centre for Autonomous Marine Operations and Systems: - Shipping and digitalization.* NTNU AMOS. 18th Oct. 2017. URL: https://www.sintef.no/globalassets/project/hfc/documents/9-utne-amos-autonomy-oct-2017-distr-2.pdf/ (visited on 8th Nov. 2021) (cit. on pp. 6, 7).

[13] C.A. Harris, A.B. Phillips, C. Dopico-Gonzales and M.P. Brito. 'Risk and Reliability Modelling for Multi-Vehicle Marine Domains'. In: *2016 IEEE/OES Autonomous Underwater Vehicles (AUV)* (2016), pp. 286–293 (cit. on pp. 6, 13, 22, 23).

[14] A.J. Sørensen and M. Ludvigsen. *Next generation of autonomous systems.* NTNU AMOS. 16th Sept. 2019. URL: https://www.gceocean.no/media/2648/190916-subsea-innovation-day_ntnu-amos.pdf (visited on 26th May 2022) (cit. on pp. 8, 9).

[15] M. Ludvigsen et al. 'Use of an Autonomous Surface Vehicle reveals small-scale diel vertical migrations of zooplankton and susceptibility to light pollution under low solar irradiance'. In: *Science Advances* 4 (2018), pp. 1–8 (cit. on p. 11).

[16] A. Dias et al. 'ROSM - Robotic Oil Spill Mitigations'. In: *OCEANS 2019 - Marseille* (2019) (cit. on p. 11).

[17] S. Brizzolara and R.A. Brizzolara. 'Autonomous Sea Surface Vehicles'. In: *Springer Handbook of Ocean Engineering.* Springer, 2016. Chap. 13, pp. 323–340 (cit. on p. 11).

[18] T.O. Fossum, P. Norgren, I. Fer, F. Nilsen, Z.C. Koenig and M. Ludvigsen. 'Adaptive Sampling of Surface Fronts in the Arctic Using an Autonomous Underwater Vehicle'. In: *IEEE Journal of Ocean Engineering* 46 (4 2021), pp. 1155–1164 (cit. on p. 12).

[19] I. Belkin, J.B. de Sousa, J. Pinto, R. Mendes and F. López-Castejón. 'Marine robotics exploration of a large-scale open-ocean front'. In: *IEEE/OES Autonomous Underwater Vehicle Workshop* (2019) (cit. on p. 12).

[20] Y. Zhang et al. 'Autonomous Tracking and Sampling of the Deep Chlorophyll Maximum Layer in an Open-Ocean Eddy by a Long-Range Autonomous Underwater Vehicle'. In: *IEEE Journal of Oceanic Engineering* 45 (4 2019), pp. 1308–1321 (cit. on p. 12).

[21] K. Lima et al. 'Comprehensive Habitat Mapping of a Littoral Marine Park'. In: *OCEANS 2019 - Marseille* (2019) (cit. on p. 12).

[22] A.G. Rumson. 'The application of fully unmanned robotic systems for inspection of subsea pipelines'. In: *Ocean Engineering* 235 (2021) (cit. on pp. 12, 13).

[23] Y. Yang, F. Khan, P. Thodi and R. Abbassi. 'Corrosion induced failure analysis of subsea pipelines'. In: *Reliability Engineering and System Safety* 159 (2017), pp. 214–222 (cit. on p. 12).

[24] I. Nilssen, Ø. Ødegård, A.J. Sørensen, G. Johnsen, M.A. Moline and J. Berge. 'Integrated environmental mapping and monitoring, a methodological approach to optimise knowledge gathering and sampling strategy'. In: *Marine Pollution Bulletin* 96 (2015), pp. 374–383 (cit. on p. 12).

[25] Z. Peng, J. Wang, D. Wang and Q.-L. Han. 'An Overview of Recent Advances in Coordinated Control of Multiple Autonomous Surface Vehicles'. In: *IEEE Transactions on Industrial Informatics* 27 (2021), pp. 732–745 (cit. on pp. 12, 13).

[26] E. Fiorelli, N.E. Leonard, P. Bhatta, D. Paley, R. Bachmayer and D.M. Fratantoni. 'Multi-AUV Control and Adaptive Sampling in Monterey Bay'. In: *IEEE/OES Autonomous Underwater Vehicles* (2004), pp. 134–147 (cit. on p. 12).

[27] C.C. Sotzig and D.M. Lane. 'Improving the coordination efficiency of limited-communication multi–autonomus underwater vehicle operations using a multiagent architecture'. In: *Journal of Field Robotics* 27 (4 2010), pp. 412–429 (cit. on p. 12).

[28] C. Wang, L. Wei, Z. Wang, M. Song and N. Mahmoudian. 'Reinforcement Learning-Based Multi-AUV Adaptive Trajectory Planning for Under-Ice Field Estimation'. In: *Sensors* 18 (4 2018) (cit. on p. 12).

[29] Z. Peng, L. Liu and J. Wang. 'Output-Feedback Flocking Control of Multiple Autonomous Surface Vehicles Based on Data-Driven Adaptive Extended State Observers'. In: *IEEE Transactions on Cybernetics* 51 (9 2021), pp. 4611–4622 (cit. on p. 13).

[30] J. Kim. 'Multi-robot global sonar survey in the presence of strong currents'. In: *Ocean Engineering* 188 (2019), pp. 278–282 (cit. on p. 13).

[31] J. Villa, J. Aaltonen, S. Virta and K.T. Koskinen. 'A Co-Operative Autonomous Offshore System for Target Detection Using Multi-Sensor Technology'. In: *Remote Sensing* 12 (2020) (cit. on p. 13).

[32] R. Costanzi, D. Fenucci, V. Manzari, A. Caiti A and R. Petroccia. 'Towards an autonomous underwater vehicles test range: At-sea experimentation of bearing-only tracking algorithms'. In: *Annual Reviews in Control* 46 (2018), pp. 304–314 (cit. on p. 13).

[33] G. Salavasidis, C. Harris, E. Rogers and A. Phillips. 'Improving the coordination efficiency of limited-communication multi–autonomus underwater vehicle operations using a multiagent architecture'. In: *Towards Autonomous Robotic Systems (TAROS)* (2016) (cit. on pp. 13, 22).

[34] P. Norgren, M. Ludvigsen, T. Ingebregtsen and V.E. Hovstein. 'Tracking and remote monitoring of an autonomous underwater vehicle using an unmanned surface vehicle in the Trondheim fjord'. In: *OCEANS 2015 - MTS/IEEE Washington* (2015) (cit. on pp. 13, 22).

[35] A.G. Rumson. 'Mapping the deep ocean with multiple AUVs'. In: *Hydro International* 22 (2 2018), pp. 24–26 (cit. on p. 13).

[36] M.F. Fallon, G. Papadopoulos, J.J. Leonard and N.M: Patrikalakis. 'Cooperative AUV Navigation using a Single Maneuvering Surface Craft'. In: *International Journal of Robotics Research* 29 (12 2010), pp. 1461–1474 (cit. on p. 13).

[37] A. Vasilijević, Đ. Nađ, F. Mandić, N. Mišković and Z. Vukić. 'Coordinated navigation of surface and underwater marine robotic vehicles for ocean sampling and environmental monitoring'. In: *IEEE/ASME Transactions on Mechatronics* 22 (3 2017) (cit. on p. 14).

[38] Y. Zhang et al. 'A system of coordinated autonomous robots for Lagrangian studies of microbes in the oceanic deep chlorophyll maximum'. In: *Science Robotics* 6 (50 2021) (cit. on p. 14).

[39] G. Antonelli et al. 'ISME activity on the use of Autonomous Surface and Underwater Vehicles for acoustic surveys at sea'. In: *ACTA IMEKO* 7 (2 2018), pp. 24–31 (cit. on p. 14).

[40] J.S. Willners, L. Toohey and Y. Petillot. 'Sampling-Based Path Planning for Cooperative Autonomous Maritime Vehicles to Reduce Uncertainty in Range-Only Localization'. In: *IEEE Robotics and Automation Letters* 4 (4 2019) (cit. on p. 14).

[41] Ø. Sture, P. Norgren and M. Ludvigsen. 'Trajectory Planning for Navigation Aiding of Autonomous Underwater Vehicles'. In: *IEEE Access* 8 (2020), pp. 116586–116604 (cit. on p. 14).

[42] T.I. Fossen. *Handbook of Marine Craft Hydrodynamics and Motion Control*. John Wiley & Sons, 2011 (cit. on p. 14).

[43] D.E. Sgarioto. 'Control system design and development for the REMUS autonomous underwater vehicle'. In: (2007) (cit. on p. 15).

[44] *Global Navigation Satellite System (GNSS)*. Princeton University. URL: https://www.princeton.edu/~alaink/Orf467F07/GNSS.pdf (visited on 22nd Nov. 2021) (cit. on p. 17).

[45] J.J. Leonard and A. Bahr. 'Autonomous Underwater Vehicle Navigation'. In: *Springer Handbook of Ocean Engineering*. Springer, 2016. Chap. 14, pp. 341–358 (cit. on pp. 17–21).

[46] J.E. Bremnes, A.H. Brodtkorb and A.J. Sørensen. 'Hybrid Observer Concept for Sensor Fusion of Sporadic Measurements for Underwater Navigation'. In: *International Journal of Control, Automation and Systems* 19(1) (2021), pp. 137–144 (cit. on pp. 17, 18, 20).

[47] K. Gade. *Inertial Navigation — Theory and Applications*. 31st Jan. 2018. URL: https://www.navlab.net/Publications/Inertial_Navigation_-_Theory_and_Applications.pdf (visited on 9th Dec. 2021) (cit. on p. 18).

[48] Alexander Bahr, John J. Leonard and Alcherio Martinoli. 'Dynamic positioning of beacon vehicles for cooperative underwater navigation'. In: *2012 IEEE/RSJ International Conference on Intelligent Robots and Systems* (2012), pp. 3760–3767 (cit. on p. 21).

[49] Y.T. Tan, R. Gao and M. Chitre. 'Cooperative path planning for range-only localization using a single moving beacon'. In: *IEEE Journal of Oceanic Engineering* 39 (2 2014), pp. 371–385 (cit. on p. 21).

[50] R. Goebel, R.G. Sanfelice and A.R. Teel. *Hybrid Dynamical Systems: Modeling, Stability, and Robustness*. Princeton University Press, 2012 (cit. on pp. 22, 23).

[51] M.S. Branicky. 'Studies in Hybrid Systems: Modeling, Analysis, and Control'. PhD thesis. Massachusetts Institute of Technology, 1995 (cit. on p. 23).

[52] M. Rausand and S. Haugen. *Risk Assessment – Theory, Methods, and Applications, Second Edition*. Wiley-Blackwell, 2020 (cit. on p. 23).

[53] Odd Ivar Haugen. *Safety assurance of complex systems Part 1: Complexity*. 4th Dec. 2019. URL: https://www.dnv.com/Publications/safety-assurance-of-complex-systems-part-1-complexity-165015 (visited on 27th May 2022) (cit. on p. 24).

[54] A. Sousa et al. 'LAUV: The Man-Portable Autonomous Underwater Vehicle'. In: *IFAC Proceedings Volumes* 45 (5 2012), pp. 268–274 (cit. on pp. 26, 28).

[55] J. Pinto et al. 'Implementation of a Control Architecture for Networked Vehicle Systems'. In: *IFAC Proceedings Volumes* 45 (2 2012), pp. 100–105 (cit. on p. 28).

[56] M. Faria et al. 'Coordinating UAVs and AUVs for oceanographic field experiments: Challenges and lessons learned'. In: *Proceedings - IEEE International Conference on Robotics and Automation* (2014), pp. 6606–6611 (cit. on p. 28).

Appendices

Two papers that were written as part of the work on this master's thesis are appended below.

Paper 1

Hybrid Tracking Controller for an ASV Providing Mission Support for an AUV

Torbjørn R. Fyrvik, Jens E. Bremnes, Asgeir J. Sørensen

Peer reviewed and to be submitted at the 14th IFAC Conference on Control Applications in Marine Systems, Robotics and Vehicles (CAMS2022)
Kongens Lyngby, Denmark

Hybrid Tracking Controller for an ASV Providing Mission Support for an AUV

Torbjørn R. Fyrvik * **Jens E. Bremnes** * **Asgeir J. Sørensen** *

* *Centre for Autonomous Marine Operations and Systems (AMOS), Department of Marine Technology, Norwegian University of Science and Technology (NTNU), Otto Nielsens veg 10, 7491 Trondheim, Norway (e-mails: torbjofy@stud.ntnu.no, jens.e.bremnes@ntnu.no, asgeir.sorensen@ntnu.no).*

Abstract: Autonomous underwater vehicles (AUVs) rely on surface support for communication with operators and position fixes to bound inertial navigation errors. By installing an acoustic modem on an autonomous surface vehicle (ASV), the ASV can carry out these tasks, replacing more expensive and less flexible manned research vessels. This paper proposes a hybrid tracking controller for an ASV providing mission support for an AUV. The proposed controller keeps the ASV in a donut-shaped safety domain about the AUV defined by the risk of collision (inner boundary) and the risk of communication loss (outer boundary). At the same time, the hybrid controller reduces power consumption and acoustic signal noise by going into standby mode when it is within the safety domain. Results from a simulation study and field trials are presented to demonstrate and validate the controller's performance. The results show that the controller performed well in the tested cases.

Keywords: Unmanned marine vehicles, autonomous surface vehicles, autonomous underwater vehicles, coordinated control, hybrid dynamical systems, collision avoidance

1. INTRODUCTION

Recent years have seen large developments in field robotics, enabled by new and improved sensor, computer, communication, and navigation technologies. Reduced dependency on human operators leads to increased human safety and has proven to be cost-efficient and more environmentally friendly (Ventikos et al., 2020; Utne et al., 2020). The transition towards higher levels of autonomy is also underway in the maritime industry, where agents with some degree of autonomy have gained significant traction (Ludvigsen and Sørensen, 2016). Two examples of such agents are autonomous surface vehicles (ASVs) and autonomous underwater vehicles (AUVs). ASVs are surface-going sensor-carrying platforms, while AUVs are sensor-carrying platforms with possibilities of under- and on-surface operation.

Some tasks are too complex for single agents to solve alone, and there is increased focus on combining multiple marine agents in robotic organizations. Robotic organizations can become powerful systems for mapping and monitoring the marine environment (Sørensen et al., 2020). One such system is an ASV aiding one or several AUVs in operation, replacing the manned support vessel that AUVs rely on. Taking the role as unmanned support vessels, ASVs can serve as communication hubs, relaying information between the AUV and the control center.

Without external aiding, AUVs rely on inertial navigation when submerged in water, leading to an unbounded error growth. External aiding can be provided by GPS on the surface or acoustic signals underwater (Ludvigsen and Sørensen, 2016). With ultra-short baseline (USBL) acoustic communication, a transducer mounted on an ASV can detect the range and bearing to an acoustic modem on the AUV, thus augmenting the inertial navigation error. USBL positioning is limited to the acoustic communication range, which depends largely on water conditions like salinity, temperature, and turbidity (Sørensen et al., 2020).

Several research groups have deployed teams of ASVs and AUVs under coordinated control. Norgren et al. (2015) used an ASV and an AUV to map an area to search for a World War II airplane wreck. The ASV maintained a constant distance and bearing relative to the estimated AUV position and orientation, functioning as a communication hub for the AUV. Vasilijević et al. (2017) presented a coordinated navigation system for an ASV and an AUV for ocean sampling and environmental monitoring. In these field trials, the ASV performed station-keeping in the middle of the AUV's operational area, which was small enough that the vehicles could communicate acoustically throughout the operation. Zhang et al. (2021) used an ASV as the communication hub for two AUVs to provide situational awareness and, if necessary, enable intervention. Other research groups have deployed larger fleets of marine robots, such as Belkin et al. (2019), Antonelli et al. (2018) and Rumson (2018).

However, several challenges remain unanswered, such as: How can an ASV adequately track an AUV while meeting operational constraints? Which risks emerge from combining these vehicles in a robotic organization, and how can they be mitigated for? The present paper attempts to answer these research questions.

The main scientific contribution of the work presented here is the development of a tracking controller for an ASV following an AUV. This is useful for aiding an AUV with USBL position fixes, as well as functioning as a communication gateway between the AUV and human operators. The tracking controller has collision avoidance properties and ensures communication between the vehicles is maintained, allowing the ASV to perform its gateway role while reducing risks. Moreover, formulating the control algorithm as a hybrid dynamical system represents another scientific contribution.

The paper is outlined as follows: Section 2 describes the system in more detail and presents the ASV tracking controller as a hybrid dynamical system, Section 3 introduces the experimental setup and discusses the results, while Section 4 concludes the paper and suggests areas of future work.

2. METHODOLOGY

2.1 Hybrid Dynamical Systems

The proposed tracking controller is modeled as a hybrid dynamical system based on the framework presented by Goebel et al. (2012). Such systems have both continuous-time and discrete-time dynamics, and their general model is expressed as

$$\mathcal{Q} = \begin{cases} \dot{x} \in \mathcal{F}(x) & \text{for } x \in \mathcal{C}, \\ x^+ \in \mathcal{G}(x) & \text{for } x \in \mathcal{D}, \end{cases} \tag{1}$$

where $\mathcal{C} \in \mathbb{R}^n$ is the flow set, $\mathcal{F} : \mathbb{R}^n \rightrightarrows \mathbb{R}^n$ is the flow map, $\mathcal{D} \in \mathbb{R}^n$ is the jump set, and $\mathcal{G} : \mathbb{R}^n \times \mathbb{R}^m \rightrightarrows \mathbb{R}^n$ is the jump map. The flow map $\mathcal{F}$ describes how the state x is allowed to change continuously when the state belongs to the flow set $\mathcal{C}$. Similarly, the jump map $\mathcal{G}$ describes how the state is allowed to change discretely when it belongs to the jump set $\mathcal{D}$.

The controller makes use of a simplified kinematic model for marine vessels described in detail in Fossen (2011). The kinematic relationship between velocities in the Earth-fixed ($\dot{\eta} \in \mathbb{R}^6$) and body-fixed ($\nu \in \mathbb{R}^6$) reference frames is expressed as

$$\dot{\eta} = \begin{bmatrix} J_1(\Theta) & 0_{3\times3} \\ 0_{3\times3} & J_2(\Theta) \end{bmatrix} \nu = J(\Theta)\nu, \tag{2}$$

where $J(\Theta) \in \mathbb{R}^{6\times6}$ is Euler angle transformation matrix. In this paper, the horizontal position component of η will be represented as $\xi = [N \;\; E]^T$, where N and E are North and East components, while ψ is the heading of the vessel relative to North. Subscript wp indicates the desired state defined by a waypoint.

2.2 Safety Domain

For the ASV to function as a communication link between the control center and the AUV, as well as supporting the AUV with navigation, USBL communication between the vehicles must be maintained. Losing communication between the vessels represents a significant system hazard, and the ASV must stay within acoustic reach of the AUV during the whole operation to reduce the risk of this hazard. Therefore, the USBL's maximum range defines an outer boundary of the ASV's safety domain, represented as a sphere centered at the AUV with radius r_{out}.

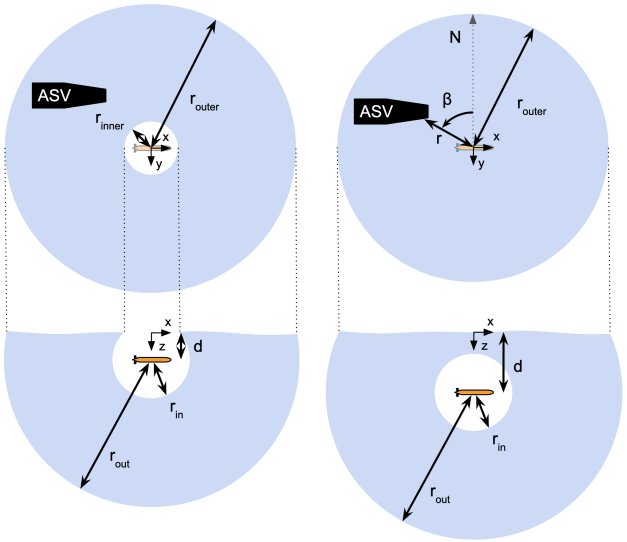

(a) $d < r_{in}$. (b) $d > r_{in}$.

Fig. 1. ASV safety domain for AUV at depth d. The bottom part of each subfigure illustrates the spheres around the AUV, while the top parts show their translations to the surface domain. For simplicity it is here assumed that the acoustic signal is not significantly affected by the surface.

However, there is often large variability in the maximum acoustic range due to water conditions and other hard-to-predict factors. Moreover, it is common that USBL fixes are not properly transmitted between the modems, meaning there is a risk that the acoustic communication is only sporadic at times. For these reasons, a safety factor α_{outer} is incorporated into the USBL modem's rated maximum range, r_0, to obtain a safety margin as per

$$r_{out} = \frac{1}{\alpha_{outer}} r_0. \tag{3}$$

At the same time, the safety domain also has an inner boundary defined by another hazard: collision between the two vehicles. The ASV must maintain a minimum safety distance to the AUV to lower the risk of this hazard. Thus, the inner boundary of the safety domain is defined by a sphere centered at the AUV with radius equal to the required safety distance between the vehicles, r_{in}.

To avoid collision in the worst-case scenario, this safety distance should be as large as the maximum expected relative displacement of the ASV relative to the AUV between two USBL fixes. Like the outer boundary, a safety factor α_{inner} is incorporated into the USBL update period, so the inner safety domain boundary is expressed as

$$r_{in} = \alpha_{inner} T_0 \cdot \dot{r}_{max}, \tag{4}$$

where T_0 is the rated USBL update period and $\dot{r}_{max}$ is the maximum relative speed between the ASV and the AUV. The safety factor incorporates uncertainty in the USBL update period and inertia in the ASV's dynamics. By choosing a sufficiently large α_{inner}, the risk of collision is kept low throughout the mission.

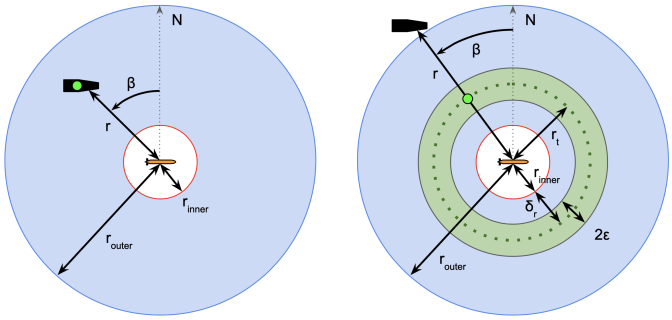

(a) Standby ($\mathcal{Q}_1$). The ASV is not using thrusters to reduce power consumption and acoustic noise from propeller.

(b) Transit ($\mathcal{Q}_2$). The ASV breaches safety domain and initiates transit towards or away from the AUV.

Fig. 2. Hybrid controller behavior. The green dots indicate ASV waypoints (WPs). When the ASV reaches the waypoint after transit, it goes back to standby mode. The dark green dotted circle is the target circle of radius $r_t = r_{inner} + \delta_r$ with the target domain indicated by the green donut around the target circle.

As seen in Fig. 1, the spheres about the AUV transform into a donut-shaped safety domain on the surface. The inner boundary of the donut is at distance r_{inner} from the AUV's position in the horizontal plane, while the outer boundary is at distance r_{outer}. For AUV depth d,

$$\begin{aligned} r_{inner} &= \begin{cases} \sqrt{r_{in}^2 - d^2} & \text{for } d \leq r_{in} \\ 0 & \text{for } d > r_{in} \end{cases} \\ r_{outer} &= \begin{cases} \sqrt{r_{out}^2 - d^2} & \text{for } d \leq r_{out} \\ 0 & \text{for } d > r_{out} \end{cases} \end{aligned} \tag{5}$$

Note that if $d > r_{in}$, the safety domain is simply a circle because the inner boundary does not touch the surface, as shown in Fig. 1b. Similarly, if $d > r_{out}$, the safety domain is non-existent on the surface, so the AUV should not dive that deeply.

The radial distance (r) and bearing (β) from the AUV to the ASV are defined as

$$\begin{aligned} r &= \sqrt{(N_{asv} - N_{auv})^2 + (E_{asv} - E_{auv})^2}, \\ \beta &= atan2\left(E_{asv} - E_{auv}, N_{asv} - N_{auv}\right). \end{aligned} \tag{6}$$

2.3 Hybrid Controller

The objective of the controller is to keep the ASV within the safety domain. However, excessive ASV control action should also be avoided to improve performance and reduce power consumption. In addition, the noise of the ASV's propeller may significantly deteriorate acoustic signals. Therefore, the tracking controller is implemented as a hybrid controller capable of switching between a standby mode and a transit mode. The controller behavior is presented graphically in Fig. 2.

The hybrid controller consists of a zero-thrust standby controller ($\mathcal{Q}_1$) and a set-point controller ($\mathcal{Q}_2$).

$\mathcal{Q}_1$ is the preferred controller when the ASV is within the safety domain (Fig. 2a). To prevent unnecessary control action, the ASV is set to standby in this area, meaning the thrusters are turned off while sensors remain on to monitor the operation.

If the ASV leaves the safety domain, however, control action is necessary. In this case, control is transferred to $\mathcal{Q}_2$, which updates the ASV's waypoint to the closest point on the target circle. This target circle, represented by the dark green line in Fig. 2, is expressed as

$$\xi_{wp,asv} = \xi_{auv} + r_t \begin{bmatrix} cos(\beta_{wp}) \\ sin(\beta_{wp}) \end{bmatrix}, \tag{7}$$

where β_{wp} is the bearing from the AUV towards the desired ASV position on the target circle. $\beta_{wp} = \beta$ represents the point on the target circle closest to the ASV. The radius of the target circle, r_t, is defined as

$$r_t = r_{inner} + \delta_r, \tag{8}$$

where δ_r is a tuning parameter that defines the margin from the safety domain's inner boundary to the target circle. When the ASV is tracking the AUV ($\mathcal{Q}_2$), a small δ_r means that the ASV moves closer to the AUV before changing to standby ($\mathcal{Q}_1$), which likely decreases the chance of leaving the outer boundary of the safety domain again. However, a small δ_r also comes with a higher risk of breaching the inner boundary.

To avoid high frequency switching between $\mathcal{Q}_1$ and $\mathcal{Q}_2$, the controller does not switch back from $\mathcal{Q}_2$ to $\mathcal{Q}_1$ until the ASV is sufficiently close to the target circle. This is quantified by the error, e, defined as

$$e = r - r_t, \tag{9}$$

which must be smaller than ε_- or ε_+, depending on the sign of e. This acceptable deviation from the target circle converts to the green target domain in Fig. 2, defined by

$$r \in [r_t - \varepsilon_-, r_t + \varepsilon_+], \tag{10}$$

where ε_- and ε_+ are tuning parameters. In this work, $\varepsilon_- = \varepsilon_+ =: \varepsilon$ is considered for simplicity. Differing values of ε_- and ε_+ can be considered in further studies. The controller accepts jumps to $\mathcal{Q}_1$ if the ASV is within the target domain, indicated by the light green area in Fig. 2.

As such, the proposed hybrid tracking controller based on the framework in (1) is formulated in (11) with subscripts 1 and 2 corresponding to $\mathcal{Q}_1$ and $\mathcal{Q}_2$, respectively. The controller state is $x = [r_{wp}, \beta_{wp}, r, \beta, q]^T$.

$$\begin{aligned} \mathcal{F}_1(x) &:= \begin{cases} \dot{r}_{wp} = \dot{r} \\ \dot{\beta}_{wp} = \dot{\beta} \\ \dot{q} = 0 \end{cases} && \text{for } x \in \mathcal{C}_1 := \\ & && \{x : q = 1\} \\ \mathcal{G}_1(x) &:= \begin{cases} r_{wp}^+ = r \\ \beta_{wp}^+ = \beta \\ q^+ = 1 \end{cases} && \text{for } x \in \mathcal{D}_1 := \\ & && \left\{ \begin{array}{l} x : |e| < \varepsilon, \\ q = 2 \end{array} \right\} \\ \mathcal{F}_2(x) &:= \begin{cases} \dot{r}_{wp} = \dot{r}_t \\ \dot{\beta}_{wp} = \dot{\beta} \\ \dot{q} = 0 \end{cases} && \text{for } x \in \mathcal{C}_2 := \\ & && \{x : q = 2\} \\ \mathcal{G}_2(x) &:= \begin{cases} r_{wp}^+ = r_t \\ \beta_{wp}^+ = \beta \\ q^+ = 2 \end{cases} && \text{for } x \in \mathcal{D}_2 := \\ & && \{x : r \notin [r_{inner}, r_{outer}]\} \end{aligned} \tag{11}$$

Once the appropriate controller has been selected in (11), the ASV waypoint is updated as per (7).

The proposed tracking algorithm relies on knowledge of the AUV's navigational states. However, the USBL communication link only provides this information sporadically. Thus, the ASV must be capable of estimating the AUV's navigational states between updates.

3. RESULTS AND DISCUSSION

3.1 Experimental Setup

To demonstrate and validate the performance of the controller, a simulation study was conducted, followed by field trials with a physical ASV and a simulated AUV.

The ASV used in the present work is a Pioner 17 from Maritime Robotics named Gretha, while the AUV is a simulated AUV modeled after a light AUV (LAUV) from OceanScan named Fridtjof.

Gretha is 5.2 m long, 2.15 m wide, has a draft of 0.3 m and weighs 810 kg. While the vehicle's rated top speed is 6 kn, its rated endurance is 24 hours at 3 kn. The on-board communication suite consists of a WiFi hotspot with more than 50 m range, LTE coverage through a 4G module, and Kongsberg MBR broadband with 15 km range. Additionally, an EvoLogics S2C R 18/34 USBL modem with range $r_0 = 3.5$ km was installed to facilitate acoustic communication with the AUV.

Fridtjof is 1.80 m long, has a diameter of 20cm and weighs 25.8 kg. The vehicle's maximum speed is 2 m/s, and the rated endurance is 8 hours at maximum speed. Fridtjof's on-board communication suite consists of a WiFi antenna with 1 km range, GSM coverage through a 3G module, and an Iridium SBD module with global coverage, as well as an underwater acoustic modem. Only the latter is used when the AUV is submerged, as the former three technologies only work in air.

When the AUV is on the surface and sufficiently close to the ASV, the vehicles communicate real-time via WiFi. When the AUV is submerged, however, they rely on the acoustic link for underwater communication. USBL position fixes are typically available every $T_0 = 5$ s, meaning communication is often limited. Moreover, experience shows that despite the 3.5 km rated range, the signal is good only up to about 500-1000 m, depending on the water conditions. It is not uncommon that signals are not properly received, especially if the distance between the acoustic modems is large or water quality is low.

The main software used for both simulations and field trials is the LSTS toolchain. This toolchain consists of DUNE on-board software,[1] Neptus command and control software,[2] and the IMC communications protocol.[3] Fridtjof is simulated in DUNE with a standard LAUV simulator, while Gretha comes with Maritime Robotics's in-house Onboard System (OBS) for control, navigation, and communication. The user interface, Maritime Robotics's version of Neptus, is called Vehicle Control Station (VCS), which has a built-in simulator for Gretha. To integrate OBS/VCS with the LSTS toolchain, a software bridge between the two interfaces was designed. The controller was implemented with Python in ROS,[4] so another software bridge was set up between IMC and ROS based on the *imc_ros_bridge* package.[5]

In the simulation study, two cases of typical AUV operation (Case 1 and Case 2) were simulated using the default LAUV simulator in DUNE, as well as the Gretha simulator in VCS. In Case 1, the AUV first does overview scans of two areas before performing closer inspection of detected areas of interest. In Case 2, the AUV continues to another area to do a third overview scan instead of performing closer inspection. AUVs normally operate on altitude control during seabed surveys, but without loss of generality, depth control is used in these test cases for simplicity. The hybrid tracking controller's performance was analyzed by running it on the ASV and studying the vehicle's resulting behavior.

After the controller was validated in numerical simulations, field trials were conducted in the Trondheimfjord in April and May 2022 with Gretha and a simulated AUV.

In Case 3, the ASV and AUV both start some distance from the operational area, which consists of a stretched-out lawnmower pattern. The length of the pattern is larger than in the simulation cases to showcase the ASV's tracking abilities. Rather than a constant altitude control law, the simulated AUV operates in the surface with a zero-depth set-point during the test to better illustrate the controller's behavior. This gives a worst-case condition with respect to the size of the anti-collision domain.

In Case 4, the AUV actively tries to breach the inner boundary, to generate challenging scenarios, by moving in an unpredictable manner, often straight towards the ASV. In essence, the AUV behaves as an adversary or a pursuer. Although this behavior is unlikely during nominal operation, it is difficult to predict how an autonomous vehicle will behave, for instance if it follows an adaptive sampling control law. Therefore, Case 4 is mainly focused on how the hybrid tracking controller prevents possibly dangerous situations when the AUV operates with high levels of autonomy. Like in Case 3, the AUV remains on the surface in Case 4.

Since the AUVs are simulated, the ASV has continuous knowledge of their navigational states. During operations with physical AUVs, it is assumed that continuous knowledge of AUVs' navigational states is made possible with a state estimator. This is out of scope of this paper and is thus not implemented here.

The testing cases for the field trials are simpler than those used in simulation because of the unpredictable and unforgiving environment of the ocean. Therefore, results from simulations and field trials are intended to complement each other.

3.2 Tuning Parameters

Several tests were run to determine suitable values for the tuning parameters. The values that yielded good performance in simulations were modified during field trials to achieve better performance. Table 1 summarizes

[1] https://github.com/LSTS/dune
[2] https://github.com/LSTS/neptus
[3] https://lsts.pt/docs/imc/master/index.html
[4] https://www.ros.org
[5] https://github.com/smarc-project/imc_ros_bridge

the numerical values, and the text below justifies the selection.

Table 1: Tuning Parameters.

Parameter	Simulations	Field Trials
α_{outer}	11.7	17.5
α_{inner}	5	5
δ_r	125 m	20 m
ε	30 m	10 m

The selection of domain-defining tuning parameters for simulations was based on a priori knowledge of the system. Firstly, the inner boundary safety factor was set to $\alpha_{inner} = 3$, yielding an inner boundary of the safety domain ($r_{inner} = 30$ m), which prevented collision in the worst-case scenario. Secondly, he outer boundary safety factor was set to $\alpha_{outer} = 11.7$, yielding $r_{outer} = 300$ m, which maintained reliable and accurate USBL fixes throughout the safety domain, while minimizing control action and consequently propeller usage. Thirdly, the margin from r_{inner} to the target circle was set to $\delta_r = 125$ m, to achieve a target circle that was approximately in the middle of the safety domain. Lastly, the acceptable distance to the target circle before changing to standby mode was set to $\varepsilon = 30$ m.

While yielding promising results in the simulations, the tuning parameters had to be adjusted during field trials for improved performance. Since the dynamics of the ASV were found to be much slower than those of the ASV simulator used during simulation-based testing, the inner boundary of the safety domain was increased to $\alpha_{inner} = 5$, giving $r_{inner} = 50$ m. Moreover, since the ASV was significantly slower than its rated top speed ($u_{max,test} = 4.9$ kn vs. $u_{max,rated} = 6$ kn), the safety factor for the safety domain's outer boundary had to be increased to $\alpha_{outer} = 17.5$, giving $r_{outer} = 200$ m. This was for the ASV to quickly reach the target circle during tracking, even with the AUV moving away from the ASV. For the ASV to remain closer to the AUV, the margin from r_{inner} to the target circle was reduced to $\delta_r = 20$ m, giving a target circle radius r_t ranging from 20 m if the AUV is deeply submerged to 70 m if the AUV is on the surface. The acceptable distance to the target circle before jumping to standby mode was reduced to $\varepsilon = 10$ m to make a smaller target domain, appropriate for a target circle closer to the safety domain's inner boundary.

3.3 Discussion

Fig. 3 shows how, despite the AUV's large operational area, the ASV does not move much in simulated Case 1. While the AUV travels 4.25 km, the ASV moves less than 620 m during the entire simulation, which is only 15% of the AUV's traveled distance. Moreover, the ASV is in standby mode for 2891 s (89% of simulation), while it is in transit mode for only 357 s (11% of simulation, 28 s collision avoidance, 329 s tracking). This is largely because each overview scan is small enough that the ASV stays mostly within the safety domain. Such behavior is beneficial because it reduces wear and tear on the propulsion system, lowers energy usage, and improves the acoustic environment. Fig. 4 helps explain how the ASV can stay mostly stationary in standby mode. Until $t = 835$ s, the

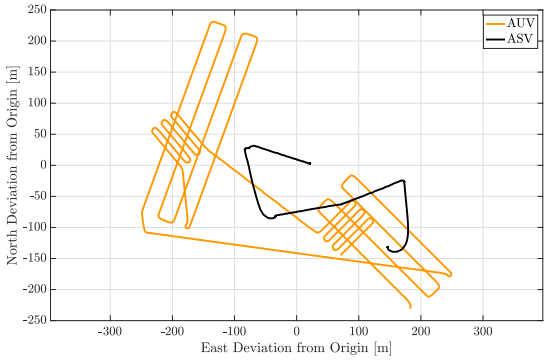

Fig. 3. Case 1: North and East movement of the two vehicles relative to the origin, defined as the center point of the operation.

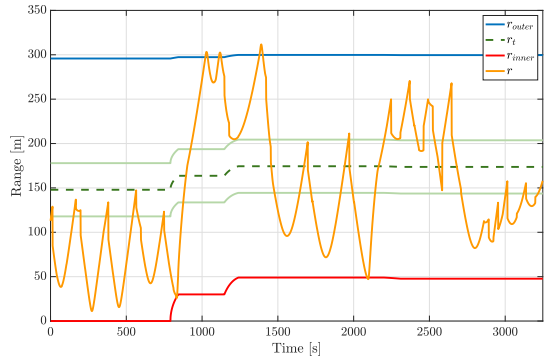

Fig. 4. Case 1: Time development of the range between the ASV and the AUV (r) compared to the radii of the outer safety boundary (r_{outer}), the target circle (r_t) surrounded by the target domain boundaries in lighter green, and the inner boundary (r_{inner}).

ASV is drifting in the middle of the AUV's lawnmower path, with the AUV sufficiently submerged that collision avoidance is not necessary. However, when the AUV transits to the Western part of its operational area, collision avoidance is initiated when the ASV breaches the inner boundary at $t = 835$ s, before tracking is initiated when the ASV breaches the outer boundary at $t = 1022$ s and again at $t = 1378$ s. One more collision avoidance is required at $t = 2095$ s, but apart from that the ASV is in standby mode.

Since the AUV transits to a different area for the third overview scan, the ASV has to move further in Case 2, as seen in Fig. 5. The AUV moves 4.99 km, while the ASV travels 1.19 km during the 1-hour simulation. Although the ASV does more tracking than in Case 1, the total distance traveled is still only 24% of that of the AUV, confirming that the ASV moves conservatively. This is validated by Fig. 6, which shows the ASV-AUV range compared to the boundaries of the safety domain. For most of the operation, the ASV is drifting within the safety domain; it spends 3115 s (81% of simulation) in standby mode and only 714 s (19% of simulation) in transit mode (680 s tracking and 34 s collision avoidance). Tracking is initiated at $t = 1240$ s, 2325 s, and 2930 s, and collision avoidance at $t = 2150$ s, and 3200 s, but the ASV quickly moves to the target domain to re-enter standby mode every time.

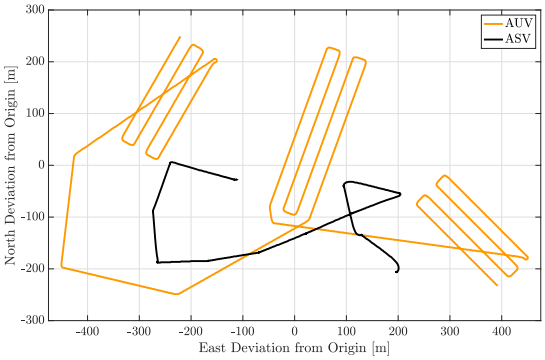

Fig. 5. Case 2: North and East movement of the two vehicles relative to the origin, defined as the center point of the operation.

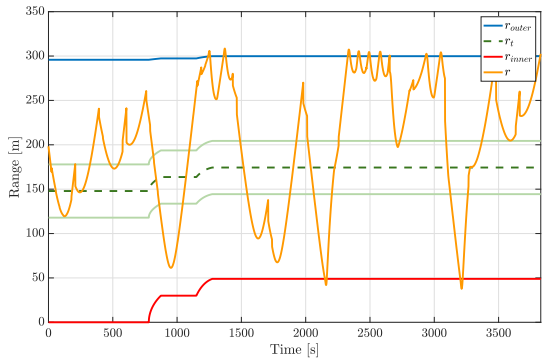

Fig. 6. Case 2: Time development of the range between the ASV and the AUV (r) compared to the radii of the outer safety boundary (r_{outer}), the target circle (r_t) surrounded by the target domain boundaries in lighter green, and the inner boundary (r_{inner}).

Like in Case 1, Case 2 shows that the hybrid tracking controller maintains a low risk of both collision and loss of communication, while not using excessive control. The ability to move autonomously without prior knowledge of the AUV's planned route makes the controller applicable to a range of operational types.

Moving onto the results from field trials, the North and East movement of both vehicles during Case 3 is presented in Fig. 7. Like in the simulated cases, the ASV travels significantly shorter than the AUV by not following the underwater vehicle to the extremities of the operation. The total distance traveled by the AUV in Case 3 is 1.98 km, while the ASV travels 1.68 km, or 85% of that of the AUV.

Fig. 8 explains the ASV's movement in Case 3 in more detail. Corrective action is taken quickly when the AUV breaches the safety domain, thus initiating a collision avoidance maneuver, which limits the range to the interval $r \in [17 \text{ m}, 233 \text{ m}]$. The ASV maintains safe operation without excessive control action, as verified by the total time spent in each operation: 798 s (53%) in standby mode and 702 s (47%) in transit mode (633 s tracking and 69 s collision avoidance). The portion spent in transit is larger than for the simulated cases because of the layout of the AUV's operational area, and since the outer boundary of

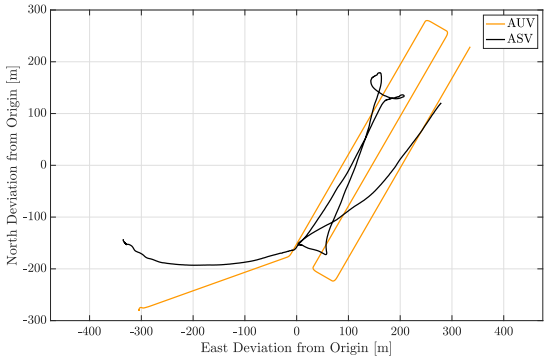

Fig. 7. Case 3: North and East movement of the two vehicles relative to the origin, defined as the center point of the operation.

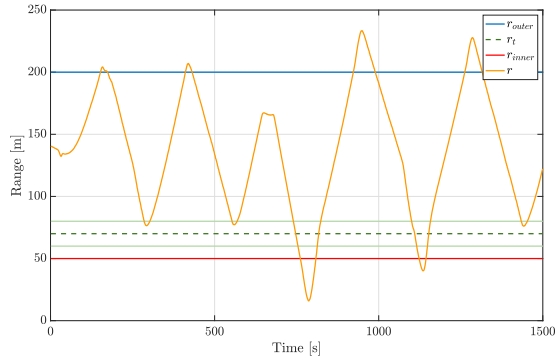

Fig. 8. Case 3: Time development of the range between the ASV and the AUV (r) compared to the radii of the outer safety boundary (r_{outer}), the target circle (r_t) surrounded by the target domain boundaries in lighter green, and the inner boundary (r_{inner}).

the safety domain was reduced to 200 m, with the target circle closer to the inner boundary.

As for Case 4, Fig. 9 shows how the ASV repeatedly breaches the safety domain's inner boundary, each time initiating a collision avoidance maneuver. Even with the AUV moving straight towards the ASV at maximum speed, it was not possible to obtain a range smaller than $r = 15.5$ m at any point during the test. This verifies the ASV's collision avoidance properties. Like in Case 3, the corrective action in Case 4 is also efficient, with only 409 s (33%) spent in transit mode (232 s tracking and 177 s collision avoidance), compared to 833 s (67%) in standby mode.

For closer inspection of the behavior seen in Fig. 9, four snapshots of the vehicles during the collision avoidance period $t \in [\ 98 \text{ s}, 235 \text{ s}]$ are presented in Fig. 10. The first snapshot (Fig. 10a) shows the ASV in collision avoidance at $t = 120$ s. As seen in Fig. 9, the ASV reaches the target domain and enters standby mode at $t = 88$ s. Because of the ASV's inertia, the vehicle is still drifting towards the AUV when collision avoidance is initiated at $t = 98$ s. Thus, it takes another 22 s until the ASV has turned around and started moving away from the AUV at $t = 120$ s, as seen in Fig. 10b, reaching the minimum range $r = 15.5$ m.

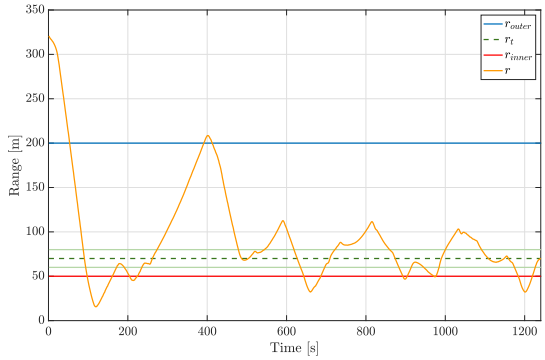

Fig. 9. Case 4: Time development of the range between the ASV and the AUV (r) compared to the radii of the outer safety boundary (r_{outer}), the target circle (r_t) surrounded by the target domain boundaries in lighter green, and the inner boundary (r_{inner}).

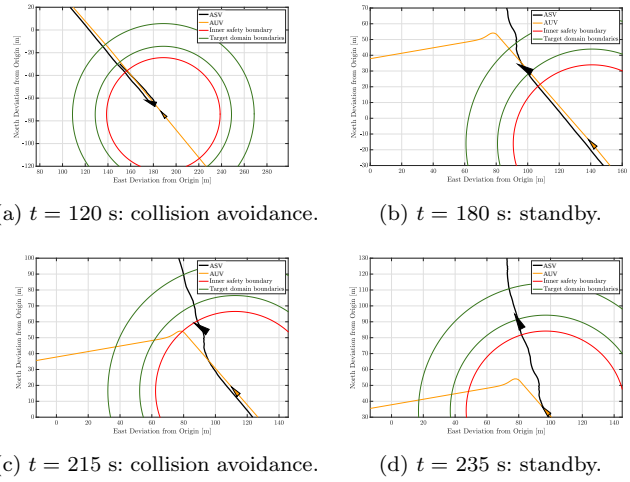

(a) $t = 120$ s: collision avoidance. (b) $t = 180$ s: standby.

(c) $t = 215$ s: collision avoidance. (d) $t = 235$ s: standby.

Fig. 10. Case 4: Snapshots of position and heading for the ASV and the AUV during collision avoidance. The red circles indicate the anti-collision domain around each AUV, while the green circles symbolize the boundaries of the target domain.

The ASV then quickly moves away from the AUV and reaches the target domain at $t = 180$ s to enter standby mode (Fig. 10b). Since the AUV is still moving the same direction, the ASV breaches the inner boundary again at $t = 215$ s (Fig. 10c), but since the ASV is now stationary and its heading is already close to the desired heading, it only takes 20 s before the ASV reaches the target domain again at $t = 235$ s (Fig. 10d). After this, the AUV changes heading, meaning the ASV can stay in standby mode until tracking is initiated at $t = 395$ s, as seen in Fig. 9.

4. CONCLUSION

The proposed hybrid controller for an ASV aiding and supporting an AUV is a simple but flexible controller with collision avoidance properties, which maintains safe operation while reducing excessive control action. Four controller tuning parameters, α_{outer}, α_{inner}, and ε, can be modified to obtain desired behavior. The controller performed well in simulation, and field trials further validated its performance. Areas of future work include dynamic selection of tuning parameters and optimal control for better performance.

ACKNOWLEDGEMENTS

This work was supported by the Research Council of Norway through the Centre of Excellence funding scheme, NTNU AMOS, project number 223254, NTNU VISTA CAROS, and the UNLOCK project, through the Research Council of Norway FRINATEK scheme, project number 274441. We would also like to thank AUR-Lab for their valuable input. The comments by two anonymous reviewers are highly appreciated for improving this article.

REFERENCES

Antonelli, G., Arrichiello, F., Caiti, A., Casalino, G., Palma, D.D., Indiveri, G., Razzanelli, M., Pollini, L., and Simetti, E. (2018). ISME activity on the use of autonomous surface and underwater vehicles for acoustic surveys at sea. *ACTA IMEKO*, 7, 24–31.

Belkin, I., de Sousa, J., Pinto, J., Mendes, R., and López-Castejón, F. (2019). Marine robotics exploration of a large-scale open-ocean front. *IEEE/OES Autonomous Underwater Vehicle Workshop*.

Fossen, T. (2011). *Handbook of Marine Craft Hydrodynamics and Motion Control*. John Wiley & Sons.

Goebel, R., Sanfelice, R.G., and Teel, A. (2012). *Hybrid dynamical systems: Modeling, stability, and robustness*. Princeton University Press.

Ludvigsen, M. and Sørensen, A. (2016). Towards integrated autonomous underwater operations for ocean mapping and monitoring. *Annual Reviews in Control*, 42, 145–157.

Norgren, P., Ludvigsen, M., Ingebregtsen, T., and Hovstein, V. (2015). Tracking and remote monitoring of an autonomous underwater vehicle using an unmanned surface vehicle in the Trondheim fjord. *OCEANS 2015 - MTS/IEEE Washington*.

Rumson, A. (2018). Mapping the deep ocean with multiple AUVs. *Hydro International*, 22, 24–26.

Sørensen, A., Ludvigsen, M., Norgren, P., Ødegård, Ø., and Cottier, F. (2020). *Sensor-Carrying Platforms*, chapter 9, 241–275. Springer.

Utne, I.B., Rokseth, B., Sørensen, A.J., and Vinnem, J.E. (2020). Towards supervisory risk control of autonomous ships. *Reliability Engineering and System Safety*, 196.

Vasiljević, A., Nad, D., Mandić, F., Mišković, N., and Vukić, Z. (2017). Coordinated navigation of surface and underwater marine robotic vehicles for ocean sampling and environmental monitoring. *IEEE/ASME Transactions on Mechatronics*, 22.

Ventikos, N.P., Chmurski, A., and Louzis, K. (2020). A systems-based application for autonomous vessels safety: Hazard identification as a function of increasing autonomy levels. *Safety Science*, 131.

Zhang, Y., Ryan, J.P., Hobson, B.W., Kieft, B., Romano, A., Barone, B., Preston, C.M., Roman, B., Raanan, B., Pargett, D., Dugenne, M., White, A.E., Freitas, F.H., Poulos, S., Wilson, S., Delong, E., Karl, D., Birch, J.M., Bellingham, J.G., and Scholin, C.A. (2021). A system of coordinated autonomous robots for Lagrangian studies of microbes in the oceanic deep chlorophyll maximum. *Science Robotics*, 6.

Paper 2

Hybrid Control Approach for an ASV Aiding Multiple-AUV Operation

Torbjørn R. Fyrvik, Jens E. Bremnes, Asgeir J. Sørensen

Draft paper for future submission.

Hybrid Control Approach for an ASV Aiding Multiple-AUV Operation

Torbjørn R. Fyrvik * **Jens E. Bremnes** * **Asgeir J. Sørensen** *

* *Centre for Autonomous Marine Operations and Systems (AMOS), Department of Marine Technology, Norwegian University of Science and Technology (NTNU), Otto Nielsens veg 10, 7491 Trondheim, Norway (e-mails: torbjofy@stud.ntnu.no, jens.e.bremnes@ntnu.no, asgeir.sorensen@ntnu.no).*

Abstract: During underwater operations, autonomous underwater vehicles (AUVs) depend on surface support as a communication link with operators and to bound errors in inertial navigation. This surface support is normally provided by a manned research vessel through acoustic signaling. Replacing the research vessel with an autonomous surface vehicle (ASV) comes with significant benefits in terms of operational domains, emissions, and efficiency. If an ASV aids multiple AUVs, the ASV should ensure that all AUVs get sufficient mission support while preventing collision with the AUVs. This paper proposes a hybrid tracking controller which implements supervisory switching to meet these two objectives for an ASV providing mission support for multiple AUVs. The controller consists of a transit controller that tracks AUVs and a standby controller that turns off the propeller to ensure good acoustic communication. While the controller nominally tracks the AUV with the least recent position fix, it switches to collision avoidance if the ASV gets too close to any AUV. Results from field trials with a physical ASV and three simulated AUVs are presented to demonstrate the controller's performance.

Keywords: Unmanned marine vehicles, unmanned surface vehicles, autonomous underwater vehicles, coordinated control, hybrid dynamical systems, collision avoidance

1. INTRODUCTION

Advances in sensor, computer, communication, and navigation technologies have recently driven large developments in field robotics. The move towards higher levels of autonomy leads to reduced dependency on human operators, which often increases operational safety and efficiency. Moreover, autonomous agents are associated with lower costs and reduced environmental impact (Ventikos et al., 2020; Utne et al., 2020). The maritime industry is not exempt from this development, and increased research and development efforts are going towards marine agents with higher levels of autonomy (Ludvigsen and Sørensen, 2016). Two examples of such agents are autonomous unmanned surface vehicles (ASVs) and autonomous underwater vehicles (AUVs). ASVs are surface-going sensor-carrying platforms, and AUVs are sensor-carrying platforms with possibilities of under- and on-surface operation.

While autonomous agents can solve a wide array of tasks, some operations require a diverse set of capabilities that cannot be provided by a single vehicle. As a result of this shortcoming, research efforts are now going towards multi-agent operations, where the agents can complement each other's capabilities. The resulting swarms of vehicles operating in different domains are called robotic organizations, which can become powerful systems for mapping and monitoring the marine environment (Sørensen et al., 2020). For instance, AUVs rely on mission support from the surface, which is normally provided by a manned research vessel. However, by replacing the manned vessel with an ASV, the system has improved capabilities, such as increased operational domains, lower emissions, and higher efficiency. The ASV's role is then to aid one or several AUVs with navigation, as well as relaying information between AUVs and the control center.

When underwater without external aiding, AUVs use inertial navigation for positioning, also known as dead-reckoning. Thus, position fixes are necessary to limit the resulting unbounded error growth. These fixes are usually provided by GPS signals when the AUV surfaces, or by acoustic signals underwater (Ludvigsen and Sørensen, 2016). Ultra-short baseline (USBL) is a suitable technology for operations where surface support is provided by a single vehicle. This is because one USBL modem can measure both the bearing and range to the underwater modem. However, the maximum range of modems largely depends on water conditions like salinity, temperature and turbidity, and the bearing uncertainty translates to a transverse position uncertainty that increases with range (Sørensen et al., 2020).

Several research groups have conducted field trials with ASVs providing mission support for AUVs. Norgren et al. (2015) used an ASV as the communication hub for an AUV that mapped the seabed, with the ASV tracking the AUV at a constant range and bearing. This is also the strategy employed by the Ocean Infinity project, where up to eight AUVs have been deployed, each with an ASV that follows its movement on the surface (Rumson, 2018).

Although this strategy is reliable, the ASVs are always moving, leading to potentially excessive control action and propeller noise that affects the acoustic signals. Moreover, it is desirable that one ASV can provide mission support for multiple AUVs.

Furthermore, Vasilijević et al. (2017) present a coordinated navigation system where an ASV performs station-keeping in the middle of the AUV's operational area to provide position fixes. In the multi-vehicle domain, Zhang et al. (2021) use an ASV to provide situational awareness and potential intervention for two AUVs, while Antonelli et al. (2018) do the same with several AUVs. However, these three research groups all give the ASV a pre-defined track to follow, regardless of AUV behavior. This gives the systems a lower level of autonomy and limits possible AUV strategies such as adaptive sampling.

Some of the challenges described above remain unsolved. This paper thus attempts to answer the research questions: How can an ASV be used to ensure reliable, safe, and autonomous operation of multiple AUVs? What are appropriate control objectives for this type of operation?

The primary scientific contribution of the present work is the development of a tracking controller algorithm for an ASV providing mission support for an AUV swarm. The mission support includes providing USBL fixes to augment the AUVs' inertial navigation error, as well as relaying relevant data from the AUVs to the operators. The proposed supervisory switching controller ensures that each AUV eventually gets a USBL fix (liveness property), while also avoiding collision with all AUVs (safety property). A secondary contribution is the formulation of the controller as a hybrid dynamical system.

The paper is outlined as follows: Section 2 describes the system in more detail and presents the ASV's supervisory switching controller as a hybrid dynamical system, Section 3 describes the experiments and discusses results, while Section 4 provides conclusions and points to areas of future work.

2. METHODOLOGY

2.1 Hybrid Dynamical Systems

The proposed tracking controller is modeled as a hybrid dynamical system based on the framework presented by Goebel et al. (2012). Such systems have both continuous-time and discrete-time dynamics, and their general model is expressed as

$$\mathcal{Q} = \begin{cases} \dot{x} \in \mathcal{F}(x) & \text{for } x \in \mathcal{C}, \\ x^+ \in \mathcal{G}(x) & \text{for } x \in \mathcal{D}, \end{cases} \tag{1}$$

where $\mathcal{C} \in \mathbb{R}^n$ is the flow set, $\mathcal{F} : \mathbb{R}^n \rightrightarrows \mathbb{R}^n$ is the flow map, $\mathcal{D} \in \mathbb{R}^n$ is the jump set, and $\mathcal{G} : \mathbb{R}^n \times \mathbb{R}^m \rightrightarrows \mathbb{R}^n$ is the jump map. The flow map $\mathcal{F}$ describes how the state x is allowed to change continuously when the state belongs to the flow set $\mathcal{C}$. Similarly, the jump map $\mathcal{G}$ describes how the state is allowed to change discretely when it belongs to the jump set $\mathcal{D}$.

The controller makes use of a simplified kinematic model for marine vessels described in detail in Fossen (2011). The kinematic relationship between velocities in the Earth-fixed ($\dot{\eta} \in \mathbb{R}^6$) and body-fixed ($\nu \in \mathbb{R}^6$) reference frames is expressed as

$$\dot{\eta} = \begin{bmatrix} J_1(\Theta) & 0_{3\times3} \\ 0_{3\times3} & J_2(\Theta) \end{bmatrix} \nu = J(\Theta)\nu, \tag{2}$$

where $J(\Theta) \in \mathbb{R}^{6\times6}$ is Euler angle transformation matrix. In this paper, the horizontal position components of η are represented as $\xi = [N \quad E]^T$, where N and E are North and East components, while ψ is the heading of the vessel relative to North. Subscript wp indicates the desired state defined by a waypoint. $i \in \{1, 2, ..., n\}$ indicates which of n AUVs that the ASV is currently providing mission support for.

2.2 Control Objectives

The controller has two objectives based on the risks of loss of communication and inter-vehicle collision: a liveness objective and a safety objective.

The *liveness objective* refers to a desired event that *should eventually happen*. Specifically, the desired event for each AUV is a reliable USBL fix. The liveliness objective thus means that the controller should ensure each AUV eventually gets its next reliable USBL fix.

A reliable USBL fix for an AUV is defined as a successfully transmitted USBL fix if the ASV is sufficiently close to the AUV, and the ASV propeller is off. The range limitation is necessary because the angular uncertainty of the USBL bearing converts to a transverse uncertainty that increases with range. Therefore, to ensure the reliability of a USBL position fix, the ASV must be sufficiently close to the AUV. Moreover, the propeller constraint is necessary because the acoustic noise produced by the propeller contributes to ambient noise that, in the worst case, may prevent USBL fixes from being correctly transmitted. Thus, the likelihood of a successful and accurate USBL fix is significantly increased if the range is small and the propeller is turned off.

On the other hand, the *safety objective* refers to an event that *should never happen*, namely collision between the ASV and an AUV. The controller should implement collision avoidance properties by ensuring that the risk of collision is kept low throughout operations.

2.3 Control Strategy

The domains defined by the control strategy are presented graphically in Fig. 1. A more in-depth description of the strategy follows subsequently.

The range (r_i) and bearing (β_i) between AUV i and the ASV are defined as

$$\begin{aligned} r_i &= \sqrt{(N_{asv} - N_{auv,i})^2 + (E_{asv} - E_{auv,i})^2}, \\ \beta_i &= atan2(E_{asv} - E_{auv,i}, N_{asv} - N_{auv,i}). \end{aligned} \tag{3}$$

To meet the safety objective, the controller takes collision-mitigating action if the ASV enters an anti-collision domain about each AUV. This domain, indicated by red

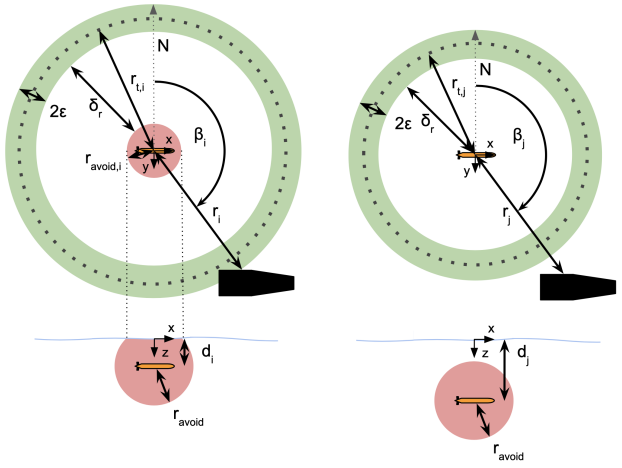

(a) $d_i < r_{avoid}$. Circular anti-collision domain on surface.

(b) $d_j > r_{avoid}$. Non-existent anti-collision domain on surface.

Fig. 1. Target and anti-collision domains for AUVs i and j at different depths. The bottom part of each subfigure shows the anti-collision sphere around each AUV, while the top part illustrates its translation to the surface, as well as the green ring-shaped target domain. δ_r and ε remain the same for all AUVs, while the other variables differ. The illustration is not to scale.

circles in Fig. 1, is a sphere centered at the AUV with radius r_{avoid} expressed as

$$r_{avoid} = \alpha T_0 \dot{r}_{max}, \tag{4}$$

where T_0 is the rated USBL update period and $\dot{r}_{max}$ is the maximum relative speed between the ASV and the AUV. α is a safety factor that can be tuned to achieve desired controller performance. The safety factor incorporates uncertainty in the USBL update period and inertia in the ASV's dynamics. By choosing a sufficiently large α, the risk of collision is kept low throughout the mission, giving the controller collision avoidance properties. However, it should be noted that large values α can lead to unnecessarily conservative behavior, as well as preventing the ASV from getting sufficiently close to the AUV to provide reliable USBL fixes.

As seen in Fig 1, the horizontal component of each AUV's sphere is a circular anti-collision domain of radius $r_{avoid,i}$ centered at $\xi_{auv,i}$. The radius of the anti-collision domain for AUV i at depth d_i is calculated as per (5).

$$r_{avoid,i} = \begin{cases} \sqrt{r_{avoid}^2 - d_i^2} & \text{for } d_i \leq r_{avoid} \\ 0 & \text{for } d_i > r_{avoid} \end{cases} \tag{5}$$

As for meeting the liveness objective, the controller must bring the ASV to the vicinity of each AUV for long enough that a reliable USBL fix can be provided. This makes for a behavior where the ASV transits to the vicinity of one AUV and turns off the propeller while waiting for a USBL fix, before repeating the same steps with the next AUV.

The vicinity of the AUV is defined as a target circle, indicated by the dashed circle in Fig. 1. The radius of the target circle is defined as

$$r_{t,i} = r_{avoid,i} + \delta_r. \tag{6}$$

δ_r is a tuning parameter that defines how far the target circle is from the anti-collision domain. A small δ_r gives higher USBL fix precision but also higher risk of entering the anti-collision domain. Hence, δ_r represents the trade-off between getting close enough to an AUV to get good USBL fixes and far enough to prevent collision.

To increase the size of the region in which the ASV can turn off the propeller, a deviation of $\varepsilon_-/\varepsilon_+$ on either side of the target circle is accepted. This acceptable deviation from the target circle converts to the green target domain in Fig. 1, defined by

$$r_i \in [r_{t,i} - \varepsilon_-, r_{t,i} + \varepsilon_+], \tag{7}$$

where ε_- and ε_+ are tuning parameters. In this work, $\varepsilon_- = \varepsilon_+ =: \varepsilon$ is considered for simplicity. Differing values of ε_- and ε_+ can be considered in further studies.

The controller must also continuously evaluate which AUV i the ASV should prioritize for mission support. During nominal operation, the controller chooses the AUV with the longest time since the last reliable USBL fix (e.g., $i = 1$). However, if the ASV enters the anti-collision domain of another AUV (e.g., $i = 2$), that vehicle must get priority. Therefore, the controller immediately selects $i = 2$ to ensure that the ASV leaves its anti-collision domain as quickly as possible. Since the ASV is then transiting towards the target domain of $i = 2$, it will turn off the propeller when it reaches its target domain to get a reliable USBL fix. Only then does the ASV resume tracking of $i = 1$. By waiting for this USBL fix, the time in which $i = 2$ stays in dead-reckoning is reduced. The AUV selection happens according to (8), with nominal operation on the top and collision avoidance on the bottom.

$$i = \begin{cases} \arg\max_k \{\tau_k\} & \text{if } \forall k : r_k > r_{avoid,k} \\ \arg\min_k \{r_k\} & \text{if } \exists k : r_k < r_{avoid,k} \end{cases} \tag{8}$$

In (8), τ_k is the time since the last reliable USBL fix for AUV k, calculated as

$$\begin{aligned} \dot{\tau}_k &= 1 \text{ for } \{r_k > r_{t,k} + \varepsilon\} \cup \{n_p \neq 0\}, \\ \tau_k^+ &= 0 \text{ for } \{r_k < r_{t,k} + \varepsilon\} \cap \{n_p = 0\}, \end{aligned} \tag{9}$$

where n_p is the propeller speed. Note that (9) is a simple incremental timer that resets if the ASV is inside the outer limit of the appropriate AUV's target domain and the propeller is off.

2.4 Hybrid Tracking Controller

The resulting supervisory switching controller is presented here as a hybrid tracking controller. It is possible and simpler to represent the controller in fully discrete dynamics, for instance as a state machine. However, the hybrid dynamical framework is chosen here to allow for further analysis of the system dynamics, such as stability analyses, at a later stage. The hybrid controller consists of a zero-

thrust standby controller ($\mathcal{Q}_1$) and a transit controller ($\mathcal{Q}_2$).

The standby controller $\mathcal{Q}_1$ is used when the ASV is in the vicinity of an AUV and waiting for signal from the AUV to provide a USBL fix. In this mode, the ASV propeller is turned off to prevent distortion of the acoustic signals, while sensors remain on to monitor the operation. To ensure a USBL fix is provided before the controller changes to transit mode, a timer τ is implemented for $\mathcal{Q}_1$. When entering standby mode, the timer jumps to T before it is decremented every second. The controller cannot jump to transit mode before the timer has reached zero. If the tuning parameter T is set high, there are higher chances of reliable USBL fixes during standby, but this means it takes longer for the ASV to initiate transit to the next AUV.

The transit controller $\mathcal{Q}_2$, on the other hand, is responsible for transiting between the vicinity of each AUV, as well as preventing collision if the ASV gets too close to any AUV. When the ASV is in transit mode, its waypoint is chosen as the closest point on the target circle around the chosen AUV. The controller is in transit mode until the ASV is sufficiently close to the target circle. This is quantified by the error, e_i, defined as

$$e_i = r_i - r_{t,i}, \tag{10}$$

which must be smaller than the tuning parameter ε for the jump to $\mathcal{Q}_1$ to occur.

Moreover, the transit controller also gives the hybrid controller its collision avoidance properties. This is obtained by accepting jumps to $\mathcal{Q}_2$ regardless of all other variables if the ASV enters the anti-collision domain of any AUV.

As such, the proposed hybrid tracking controller based on the framework in (1) is formulated in (11) with subscripts 1 and 2 corresponding to $\mathcal{Q}_1$ and $\mathcal{Q}_2$, respectively. The controller state is $x_i = [r_{wp,i}, \beta_{wp,i}, r_i, \beta_i, q, \tau]^T$.

$$\begin{aligned}
\mathcal{F}_1(x_i) &:= \begin{cases} \dot{r}_{wp,i} = \dot{r}_i \\ \dot{\beta}_{wp,i} = \dot{\beta}_i \\ \dot{q} = 0 \\ \dot{\tau} = -1 \end{cases} && \text{for } x_i \in \mathcal{C}_1 := \\
&&& \{x_i : q = 1, \tau \in (0, T]\} \\
\mathcal{G}_1(x_i) &:= \begin{cases} r^+_{wp,i} = r_i \\ \beta^+_{wp,i} = \beta_i \\ q^+ = 1 \\ \tau^+ = T \end{cases} && \text{for } x_i \in \mathcal{D}_1 := \\
&&& \left\{ \begin{array}{l} x_i : |e_i| < \varepsilon, \\ q = 2 \end{array} \right\} \\
\mathcal{F}_2(x_i) &:= \begin{cases} \dot{r}_{wp,i} = \dot{r}_{t,i} \\ \dot{\beta}_{wp,i} = \dot{\beta}_i \\ \dot{q} = 0 \\ \dot{\tau} = 0 \end{cases} && \text{for } x_i \in \mathcal{C}_2 := \\
&&& \{x_i : q = 2\} \\
\mathcal{G}_2(x_i) &:= \begin{cases} r^+_{wp,i} = r_{t,i} \\ \beta^+_{wp,i} = \beta_i \\ q^+ = 2 \\ \tau^+ = 0 \end{cases} && \text{for } x_i \in \mathcal{D}_2 := \\
&&& \left\{ \begin{array}{c} \{x_i : (q, \tau) = (1, 0)\} \\ \cup \\ \{x_i : r_i < r_{avoid,i}\} \end{array} \right\}
\end{aligned} \tag{11}$$

Once the appropriate controller has been selected in (11), the ASV waypoint is updated as per

$$\xi_{wp,asv} = \xi_{auv,i} + r_{t,i} \begin{bmatrix} cos(\beta_{wp,i}) \\ sin(\beta_{wp,i}) \end{bmatrix}. \tag{12}$$

The complete controller algorithm follows the above steps and is presented in Algorithm 1.

Algorithm 1: Controller Algorithm

```
initialization;
while Not interrupted do
    select AUV ;                    /* See (8) */
    select controller ;             /* See (11) */
    set waypoint ;                  /* See (12) */
end
```

The proposed tracking algorithm relies on knowledge of the AUVs' navigational states. Between USBL fixes, the ASV should be able to estimate the AUVs' states.

3. RESULTS AND DISCUSSION

3.1 Experimental Setup

To test the proposed hybrid tracking controller, an ASV was set to aid three simulated AUVs.

The ASV used in these field trials is a Pioner 17 from Maritime Robotics named Gretha. Gretha is 5.2 m long, 2.15 m wide, has a draft of 0.3 m and weighs 810 kg. The vehicle's rated endurance is 24 hours at 3 kn, and the observed maximum speed during field trials was 4.9 kn. The on-board communication suite consists of a WiFi hotspot with more than 50 m range, LTE coverage through a 4G module, and Kongsberg MBR broadband with 15 km range. Additionally, an EvoLogics S2C R 18/34 USBL modem was installed to facilitate acoustic communication with real AUVs in later field trials, with a rated period of USBL position fixes $T_0 = 5$ s and rated range $r_0 = 3.5$ km.

The AUVs are simulated with the LSTS toolchain, which consists of DUNE on-board software, [1] Neptus command and control software, [2] and the IMC communications protocol. [3] Gretha, conversely, comes with Maritime Robotics's in-house Onboard System (OBS) for control, navigation, and communication. The user interface, Maritime Robotics's version of Neptus, is called Vehicle Control Station (VCS), which has a built-in simulator for Gretha. To integrate OBS/VCS with the LSTS toolchain, a software bridge between the two interfaces was designed. The controller was implemented with Python in ROS, [4] so another software bridge was set up between IMC and ROS based on the *imc_ros_bridge* package. [5]

Deploying Gretha and simulating three AUVs with the default AUV simulator in DUNE, two cases of a typical AUV operation were tested. The supervisory switching controller's performance was analyzed by running it on the ASV and studying the vehicle's resulting behavior.

[1] https://github.com/LSTS/dune
[2] https://github.com/LSTS/neptus
[3] https://lsts.pt/docs/imc/master/index.html
[4] https://www.ros.org
[5] https://github.com/smarc-project/imc_ros_bridge

In Case 1, each AUV does a lawnmower pattern, with the operational areas separated by a few hundred meters. This closely resembles a possible multi AUV operation, where the AUVs can do simultaneous overview scans of the seabed. It is common for AUVs to maintain a constant altitude above the seabed during surveys, but to better showcase the behavior of the controller, the simulated vehicles instead operate in the surface with a zero-depth set-point during the test. This also means that the target circle and collision avoidance circle radii are the same for all three vehicles, i.e., $r_{avoid,i} = r_{avoid}$ and $r_{t,i} = r_t$ for each AUV i.

In Case 2, the AUVs' waypoints are updated manually to create situations that demonstrate the ASV's anti-collision properties. Although it is unlikely that the AUVs will actively attempt to enter the anti-collision domain during nominal operation, it is difficult to predict how an autonomous vehicle will behave, for instance if it follows an adaptive sampling control law. Therefore, Case 2 is mainly focused on how the hybrid tracking controller prevents possibly dangerous situations when the AUVs operate with high levels of autonomy. The AUVs operate in the surface in Case 2 as well.

Since the AUVs are simulated, the ASV has continuous knowledge of their navigational states. During operations with real AUVs, it is assumed that continuous knowledge of AUVs' navigational states is made possible with a state estimator. This is out of scope of this paper and is thus not implemented here. Moreover, since the ASV does not receive actual acoustic signals from the simulated AUVs, transmission of USBL fixes must also be simulated. This is done by assuming that the ASV will provide at least one fix if it is in standby within the outer boundary of the target domain for T seconds, where T is one of the controller tuning parameters.

3.2 Tuning Parameters

Several tests were run to determine suitable values for the tuning parameters. It was found that $\alpha = 5$ gave an appropriately large collision avoidance zone around the AUV. With this safety factor, the radius of the spherical anti-collision domain is $r_{avoid} = \alpha T_0 \dot{r}_{max} = 50$ m, using $T_0 = 5$ s and $\dot{r}_{max} = 2$ m/s. Moreover, a distance $\delta_r = 20$ m from the anti-collision domain to the target circle was found to give good performance. This translates to target circles of radius $r_{t,i} = r_i + 20\text{m} \in [20\text{m}, 70\text{m}]$ centered at $\xi_{auv,i}$.

As for the tuning parameters defining the discrete dynamics of the controller, $\varepsilon = 10$ m was chosen as the acceptable distance to waypoint before the ASV can change from $\mathcal{Q}_2$ to $\mathcal{Q}_1$. Moreover, $T = 10$ s was used to yield satisfactory performance.

3.3 Discussion

As seen in Fig. 2, the ASV shuttles between the operational areas of the three AUVs during Case 1. The triangular path of the ASV highlights how the vehicle does not have to transit to the exact position of the AUV before providing the USBL fix, but rather reduces the traveled distance by stopping in the target domain.

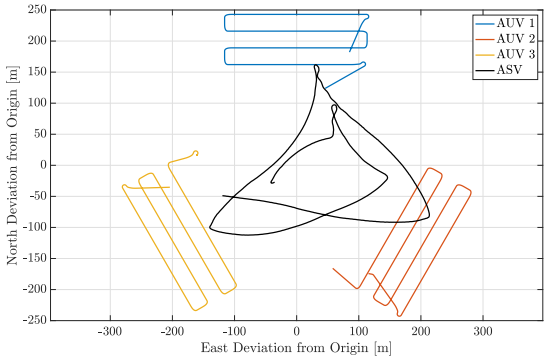

Fig. 2. Case 1: North and East movement of the four vehicles relative to the origin, defined as the center point of the operation.

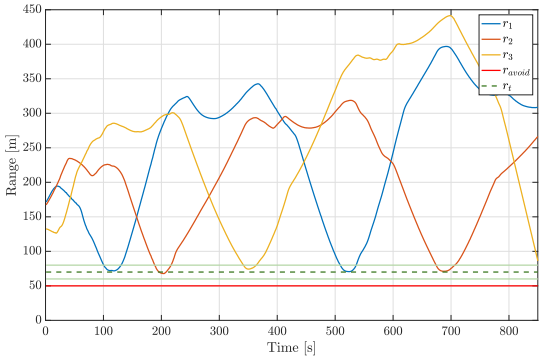

Fig. 3. Case 1: Range between the ASV and each AUV i (r_i), and radii of the collision avoidance circle (r_{avoid}) and target circle (r_t) as time series.

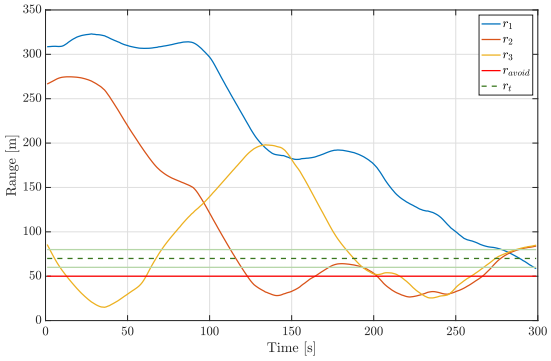

Fig. 4. Case 2: Range between the ASV and each AUV i (r_i), and radii of the collision avoidance circle (r_{avoid}) and target circle (r_t) as time series.

Fig. 3 explains the ASV's behavior in more detail. The ASV moves towards the AUVs in cyclical order, transiting towards one until the range is within the target domain, waiting $T = 10$ s, and then transiting towards the next AUV. Due to the orientation of the AUVs' operational areas relative to each other, the ASV never enters the anti-collision zone of any AUV. Since it reaches significantly higher speeds than the AUVs, the ASV quickly transits between the operational areas, and the time between two consecutive USBL fixes does not exceed 500 s for any AUV.

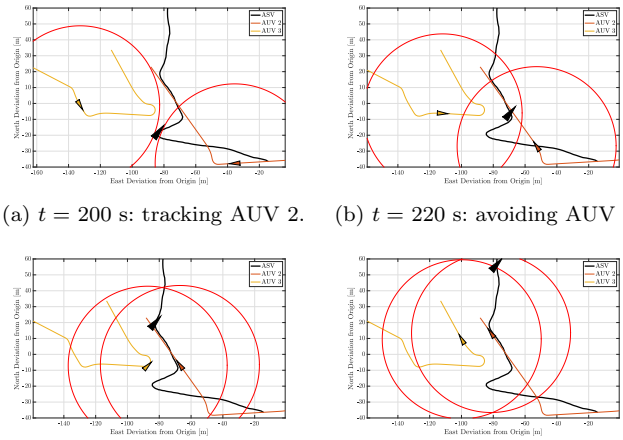

(a) $t = 200$ s: tracking AUV 2. (b) $t = 220$ s: avoiding AUV 2.

(c) $t = 240$ s: avoiding AUV 3. (d) $t = 260$ s: avoiding AUV 2.

Fig. 5. Case 2: Snapshots of position and heading for the ASV, AUV 2 and AUV 3 during collision avoidance. The red circles indicate the anti-collision domain around each AUV.

Fig. 4 shows how the AUVs repeatedly get so close that the ASV enters their anti-collision domains during Case 2, requiring corrective action by the supervisory switching controller. This corrective action effectively prevents collision, with no AUV getting closer to the ASV than AUV 3 at $t = 40$ s with $r_3 = 15$ m. Although it is longer since AUV 1 has received USBL fixes than the two other vehicles towards the end of case, the ASV focuses its control action on AUV 2 and 3. This shows how anti-collision (safety objective) gets priority over USBL fixes (liveness objective).

Since both AUV 2 and 3 are within the anti-collision domain in the time frame $t \in [200 \text{ s}, 260 \text{ s}]$, snapshots of the position and heading of these vehicles, as well as the ASV, are shown in Fig. 5 for further analysis.

Following the results from Fig. 4, at $t = 200$ s (Fig. 5a), the ASV has just come out of standby mode providing a USBL fix for AUV 3 and started transit towards AUV 2. Soon after, however, the ASV enters the anti-collision domain of AUV 2 and needs to turn around to prevent collision. This is reflected in Fig. 5b, where the ASV is moving away from AUV 2 at $t = 220$ s. At $t = 240$ s (Fig. 5c), the range to AUV 3 has gotten smaller than that of AUV 2, as verified by Fig. 4. This means that the ASV switches to collision avoidance for AUV 3. By $t = 260$ s (Fig. 5d), the ASV has moved out of the anti-collision domain of both vehicles. Since the ASV is significantly faster than the AUVs, it quickly moves out of the anti-collision domains despite both AUVs actively moving towards it.

4. CONCLUSION

The proposed supervisory switching controller for an ASV providing mission support for multiple AUVs performed well in field trials with a physical ASV and three simulated AUVs. Implemented as a hybrid dynamical system, the controller ensured that each AUV eventually received communication and navigation support, while upholding safety by preventing collisions with all AUVs. The four tuning parameters (α, δ_r, ε and T) were tuned to achieve desired behavior. Areas of future work include field trials with physical AUVs, dynamic selection of tuning parameters and detailed analysis of the system dynamics, such as stability analysis of the hybrid controller.

ACKNOWLEDGEMENTS

This work was supported by the Research Council of Norway through the Centre of Excellence funding scheme, NTNU AMOS, project number 223254, NTNU VISTA CAROS, and the UNLOCK project, through the Research Council of Norway FRINATEK scheme, project number 274441. We would also like to thank AUR-Lab for their valuable input. The comments by two anonymous reviewers are highly appreciated for improving this article.

REFERENCES

Antonelli, G., Arrichiello, F., Caiti, A., Casalino, G., Palma, D.D., Indiveri, G., Razzanelli, M., Pollini, L., and Simetti, E. (2018). ISME activity on the use of autonomous surface and underwater vehicles for acoustic surveys at sea. *ACTA IMEKO*, 7, 24–31.

Fossen, T. (2011). *Handbook of Marine Craft Hydrodynamics and Motion Control*. John Wiley & Sons.

Goebel, R., Sanfelice, R.G., and Teel, A. (2012). *Hybrid dynamical systems: Modeling, stability, and robustness*. Princeton University Press.

Ludvigsen, M. and Sørensen, A. (2016). Towards integrated autonomous underwater operations for ocean mapping and monitoring. *Annual Reviews in Control*, 42, 145–157.

Norgren, P., Ludvigsen, M., Ingebregtsen, T., and Hovstein, V. (2015). Tracking and remote monitoring of an autonomous underwater vehicle using an unmanned surface vehicle in the Trondheim fjord. *OCEANS 2015 - MTS/IEEE Washington*.

Rumson, A. (2018). Mapping the deep ocean with multiple AUVs. *Hydro International*, 22, 24–26.

Sørensen, A., Ludvigsen, M., Norgren, P., Ødegård, Ø., and Cottier, F. (2020). *Sensor-Carrying Platforms*, chapter 9, 241–275. Springer.

Utne, I.B., Rokseth, B., Sørensen, A.J., and Vinnem, J.E. (2020). Towards supervisory risk control of autonomous ships. *Reliability Engineering and System Safety*, 196.

Vasilijević, A., Nad, D., Mandić, F., Mišković, N., and Vukić, Z. (2017). Coordinated navigation of surface and underwater marine robotic vehicles for ocean sampling and environmental monitoring. *IEEE/ASME Transactions on Mechatronics*, 22.

Ventikos, N.P., Chmurski, A., and Louzis, K. (2020). A systems-based application for autonomous vessels safety: Hazard identification as a function of increasing autonomy levels. *Safety Science*, 131.

Zhang, Y., Ryan, J.P., Hobson, B.W., Kieft, B., Romano, A., Barone, B., Preston, C.M., Roman, B., Raanan, B., Pargett, D., Dugenne, M., White, A.E., Freitas, F.H., Poulos, S., Wilson, S., Delong, E., Karl, D., Birch, J.M., Bellingham, J.G., and Scholin, C.A. (2021). A system of coordinated autonomous robots for Lagrangian studies of microbes in the oceanic deep chlorophyll maximum. *Science Robotics*, 6.

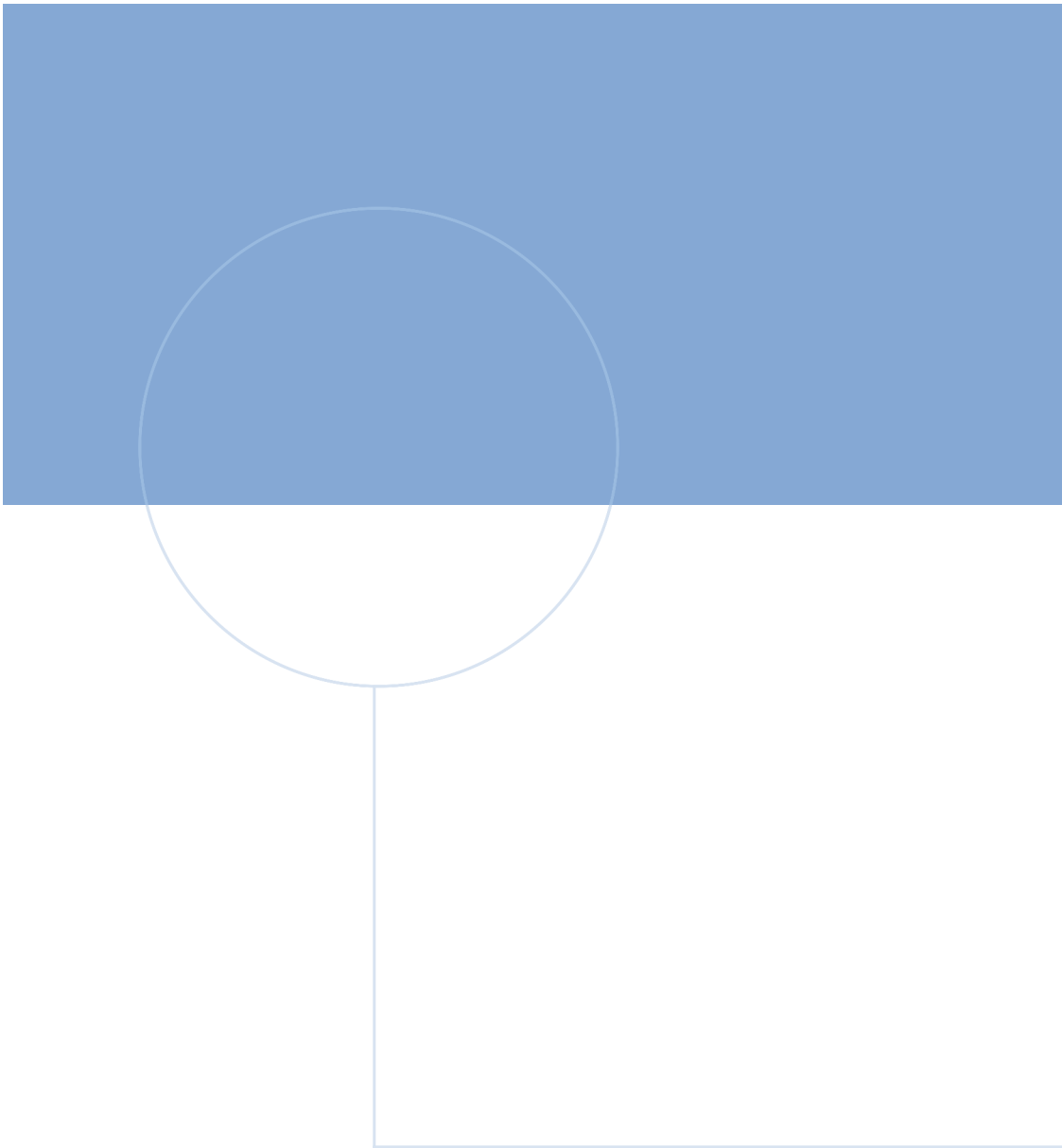

NTNU

Kunnskap for en bedre verden